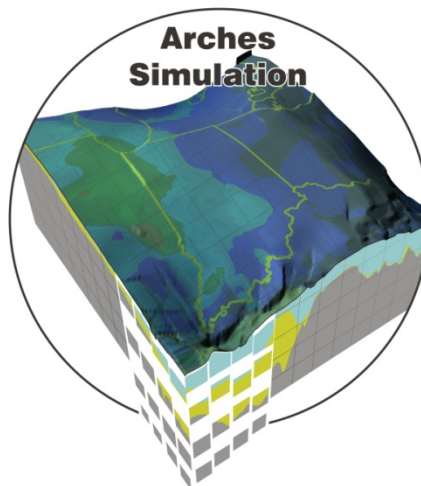


CONCEPTUAL MODEL SUMMARY REPORT SIMULATION FRAMEWORK FOR REGIONAL GEOLOGIC CO₂ STORAGE ALONG ARCHES PROVINCE OF MIDWESTERN UNITED STATES

TOPICAL REPORT



August 2011

Reporting Period: March 1, 2010 - June 30, 2011

DOE Award Number: DE-FE0001034

Ohio Department of Development Grant Agreement: CDO/D-10-03

Energy Systems & Carbon Management
Battelle Memorial Institute
505 King Avenue
Columbus, OH 43201



This report was prepared as an account of work sponsored by an agency of the United States Government. Neither the United States Government nor any agency thereof, nor any of their employees, makes any warranty, express or implied, or assumes any legal liability or responsibility for the accuracy, completeness, or usefulness of any information, apparatus, product, or process disclosed, or represents that its use would not infringe privately owned rights. Reference herein to any specific commercial product, process, or service by trade name, trademark, manufacturer, or otherwise does not necessarily constitute or imply its endorsement, recommendation, or favoring by the United States Government or any agency thereof. The views and opinions of authors expressed herein do not necessarily state or reflect those of the United States Government or any agency thereof.

ABSTRACT

A conceptual model was developed for the Arches Province that integrates geologic and hydrologic information on the Eau Claire and Mt. Simon formations into a geocellular model. The conceptual model describes the geologic setting, stratigraphy, geologic structures, hydrologic features, and distribution of key hydraulic parameters. The conceptual model is focused on the Mt. Simon sandstone and Eau Claire formations. The geocellular model depicts the parameters and conditions in a numerical array that may be imported into the numerical simulations of carbon dioxide (CO₂) storage. Geophysical well logs, rock samples, drilling logs, geotechnical test results, and reservoir tests were evaluated for a 500,000 km² study area centered on the Arches Province. The geologic and hydraulic data were integrated into a three-dimensional (3D) grid of porosity and permeability, which are key parameters regarding fluid flow and pressure buildup due to CO₂ injection. Permeability data were corrected in locations where reservoir tests have been performed in Mt. Simon injection wells. The final geocellular model covers an area of 600 km by 600 km centered on the Arches Province. The geocellular model includes a total of 24,500,000 cells representing estimated porosity and permeability distribution. CO₂ injection scenarios were developed for on-site and regional injection fields at rates of 70 to 140 million metric tons per year.

Table of Contents

ABSTRACT	iii
List of Figures	v
List of Tables	vi
List of Appendices	vii
List of Acronyms	viii
EXECUTIVE SUMMARY	ix
Section 1.0: INTRODUCTION	1
1.1 Background	1
1.2 Objectives	1
1.3 Methods	2
1.4 Assumptions/Limitations	2
Section 2.0: GEOLOGIC FRAMEWORK	4
2.1 Geologic Setting	4
2.2 Regional Structure	8
2.3 Stratigraphy	11
2.4 Hydrostratigraphic Units	13
2.5 Geologic Cross Sections	15
2.6 Structure Maps	19
Section 3.0: HYDRAULIC PARAMETERS	21
3.1 Rock Core Testing Program	21
3.2 Core Testing Methods/Types	21
3.2.1 Routine Analysis	22
3.2.2 Special Core Analysis (SCAL)	23
3.3 Results from Core	24
3.3.1 Historical/Existing Core Data Results	26
3.3.2 Routine Porosity/Permeability Core Analysis Results from Arches Study	28
3.3.3 SCAL Results from Arches Study	32
3.3.3.1 MICP Results	32
3.3.3.2 Geomechanical Results	36
3.3.3.3 Relative Permeability Results	37
3.4 Knox and Precambrian Layer Porosity and Permeability	39
3.5 Reservoir Pressure	39
3.6 Density/Salinity	42
3.7 Reservoir Temperature	43
3.8 Compressibility/Geomechanical	46
3.9 Other Model Input	47
Section 4.0: GEOCELLULAR MODEL DEVELOPMENT	49
4.1 Geophysical Log Database	49
4.2 Geostatistical Analysis	51
4.3 3D Porosity Grid	56
4.4 Porosity–Permeability Transform Estimate	59
4.5 Injection Well Reservoir Test Permeability Correction Factors	61
Section 5.0: SIMULATION SCENARIOS	68

5.1	CO ₂ Sources in the Arches Province	68
5.2	On-Site Injection	69
5.3	Regional Injection Fields.....	69
5.4	Pipeline Routing Study.....	70
5.5	Other Simulation Scenarios.....	72
Section 6.0: CONCLUSIONS		73
Section 7.0: REFERENCES		75

List of Figures

Figure 2-1.	3D Surface Image of the Mt. Simon Sandstone Illustrating Major Geologic Structures in the Region	5
Figure 2-2.	Stratigraphic Correlation and CO ₂ Sequestration Chart of Geologic Units in the Midwestern U.S. (MRCSP, 2005).....	6
Figure 2-3.	Diagram Illustrating Depositional Setting of Basins and Arches in Middle Devonian Time (from Blakey, 2008)	7
Figure 2-4.	Isopach Map (ft) of Cambrian Basal Sandstones in the Midwestern United States Hydrologic Features	9
Figure 2-5.	Geologic Block Diagram Illustrating Hydrologic Features and Flow Cycles in Arches Province	10
Figure 2-6.	Cambrian Basal Sandstone Distribution in Midwestern U.S.	12
Figure 2-7.	Cambrian Basal Sandstone Distribution in Midwestern U.S.	13
Figure 2-8.	Draft Conceptual Diagram for Arches Simulations	14
Figure 2-9.	Location Map of Geological Cross Sections Prepared for Arches Province	16
Figure 2-10.	Example Geologic Cross Section in Northern Indiana	17
Figure 2-11.	Comparison of Isopach Maps for the Mt. Simon Sandstone in Kentucky	18
Figure 2-12.	Study Area Showing Structure and Isopach Maps Respectively for the Knox (a, b), Eau Claire Formation (c, d), and Mt. Simon Sandstone (e, f).....	20
Figure 3-1.	Map Showing Historical and New/Arches Core Data Well Locations	24
Figure 3-2.	Map Showing Mt. Simon Historical and New/Arches Average Core Porosity Data.....	25
Figure 3-3.	Map Showing Mt. Simon Historical and New/Arches Core Permeability Data	26
Figure 3-4.	Map Showing Mt. Simon Historical Core Porosity Data.....	27
Figure 3-5.	Map Showing Mt. Simon Historical Core Permeability Data	27
Figure 3-6.	Map Showing Mt. Simon New/Arches Project Core Porosity Data	28
Figure 3-7.	Map Showing Mt. Simon New/Arches Project Core Permeability Data	29
Figure 3-8.	Permeability-Porosity Crossplot Showing Data from Routine New/Arches Core Analysis	30
Figures 3-9 a-c.	(a) Crossplot of Horizontal and Vertical Permeability to Air, (b) Crossplot of Horizontal and Vertical Porosity, (c) Crossplot of Horizontal and Vertical Grain Density.....	31
Figure 3-10.	Mercury Saturation Plot for MICP Test Samples	34
Figure 3-11.	Pore Throat Radius Plot for MICP Test Samples	34
Figure 3-12.	Leverett J Function Plot for MICP Test Samples	35
Figure 3-13.	Leverett J-Function (Dimensionless Capillary Pressure) Plot of Mt. Simon MICP Data....	35
Figure 3-14.	Leverett J-Function (Dimensionless Capillary Pressure) Plot of Eau Claire MICP Data....	35
Figure 3-15.	lot of Stress-Strain Curve Results from Sample #1.....	36
Figure 3-16.	Liquid Production from Eau Claire Sample from CO ₂ Relative Permeability Test in Well 3416560005, Warren County, Ohio (sample depth 3152.7 ft).....	38

Figure 3-17.	Liquid Production from Mt. Simon Sample from CO ₂ Relative Permeability Test in Well IN16209, Jasper County, Indiana (sample depth 3087 ft).....	39
Figure 3-18.	Mt. Simon Reservoir Pressure (psi)	42
Figure 3-19.	Mt. Simon Fluid Density.....	43
Figure 3-20.	Isopach of Final Temperature Gradient Dataset	45
Figure 4-1.	Schematic Diagram Showing Geocellular Model Development Process	49
Figure 4-2.	Location Map Showing Well Locations Where Geophysical Porosity Logs Were°Evaluated	50
Figure 4-3.	Average Porosity in Mt. Simon Sandstone Based on Log Data.....	51
Figure 4-4.	Empirical Variograms of the Mt. Simon Formation	54
Figure 4-5.	Map Showing Ratio of Dolomite to Shale Based on Gamma Ray Logs in the Eau Claire Formation	55
Figure 4-6.	Empirical Variograms of Eau Claire Dolomite.....	56
Figure 4-7.	3D Porosity Model	57
Figure 4-8.	3D Porosity Distribution for Eau Claire.....	58
Figure 4-9.	3D Porosity Distribution for Mt. Simon	58
Figure 4-10.	Ranges of Values for Porosity and Permeability within the Eau Claire and Mt. Simon Formations	60
Figure 4-11.	Map of Log-Derived Permeability Transform Data.....	62
Figure 4-12.	Map of Pressure Fall-off Permeability Data	63
Figure 4-13.	Map of Permeability Correction Factor	64
Figure 4-14.	3D Permeability Model	65
Figure 4-15.	3D Permeability Distribution for Eau Claire.....	66
Figure 4-16.	3D Log Permeability Distribution for Mt. Simon	66
Figure 4-17.	3D Porosity Distribution at 5X Vertical Exaggeration	67
Figure 5-1.	Distribution of Large CO ₂ Point Sources in the Arches Province	69
Figure 5-2.	Pipeline Routing Analysis Results	71

List of Tables

Table 2-1.	Conceptual Model Hydrostratigraphic Units	15
Table 3-1.	Summary of Average Permeability and Porosity Measured in Core Samples from Existing and New/Arches Project Samples (by well)	25
Table 3-2.	Summary Average Permeability and Porosity Measured in Core Samples from Existing Samples (by well)	26
Table 3-3.	Summary of Average Permeability, Average Porosity, and Average Grain Density Measured in Core Samples from New/Arches Project Samples (by well).....	28
Table 3-4.	Summary Comparison of Vertical and Horizontal Permeability, Porosity, and Grain Density Measured from New/Arches Core Samples in Mt. Simon	31
Table 3-5.	Summary of Test Results from MICP	33
Table 3-6.	Summary of Triaxial Compressive Test.....	37
Table 3-7.	Summary of Brazilian Indirect Tensile Test	37
Table 3-8.	Summary of Relative Permeability Tests.....	38
Table 3-9.	Mt. Simon Reservoir Pressure Data.....	40
Table 3-10.	Example of Source Data.....	44
Table 3-11.	Summary of Geomechanical Data for Eau Claire and Mt. Simon Formations	46
Table 3-12.	Mt. Simon Rock Core CO ₂ -Water Relative Permeability Data from East Bend	48
Table 4-1.	Covariance Parameters Determined Using SGeMS Variogram Tools	53
Table 4-2.	Parameters of Eau Claire Dolomite Covariance Structure	56

Table 4-3. Type of Data and Number of Wells Used to Determine the Permeability Correction Factor (f_{corr})	62
---	----

List of Appendices

(appendices included separately on DVD in digital format)

- Appendix A. Analysis of the Southern Margin of the Mt. Simon
- Appendix B. Arches Core Test Results
- Appendix C. Geocellular Model Data

List of Acronyms

2D	two-dimensional
3D	three-dimensional
CO ₂	carbon dioxide
GIS	geographic information system
mD	millidarcy
MICP	mercury injection capillary pressure
MRCSP	Midwest Regional Carbon Sequestration Partnership
MVA	monitoring/verification/accounting
NETL	National Energy Technology Laboratory
psi	pounds per square inch
QA/QC	quality assurance/quality control
SCAL	special core analysis
Ss	sub sea
U.S. DOE	U.S. Department of Energy

EXECUTIVE SUMMARY

This report presents a summary of the conceptual model for the Arches Province in the Midwestern U.S. The Arches Simulation project is designed to develop a simulation framework for regional geologic carbon dioxide (CO₂) storage infrastructure along the Arches Province through: 1) development of a geologic model, and 2) advanced reservoir simulations of large-scale CO₂ storage along the province. The objective of the conceptual model task was integration of the various geologic and hydrologic information into a geocellular model, which comprises the basis for the numerical model. Geologic information includes general geologic setting, stratigraphy, structure of the rock formations, hydrologic features, and description of the hydrostratigraphic units. The conceptual model was also aimed at compilation of hydraulic parameters that describe the physical conditions and controls in the rock formations being considered for CO₂ storage. The ultimate objective of the conceptual model was development of a geocellular model. The geocellular model represents the parameters and conditions in a numerical array, or regularly spaced grid, that may be imported into the numerical model.

The Arches Province in the Midwestern U.S. has been identified as a major area for CO₂ sequestration because of the intersection of reservoir thickness and permeability along the province. The province includes areas of Indiana, Kentucky, Michigan, and Ohio along several arch structures between the Appalachian, Illinois, and Michigan sedimentary basins. The main injection target is the Mt. Simon sandstone due to its depth, thickness, hydraulic properties, and brine salinity.

The Arches Simulation project is a three-year effort and part of the U.S. Department of Energy (DOE)/National Energy Technology Laboratory (NETL) program on monitoring/verification/accounting (MVA), simulation, and risk assessment of CO₂ sequestration in geologic formations. The project is supported by U.S. DOE/NETL under agreement DE-FE0001034 and Ohio Department of Development under agreement CDO/D-10-03. The project research team consists of Battelle Memorial Institute, Battelle Pacific Northwest Division, Geological Surveys of Ohio, Indiana, and Kentucky, and Western Michigan University.

Initial work on the project involved compiling and interpreting information on the deep rock formations, Mt. Simon injection well operations, and geotechnical data. The conceptual model describes the geologic setting, stratigraphy, geologic structures, hydrologic features, and distribution of key hydraulic parameters. Geophysical well logs, rock samples, drilling logs, geotechnical test results, and reservoir tests were evaluated for a 500,000 km² study area centered on the Arches Province:

- Information from over 500 wells that penetrate the deeper rock zones in the Midwest U.S.,
- Geophysical well logs from 496 wells,
- Approximately 4,000 rock core test results in Eau Claire or Mt. Simon intervals,
- 105 additional standard permeability and porosity tests on Mt. Simon/Eau Claire rock samples,
- Completion of geomechanical tests on 11 rock samples,
- 16 mercury injection capillary pressure tests on rock samples,
- 10 other advanced saturation tests on rock core samples,
- Deep well injection operational data from 48 wells in the study area,
- Pressure fall-off reservoir test data from 31 wells,
- Compilation and analysis of a total of 960,000 porosity data from geophysical logs,
- Many other geological maps, research, and publications.

The geologic and hydraulic data were integrated into a geocellular model. The data were integrated into a three-dimensional (3D) grid of porosity and permeability, which are key parameters regarding fluid flow and pressure buildup due to CO₂ injection. Permeability data were corrected in locations where reservoir

tests have been performed in Mt. Simon injection wells. The final geocellular model covers an area of 600 km by 600 km centered on the Arches Province. The geocellular model includes a total of 24,500,000 cells representing estimated porosity and permeability distribution.

Development of the conceptual model revealed several key conclusions regarding the geologic framework for CO₂ storage in the Arches Province:

- The Mt. Simon sandstone and equivalent basal sandstone interval are present from Iowa to West Virginia. The Arches Province is located along the east-central extent of the overall extent, and the nature of the rock formation varies across the study area. Many of these trends were exhibited in maps of hydraulic and geotechnical parameters.
- Interpretation of the Mt. Simon was refined in the Arches Province to define the distribution of the formation in more detail. The mapping was based on detailed geologic cross sections which built upon previous work performed by the Midwest Regional Carbon Sequestration Partnership (MRCSP) and other research.
- Hydrostratigraphic units were identified to aid in delineation of formation structure, which defines the overall framework of the model. In developing the conceptual model, it was determined that there is often no clear break between hydrostratigraphic units. Thus, the Cambrian basal sandstone and Eau Claire formation were represented with a variable distribution of input parameters.
- A major result of this portion of this research was revision to the southern margin of the Mt. Simon sandstone into Kentucky. New seismic interpretations and well data collected from recent CO₂ injection tests were used to re-interpret the southern boundary of the Mt. Simon sandstone and examine the manner in which the sandstone thins south- and eastward. Structures associated with the Rough Creek Graben and Rome Trough influence the southern limit of the sandstone, causing thinning or absence on structural highs.
- Geostatistical analysis of geophysical porosity data was completed for the Mt. Simon and Eau Claire intervals. Geostatistical analysis for the Mt. Simon suggests a fairly erratic dataset. Subsampling methods were necessary to interpret the data and indicated lateral correlation range of 50 to 60 km.
- There are 131 large CO₂ point sources in the Arches Province with combined emissions of approximately 286 million metric tons CO₂ per year. However, the 53 sources greater than 1 million metric tons CO₂ per year account for over 90% of total emissions. Based on review of these sources, on-site injection and regional storage field scenarios were identified for simulation. A study of pipeline routing was used to identify seven potential locations for regional storage fields.

The model has several inherent assumptions and limitations related to depicting the nature of deep rock formations. This is a basin-scale simulation study, and many trends in geology and input parameters were generalized. In general, any CO₂ storage project would require more detailed investigation of rock formations in the project area. Research was focused on the Arches Province, and areas outside this region were not reviewed in detail. The conceptual model was intended to provide general guidance for a large region of the Midwestern U.S. A CO₂ storage project would require field work such as seismic surveys, drilling, geophysical logging, reservoir tests, detailed reservoir modeling, and system design. The results of this report shall not be viewed or interpreted as a definitive assessment of suitability of candidate geologic CO₂ storage formations, the presence of suitable caprocks, or sufficient injectivity to allow CO₂ sequestration to be carried out in an economic manner.

Section 1.0: INTRODUCTION

The Arches Simulation project is designed to develop a simulation framework for regional geologic carbon dioxide (CO₂) storage infrastructure along the Arches Province through development of a geologic model and advanced reservoir simulations of large-scale CO₂ storage along the province. This report presents a summary of the conceptual model, which includes input information for the numerical simulations. The conceptual model describes the geologic framework, hydraulic parameters, geocellular model development, and simulation scenarios for the Arches Simulation project.

1.1 Background

The Arches Province in the Midwestern U.S. has been identified as a major area for CO₂ sequestration because of the intersection of reservoir thickness and permeability along the province. The province includes areas of Indiana, Kentucky, Michigan, and Ohio along several arch structures between the Appalachian, Illinois, and Michigan sedimentary basins. The main injection target is the Mt. Simon sandstone due to its depth, thickness, hydraulic properties, and brine salinity. There are many existing CO₂ sources in proximity to the Arches Province, and the area is adjacent to the Ohio River Valley corridor of coal-fired power plants such that it may be feasible to access the area with a pipeline network.

The Arches Simulation project is a three-year effort and part of the United States Department of Energy (U.S. DOE)/National Energy Technology Laboratory (NETL) program on innovative and advanced technologies and protocols for monitoring/verification/accounting (MVA), simulation, and risk assessment of CO₂ sequestration in geologic formations. The project is supported by U.S. DOE/NETL under agreement DE-FE0001034 and Ohio Department of Development under agreement CDO/D-10-03. The work includes seven main tasks aimed at compiling hydrogeological information on the Mt. Simon sandstone and confining layers, development of model framework, preliminary variable density flow simulations, multiple-phase model runs of regional storage infrastructure scenarios, and analyzing implications for regional storage feasibility. The research team consists of Battelle Memorial Institute, Battelle Pacific Northwest Division, Geological Surveys of Ohio, Indiana, and Kentucky, and Western Michigan University.

Initial work on the project involved compiling and interpreting information on the deep rock formations, Mt. Simon injection well operations, and geotechnical data. This information was integrated into the conceptual model. The conceptual model will feed numerical simulations of large-scale CO₂ storage in the Arches Province region. As with any modeling effort for geological environments, much of the input data is subject to change based on evolution of the understanding of the deep rock formations and advancement of the numerical simulations.

1.2 Objectives

The overall objective of this project is to develop a simulation framework for regional geologic CO₂ storage infrastructure along the Arches Province of the Midwestern U.S. The goal of this project is to build a geologic model for the Arches Province and complete advanced reservoir simulations necessary for effective implementation of large-scale CO₂ storage in the region. The project is focused on connecting a very strong set of existing field data to advanced simulation concepts and address key emerging issues in sequestration modeling. The work will represent applied simulation of CO₂ storage—the widespread application along a major, regional geologic structure in an area of the country with a dense concentration of large CO₂ sources.

The objective of the conceptual model task was integration of the various geologic and hydrologic information into a geocellular model, which comprises the basis for the numerical model. Geologic information includes general geologic setting, stratigraphy, structure of the rock formations, hydrologic features, and description of the hydrostratigraphic units. The conceptual model was also aimed at compilation of hydraulic parameters that describe the physical conditions and controls in the rock formations being considered for CO₂ storage. The ultimate objective of the conceptual model was development of a geocellular model. The geocellular model represents the parameters and conditions in a numerical array, or regularly spaced grid, that may be imported into the numerical model.

1.3 Methods

Development of the conceptual model was a combined effort involving the whole project team. Research was focused on the Mt. Simon sandstone and the Eau Claire formation, because these are the main rock formations suitable for CO₂ storage in the Arches Province. A general study area was defined that encompassed the Arches Province. Some additional information was collected in the surrounding geologic basins to delineate regional trends. Analysis of the geologic information required review of geophysical well logs, rock samples, drilling logs, geotechnical test results, and reservoir tests. Data were tabulated and integrated into geologic interpretation software. Geologic cross sections and maps were prepared to aid in description of the geologic setting. Hydrologic information was compiled from geophysical well logs, rock core tests, reservoir tests, and other sources. To expand the database on geotechnical information regarding the Mt. Simon sandstone and Eau Claire formation, additional rock core testing was completed on previously untested rock core available at the state core repositories. Once compiled, the geologic and hydraulic data were integrated into a geocellular model. Data were extrapolated into a three-dimensional (3D) grid of porosity and permeability, which are key parameters regarding fluid flow and pressure buildup due to CO₂ injection. A method was also employed to correct permeability data where reservoir tests have been performed in Mt. Simon injection wells. The geocellular model was translated into numerical array of parameters with geologic interpretation and visualization software.

1.4 Assumptions/Limitations

The conceptual model is a simplified version of reality. Consequently, the model has inherent assumptions and limitations related to depicting the nature of deep rock formations. Major assumptions and limitations to the conceptual model are listed as follows:

- Research was focused on the Arches Province. Adjacent areas in the Appalachian Basin, Illinois Basin, Michigan Basin, Ontario Province, and Wisconsin were not reviewed in detail. Readers are referred to other studies on these areas by the MRCSP (Appalachian Basin and Michigan Basin), Midwest Geological Sequestration Consortium (Illinois Basin), Ontario Ministry of Natural Resources (Ontario), Wisconsin Geological Survey (Wisconsin), and other research on these areas.
- Since this is a basin-scale simulation study, it was necessary to generalize many trends in geology and input parameters. In general, any CO₂ storage project would require more detailed investigation of rock formations in the project area.
- Data coverage should be considered when examining maps and figures. Many areas of the Arches Province have not been characterized with deep wells. Therefore, large areas of the study area have very sparse data coverage where average values were assumed.
- Geological information on the Mt. Simon has been collected over a period of many decades. Therefore, quality of the information varies. Efforts were made to retain as much useful

information as possible, but some data were screened out because of unacceptable quality or contrast with surrounding data.

- The geocellular model was prepared for input to a numerical flow model. Therefore, some adjustments were made to accommodate model requirements such as minimum thickness and smoothing over abrupt breaks in reservoir properties. In several cases, the model input represents a reduction of a large amount of data.
- Similarly, the conceptual model may not address many geologic features of the Mt. Simon sandstone and Eau Claire formation, because they are not input parameters for the numerical model. Several recent articles have addressed geological factors for Cambrian age rock formations in the Midwestern U.S. (Bowen et al., 2011; Barnes et al., 2009; Leetaru and McBride, 2009; Medina et al., 2009; Ebberts and George, 2000), and readers are referred to these articles for more information.

Implementation of a CO₂ storage project is a multi-year effort involving site screening, site assessment, characterization, testing, and system design. The conceptual model was intended to provide general guidance for a large region of the Midwestern U.S. A site-specific CO₂ storage project would require field work such as seismic surveys, drilling, geophysical logging, reservoir tests, detailed reservoir modeling, and system design. The results of this report shall not be viewed or interpreted as a definitive assessment of suitability of candidate geologic CO₂ storage formations, the presence of suitable caprocks, or sufficient injectivity to allow CO₂ sequestration to be carried out in an economic manner.

Section 2.0: GEOLOGIC FRAMEWORK

This section describes the geologic framework for the Arches Province. The geologic framework includes stratigraphic relationship of rocks, structural distribution of rock formations, hydrologic features, and delineation of hydrostratigraphic units. Characterization of these items involved analysis of several hundred well logs, inspection of rock samples, review of geotechnical test data, construction of geologic cross sections, and development of maps.

2.1 Geologic Setting

The Arches Province is an informal term to describe a geographical area in Illinois, Indiana, Kentucky, Michigan, Ohio, Ontario, and Wisconsin along several regional geologic structures: the Cincinnati Arch, Indiana-Ohio Platform, Kankakee Arch, and the Findlay Arch (Figure 2-1). Thick sequences of sedimentary rocks overlie Precambrian age crystalline basement rock in the region. The sedimentary rocks consist of layers of shale, anhydrite, siltstone, dolomite, limestone, and sandstone deposited in the Paleozoic Era approximately 250 to 570 million years ago. Cambrian System rocks are thought to have been deposited when the Laurentian continental plate separated from the Baltica plate and the Iapetus Ocean formed 505 to 570 million years ago. The rock formations have subsequently undergone periods of deformation and diagenesis that defines their current character. Below the sedimentary rock layers are very old crystalline and dense sedimentary Precambrian rocks more than 1 billion years old. Relatively thin, unconsolidated alluvial and glacial sediments are present on the surface in the region.

Rock units have been identified based on their age and character as determined in oil and gas wells drilled throughout the region. In general, these borings are more concentrated in areas where oil and gas are present. In addition, there have been more penetrations in shallower zones. Figure 2-2 lists Paleozoic stratigraphy as defined by the MRCSP research. The focus of the Arches Simulation project is the lower Cambrian age rocks, because these have the most suitable pressure/temperature conditions for CO₂ storage in supercritical fluid or liquid state. Specifically, the Mt. Simon sandstone is considered the most appealing zone for CO₂ storage in the Arches Province. The Eau Claire-Conasauga formations are considered the main containment unit above the Mt. Simon. Younger formations in the Knox supergroup overlie the Eau-Claire-Conasauga. These rock formations were not studied as part of this project, but may contain promising zones for CO₂ storage in some areas (Greb et al., 2009). Precambrian rocks are generally considered impermeable in much of the region, and comprise the lowermost unit addressed in the conceptual model.

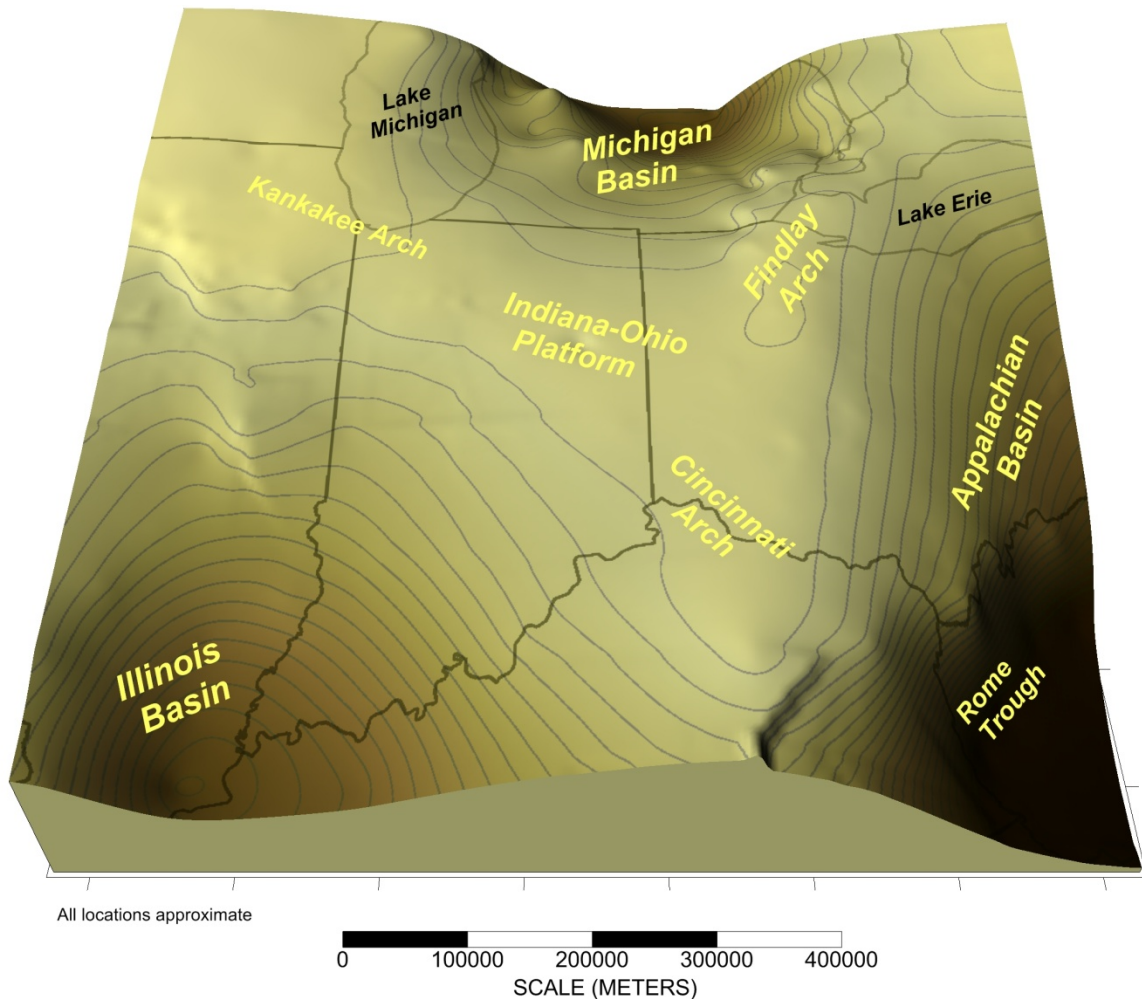
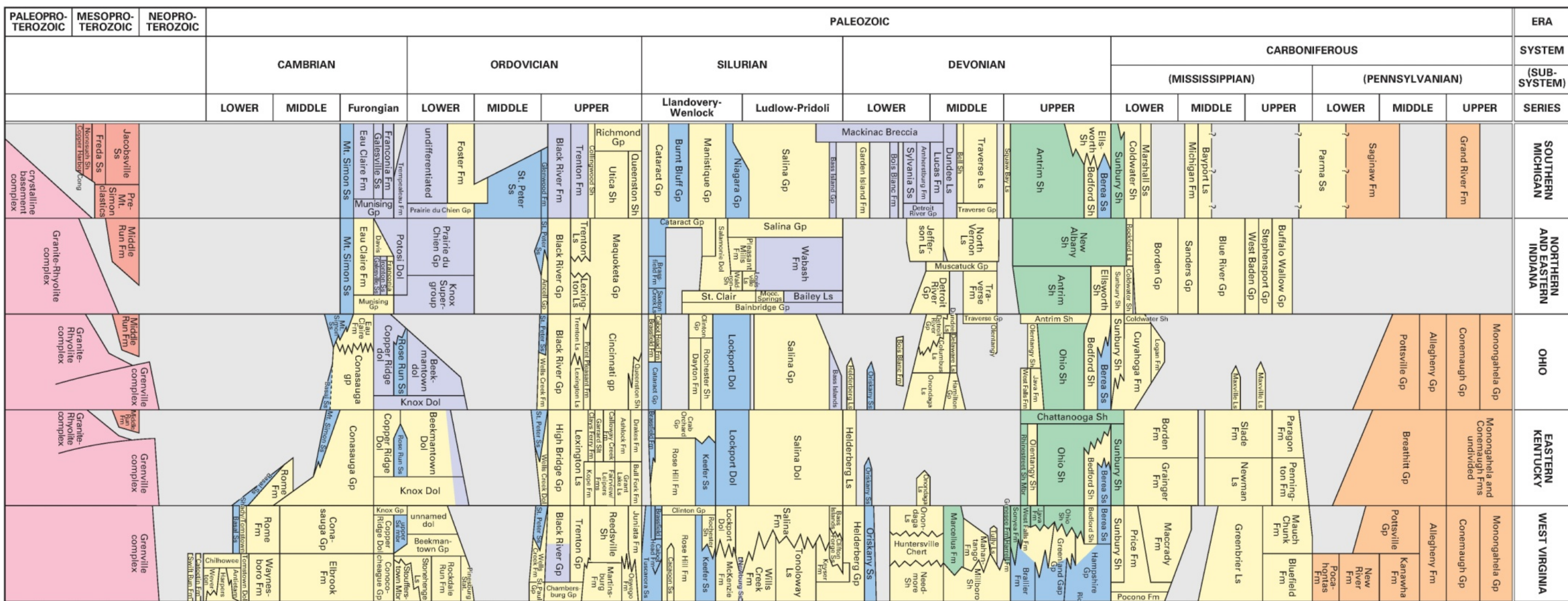


Figure 2-1. 3D Surface Image of the Mt. Simon Sandstone Illustrating Major Geologic Structures in the Region



Precambrian rocks are generally more than 1 billion years old and consist of variable distribution of crystalline metamorphic and igneous rocks along with some areas of dense sedimentary sandstones. The Grenville Front extends from south-central Kentucky, through western Ohio and into eastern Michigan. The front is a structural thrust fault feature formed in the Proterozoic era. East of the Grenville Front, rocks are metamorphic that have been intruded by igneous rocks. West of the front, Precambrian rocks are more variable, reflecting the East Continent rift basin (Drahovzal, 1992), Granite-Rhyolite province, the Penokean province, and the mid-continent rift system (Shrake et al., 1990; Santos, 2001). The Precambrian unconformity represents the surface separating Paleozoic Cambrian rocks from underlying Precambrian. This surface was subject to prolonged exposure and erosion. Local erosional valleys and knolls may exist on the surface. However, these features are difficult to identify without seismic surveys and/or many deep borings.

Above the Precambrian surface, a Cambrian basal sandstone interval is present in most of the study area. These Cambrian rocks include a distribution of clastic and carbonate rocks. Deposition of basal sandstones is considered to have occurred during the late stages of a Precambrian failed rift system and continued during subsequent sea level rise (Figure 2-3). The coarse nature of much of the Cambrian basal sandstones indicates that sediments were rapidly eroded off Precambrian highlands. Bowen et al. (2010) suggest the depositional system included braided fluvial channels with localized alluvial fans that merged into a tidally dominated nearshore environments. MRCSP research (Wickstrom et al., 2005) concluded that the basal sandstone transitions from the Mt. Simon sandstone in eastern Indiana and western Ohio to more dolomitic Conasauga sandstones in eastern Ohio and eastern Kentucky. Both studies concluded that localized zones of coarse, feldspathic sandstone may be present near basement rock highs. Analysis of basal sandstone depositional systems was not the focus of the conceptual model, because several studies have addressed these items (Leetaru, 2009; MGSC, 2005; Medina and Rupp, 2010; Ochoa, 2011; Saeed, 2002). However, results of the conceptual model generally confirm conclusions reached in recent research.

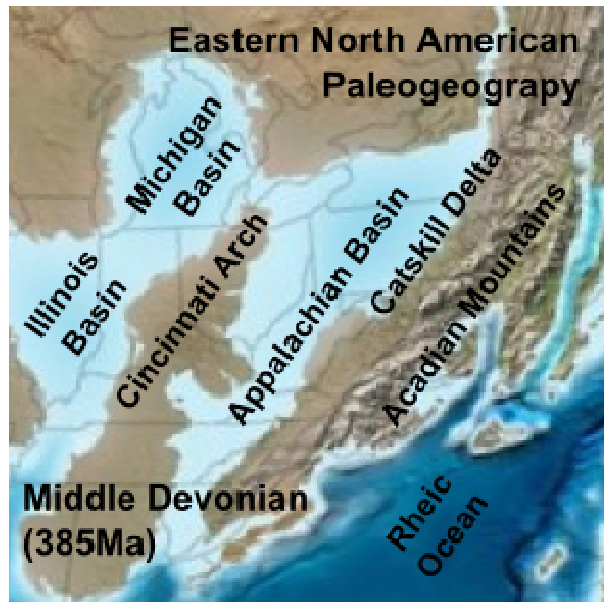


Figure 2-3. Diagram Illustrating Depositional Setting of Basins and Arches in Middle Devonian Time (from Blakey, 2008)

The Eau Claire and Conasauga formations overlie the basal sandstone throughout the study area. The Eau Claire is a variable shale, sandstone, and dolomite unit (Nuefelder, 2011). The Eau Claire transitions to Conasauga formation into the Appalachian Basin in eastern Ohio and eastern Kentucky. The formations have poorly developed porosity often filled with diagenetic feldspar, clay minerals, dolomite and/or quartz cement (Wickstrom et al., 2005). As such these formations are generally considered a confining layer. However, in some areas, the Eau Claire formation contains significant porosity such that injection wells are completed across the lower Eau Claire. The Eau Claire overlies the basal sandstone conformably. The unit is thought to have been deposited in middle to later Cambrian time as transgressive seas covered the region. Deposition is considered to have continued from Mt. Simon deposition, and the contact between the two units is not well defined in many areas.

The Knox Supergroup includes several late-Cambrian to middle-Ordovician carbonate formations. In the study area, the Knox is comprised of dense dolomite and limestone rock formations. However, there are zones with vugular or fracture porosity that have been used for deep well injection (Greb, 2010). The Knox Unconformity is a major geologic unconformity present at the top of the Knox interval in most of the study area. The Knox interval was not characterized in detail for the conceptual model because the unit will be represented as a general, upper-bounding layer in the numerical simulation. Similarly, younger rock formations that overlie the Knox were not addressed in the conceptual model, although these rocks do influence hydrologic conditions in the region.

2.2 Regional Structure

Rock formations form broad arches and basin structures in the Midwestern United States (Figure 2-1). Sedimentary strata thicken to over 5,000 m in the Appalachian Basin, Illinois Basin, and the Michigan Basin. These deep basins form major boundaries to fluid flow because fluids are limited from migrating across the deeper zones of the basins. In the northwest portion of the study area (Wisconsin and Minnesota), Paleozoic formations become shallower and outcrop at the surface or are truncated in the subsurface along the Canadian Shield (Mossier, 1992). In the northeastern portion of the study area (Ontario Province), the Findlay Arch continues into the Algonquin Arch. Paleozoic rock formations also shallow along the western St. Lawrence Platform to the erosional limit of Paleozoic rocks (Shafeen et al., 2004). Cambrian age rock formations are truncated in the subsurface in this area.

The arch structures are considered to have formed during major Paleozoic tectonic orogenies. Most structural relief along the arches is considered the result of differential subsidence with the surrounding basins rather than tectonic arching (Wickstrom et al., 1992). Thus, pervasive faulting and fracturing are not present along the arch structures, as might be found in more localized rock folds. The Rome Trough is a significant structural feature present in the southeastern portion of the study area. The trough is a northeast-trending graben bounded by normal faults. Faulting is also present in the Kentucky River Fault System and Rough Creek Fault System in Kentucky. The Wabash Valley and Cottage Grove Fault Systems are present in Southern Illinois. These major fault systems are generally located on the periphery of the Arches Province. Faults that have been identified in the Arches Province are more isolated features, which appear to be associated with basement displacement along the Precambrian rocks. Several faults have been proposed in northwestern Ohio (Bowling Green Fault System, Maumee Fault, Auglaize Fault, Anna-Champaign Fault). The Royal Center Fault, Fortville Fault, and the Mt. Carmel fault have been identified in Indiana. The Sandwich fault zone and several gentle anticlines have been proposed in northeastern Illinois. These faults appear to have limited displacement and extent such that they do not affect the flow of fluids in the subsurface formations being addressed. In general, the features were accounted for by variations in layer thickness/structure but explicit representation in the simulations was not completed.

While the features in the Arches Province are notable from a regional perspective, the structures cover tens of thousands square kilometers. On a local basis, rock layers are nearly flat with very little dip. The center of the study area is the Indiana-Ohio Platform, where rock formations are essentially flat lying. Even along the arch structures, dip is very low, on the order of 10 to 20 ft per mile. Rocks dip more steeply into the basins, where total sedimentary thickness exceeds 5,000 m.

The Cambrian basal sandstones may be correlated across a very large area of the U.S. As mentioned earlier, the arch structures are more the result of subsidence along the surrounding basins. Isopach maps of Cambrian basal sandstones better illustrate the depositional center of the rock formations. As shown in Figure 2-4, the depositional center of the Cambrian basal sandstones is located in what is currently northeastern Illinois, where the unit is over 2,000 ft thick. As shown, the thickness of the Cambrian basal sandstones thins away from this depocenter. The depositional environment across the interval varied substantially during the period of deposition. The rocks were then subjected to several hundred million years of diagenesis and alteration. The current nature of these rocks reflects these developments.

This total thickness is now superimposed on the current geologic structures. As such, the depositional center of the Cambrian basal sandstone interval does not coincide with the center of the basins. The Arches Province covers the east-central portion of the total extent of the Cambrian basal sandstone interval. In this area, the interval generally thickens from 100 ft on the edge of the Appalachian basin to over 2,000 ft in the northern portion of the Illinois basin.

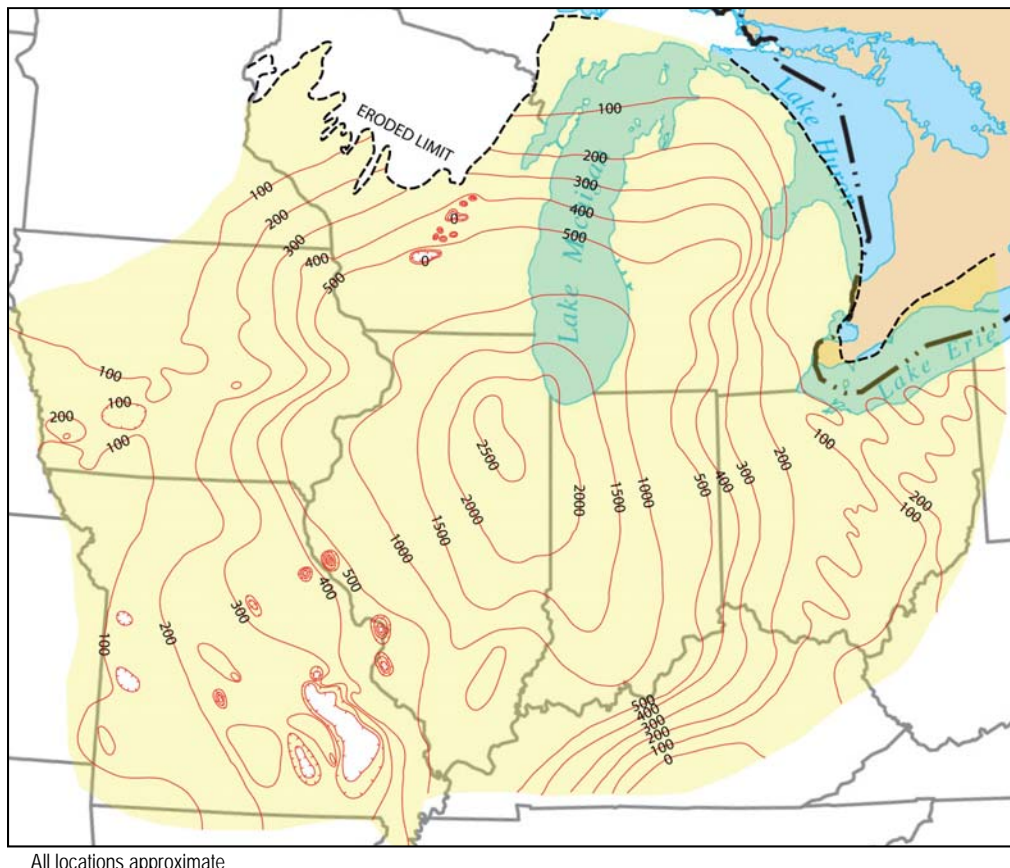


Figure 2-4. Isopach Map (ft) of Cambrian Basal Sandstones in the Midwestern United States Hydrologic Features

Fluid flow in the deep rock formations is influenced by several factors, including topography, geologic structure, fluid density, rock permeability, tectonic forces, compaction, temperature variations, surface water bodies, and freshwater infiltration. Deep rock formations are fairly isolated and saturated with dense saline fluid throughout much of the Arches Province. As described in fundamental theory (Tóth, 1963), fluid flow cycles in these deeper zones are very slow, on the order of hundreds of thousands to millions of years (Figure 2-5). In addition, deep wells may disturb hydrologic conditions with introduced drilling fluids. As such, flow directions and velocities are difficult to determine. Hydraulic gradients created by large-scale CO₂ injection would probably be much greater than any pre-existing conditions. Consequently, these pre-existing gradients were not considered a major factor in the conceptual model.

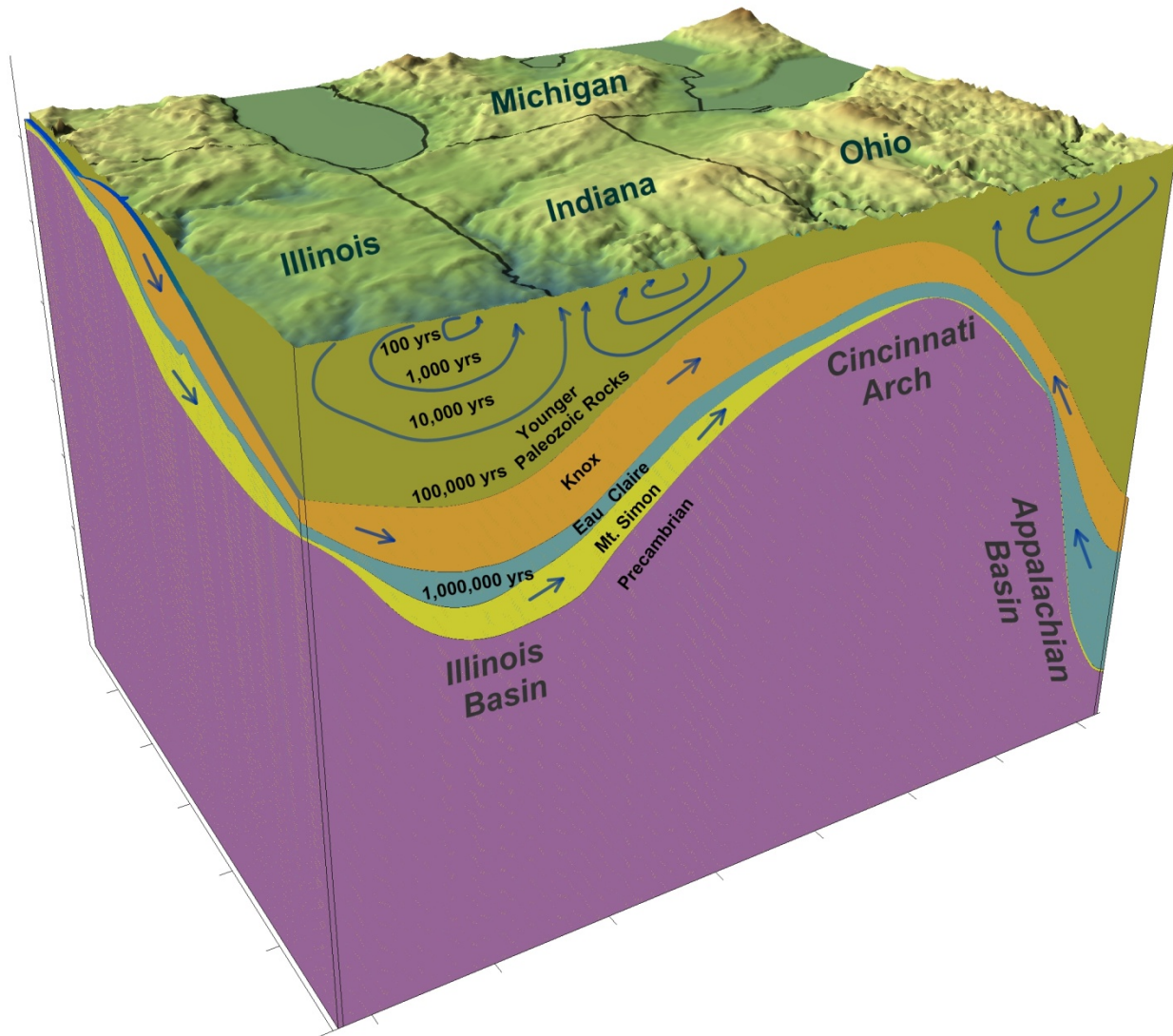


Figure 2-5. Geologic Block Diagram Illustrating Hydrologic Features and Flow Cycles in Arches Province

The basin and arch structures in the study area are major hydrologic features. Fluid density generally increases substantially into the basins, reaching levels over 1.3 kg/L at depths in some areas. Conversely, fluid density is generally lower along the arch structures. Fluid density in northern Illinois and Wisconsin

is near 1.0, and the Mt. Simon formation is considered a freshwater aquifer in these areas. Reservoir pressures reflect these density variations along with depth. Reservoir pressures are near freshwater gradients (0.433 pounds per square inch [psi]/ft) in shallow zones, while the deeper basins may have a pressure gradient of 0.48 psi/ft or greater. These pressure gradients may be a result of fluid density and/or trapped fluids in the deeper portions of the basins.

Studies on potentiometric surface maps of equivalent freshwater heads in the Mt. Simon suggested flow directions converging toward northwest Ohio (Clifford, 1973; Warner, 1988). This research matches other hypotheses that suggest fluids are migrating out of basins into arches due to tectonic forces compressing the basins. However, other research has indicated flow directions from the arches into the basins, possibly due to surface water infiltration along arch structures (Gupta, 1993). Lake Michigan is present in the northwestern portion of the study area, and Lake Erie is present in the northwestern portion of the study area. However, the lakes are relatively recent features and not directly connected to the Mt. Simon or Eau Claire.

Permeability of rock formations is a large control on flow in the study area. The Cambrian basal sandstone has a variable distribution across the Arches Province. The formation transitions from a clastic sandstone in the western portion of the study area into the carbonate Conasauga formation into the Appalachian Basin. The Conasauga formation generally has much lower permeability than the Mt. Simon sandstone. Other trends in permeability are present in the basin. In addition, vertical variations in permeability are present within the Cambrian basal sandstones. Recent research on the Mt. Simon sandstone suggests that the porosity of the formation decreases with depth into the basins (Medina et al., 2008). Similar variations are present in the Eau Claire formation, which may have dominant sandstone, carbonate, or shale lithology depending on location and depth.

Other hydrologic features in the Arches Province include faults and other structural limits. In northern Kentucky, Cambrian rock formations are abruptly faulted several hundred feet, essentially marking a limit to the extent of the Mt. Simon. In the far northeastern and northwestern portions of the study area, Cambrian rock formations are truncated by underlying Precambrian basement rocks.

2.3 Stratigraphy

The geologic model covers Knox through Precambrian rock formations, but it is focused on the Eau Claire and Mt. Simon formations (Figure 2-6). Precambrian rocks include crystalline metamorphic and igneous rocks along with some areas of dense sedimentary sandstones. Rocks include the crystalline Grenville Complex east of the Grenville Front. West of the front, basement rock reflects the East Continent rift basin, Eastern Granite-Rhyolite province, the mid-continent rift system, the Middle Run Formation, and Penokean Province. Few wells have penetrated these deeper Precambrian rocks, so they are not well understood. Some boring logs indicate weathered zones or washouts at the contact of Precambrian rocks and overlying sedimentary strata.

The Cambrian basal sandstone interval includes a complex distribution of Mt. Simon sandstone in Michigan, Indiana, western Kentucky, Illinois, and western Ohio and dolomitic sandstones of the Conasauga Group in eastern Ohio and eastern Kentucky (Figure 2-7). The unit may be correlated with the Potsdam sandstone into New York and Pennsylvania and sandstone units in the Rome Trough in West Virginia, eastern Kentucky, and Pennsylvania (Wickstrom et al., 2005). The eastern portion of the study area includes a region where the basal Conasauga sandstones have been delineated. The Mt. Simon is considered the main CO₂ storage interval in the Arches Province. The area in eastern Ohio and Kentucky was included in the model to provide coverage along the Findlay arch and to accommodate numerical boundary conditions.

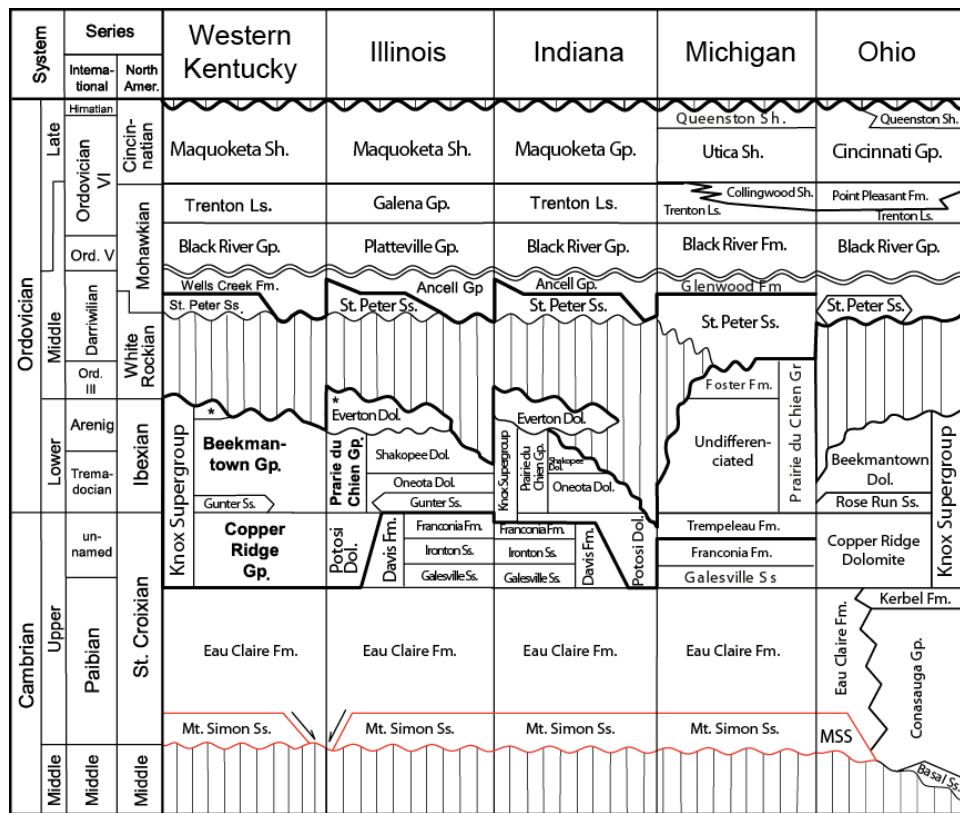


Figure 2-6. Cambrian Basal Sandstone Distribution in Midwestern U.S.

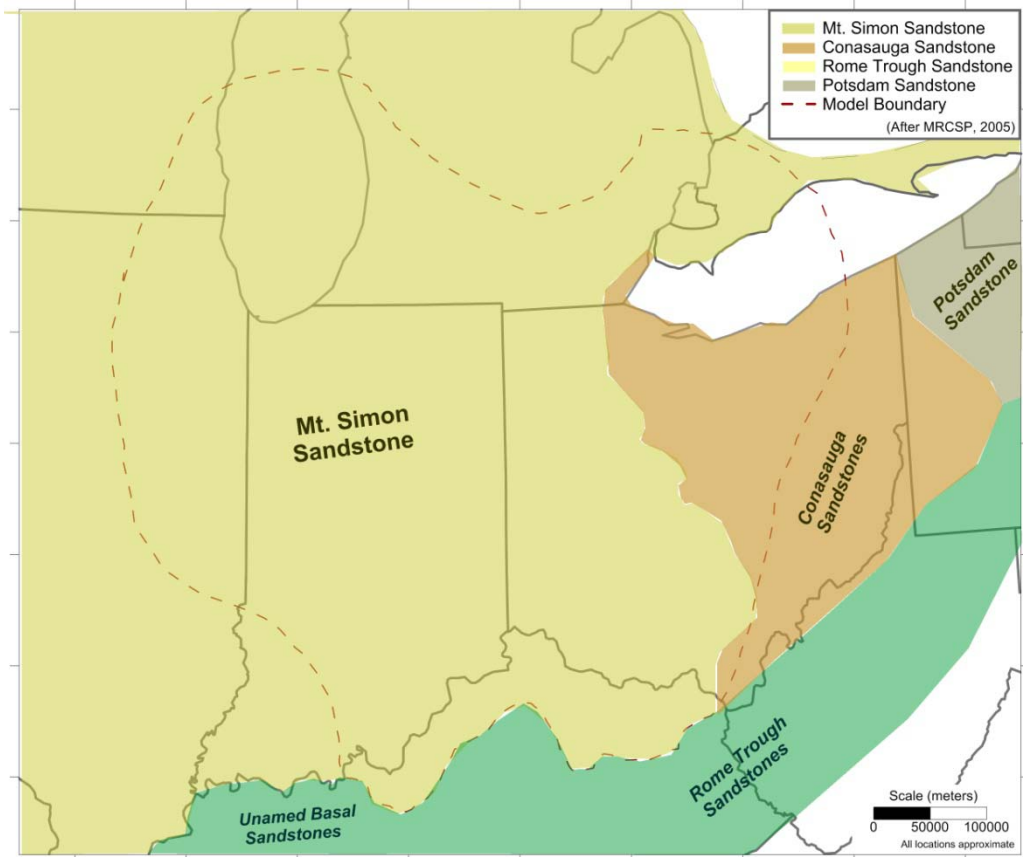


Figure 2-7. Cambrian Basal Sandstone Distribution in Midwestern U.S.

The Eau Claire conformably overlies the Cambrian basal sandstone and consists of “dark gray, red and green shales; dolomitic, feldspathic, and partly glauconitic siltstone; very fine-grained to fine-grained, well-sorted sandstone (often felspathic and lithic); silty to sandy dolostone; and oolitic limestone” (Wickstrom et al., 2005). The Eau Claire formation is classified in the lower part of the Munising group. The formation has been identified in Illinois, Indiana, lower Michigan, western Ohio, northern Kentucky, and southwestern Ontario province. The Eau Claire transitions into the Conasauga Group from central Ohio eastward into the Appalachian Basin.

The Knox interval includes a variety of carbonate units unconformably overlying the Eau Claire. The upper limit of the interval is defined by the Knox Unconformity, a major erosional unconformity between lower and upper Ordovician rocks. The interval includes the Beekmantown, Copper Ridge, Prairie Du Chien, Potosi, Davis, Franconia, Ironton, Galesville, Trempealeau, and many other regional or driller-named formations. In general, the lower Knox is characterized by dense dolomite or limestone carbonate lithology, and the upper Knox is characterized by a series of thick shale units.

2.4 Hydrostratigraphic Units

Hydrostratigraphic units were defined to aid in development of the numerical model. Hydrostratigraphic units are a major control on fluid flow. These units represent rock intervals with similar hydraulic properties. In developing the conceptual model, it was determined that there is often no clear break between hydrostratigraphic units. For example, the boundary between the Mt. Simon sandstone and the Eau Claire is more gradational in certain areas. In developing the conceptual model, interpretation of

formation contacts from well logs was indefinite at times. In addition, the Arches Province covers a large area where the character of rock formations changes substantially. For example, the Eau Claire formation is more of a sandy dolomite in areas of southwestern Michigan, whereas in areas of eastern Indiana and western Ohio it has been identified as shale dominant lithology.

Based on this conclusion, the Cambrian basal sandstone and Eau Claire formation were represented with a variable distribution of input parameters (Figure 2-8). The formations were mapped based on stratigraphic correlation and detailed geologic cross sections (Table 2-1). The hydrostratigraphic units aid in delineation of formation structure, which defines the overall framework of the model. However, a sharp contact between reservoir and confining unit was not explicitly defined in the conceptual model.

The Precambrian unit includes crystalline and meta-sedimentary basement rock, which has mostly been observed as impermeable. Thus, this unit is the lower bound of the model. The Mt. Simon sandstone is considered the main injection interval for CO₂ storage. In the conceptual model, the unit includes other Cambrian basal sandstone formations, mainly identified in eastern Ohio and Kentucky. The nature of flow between these units is not entirely clear. Since the model covers some areas into Eastern Ohio and Kentucky, the Conasauga sandstone units were binned with the Mt. Simon unit. The transition in rock character is captured by reduction of porosity and permeability in these areas. The Eau Claire includes variable shale, sandstone, and dolomite units that also grade into the Conasauga Group in the eastern portion of the study area. The Knox unit includes a group of several carbonate rock formations. Both the Knox and Precambrian were represented as simple, homogenous units in the conceptual model.

	Illinois	Indiana	Michigan	Ohio	Kentucky	Numerical Model
ORDOVICIAN	Knox Eminence Potosi Franconia Ironton Galesville	Knox Franconia Ironton Galesville	Trempealeau Franconia Ironton Galesville	Beekmantown Copper Ridge	Knox Beekmantown Copper Ridge	Knox
CAMBRIAN	Eau Claire	Eau Claire	Eau Claire	Eau Claire	Conasauga	Eau Claire
	Mt. Simon	Mt. Simon	Mt. Simon	Mt. Simon	Mt. Simon	Mt. Simon
	Precambrian Granite- Rhyolite Complex	Precambrian Granite- Rhyolite Middle Run	Precambrian Granite- Rhyolite Complex	Precambrian Middle Run Grenville	Precambrian Middle Run Grenville	Precambrian Granite- Rhyolite Middle Run

Figure 2-8. Draft Conceptual Diagram for Arches Simulations

Table 2-1. Conceptual Model Hydrostratigraphic Units

Hydrostratigraphic Unit	Description	Subunits
Knox	Group of several carbonate rock formations overlying Eau Claire	Beekmantown, Copper Ridge, Prairie Du Chien, Potosi, Davis, Franconia, Ironton, Galesville, Trempeleau, others
Eau Claire (Conasauga)	Variable shale, sandstone, and dolomite unit	Eau Claire, Conasauga Group
Mt. Simon sandstone (Cambrian Basal SS)	Mt. Simon sandstone that transitions to unnamed Conasauga sandstones in eastern Ohio and Kentucky	Upper Mt. Simon
		Middle Mt. Simon
		Lower Mt. Simon
Precambrian	Crystalline and meta-sedimentary basement rock	Grenville complex, Middle Run, Granite-Rhyolite complex, other crystalline basement

2.5 Geologic Cross Sections

In the first year of the project, a geologic database was generated, including approximately 500 well logs, Mt. Simon injection data, geotechnical parameters, core test results, and other geologic information. The logs were analyzed to determine the depth of key formations, including the Knox, Eau Claire, Mt. Simon, and Precambrian. These logs were integrated into a PETRA geological model that outlines the 3D distribution of the rock formations and geotechnical rock properties.

Based on this information, geologic cross sections through the Arches Province were constructed to better understand the distribution of the rock formations. As shown in Figure 2-9, these cross sections provide comprehensive coverage across the study area. Together, these cross sections define the structural framework of the model. The cross sections were utilized to delineate formation tops and variations in lithology. Cross sections were developed with a combination of geophysical log data, rock core examination, rock cuttings, and well logs (Figure 2-10).

The cross sections were developed by project team members for their respective states. Thus, they represent consensus interpretation of Mt. Simon and Eau Claire distribution. The work represents a continuation of efforts initiated in MRCSP Phase I (MRCSP, 2005) and Phase II research (Medina et al., 2010). Several areas evaluated as part of the initial MRCSP research were re-examined and the interpretation of Mt. Simon and Eau Claire formation tops was revised. Overall, the layer tops used in this research were selected by each respective state geological survey. Data for Illinois, Pennsylvania, and West Virginia were retained from the MRCSP database. Some supplemental information in Wisconsin and Ottawa Province was obtained from previous modeling studies (Gupta, 1993).

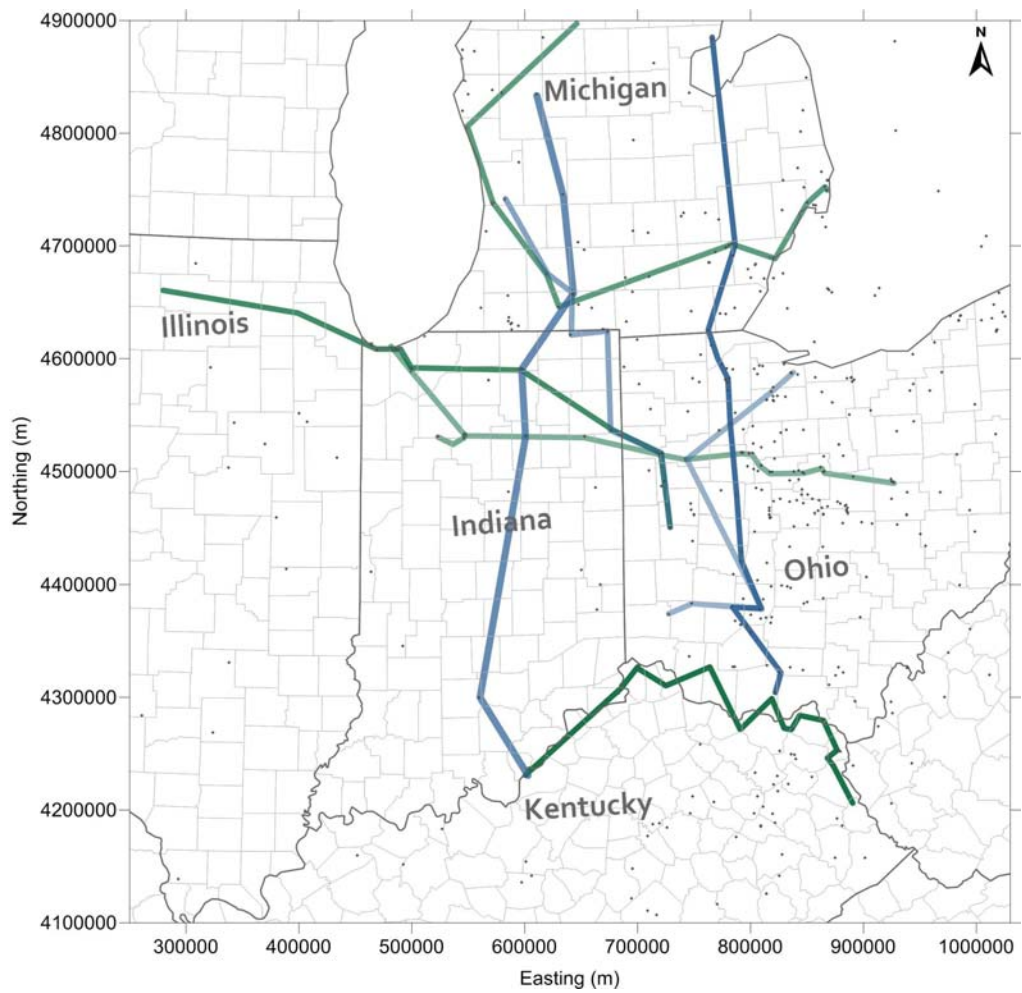


Figure 2-9. Location Map of Geological Cross Sections Prepared for Arches Province

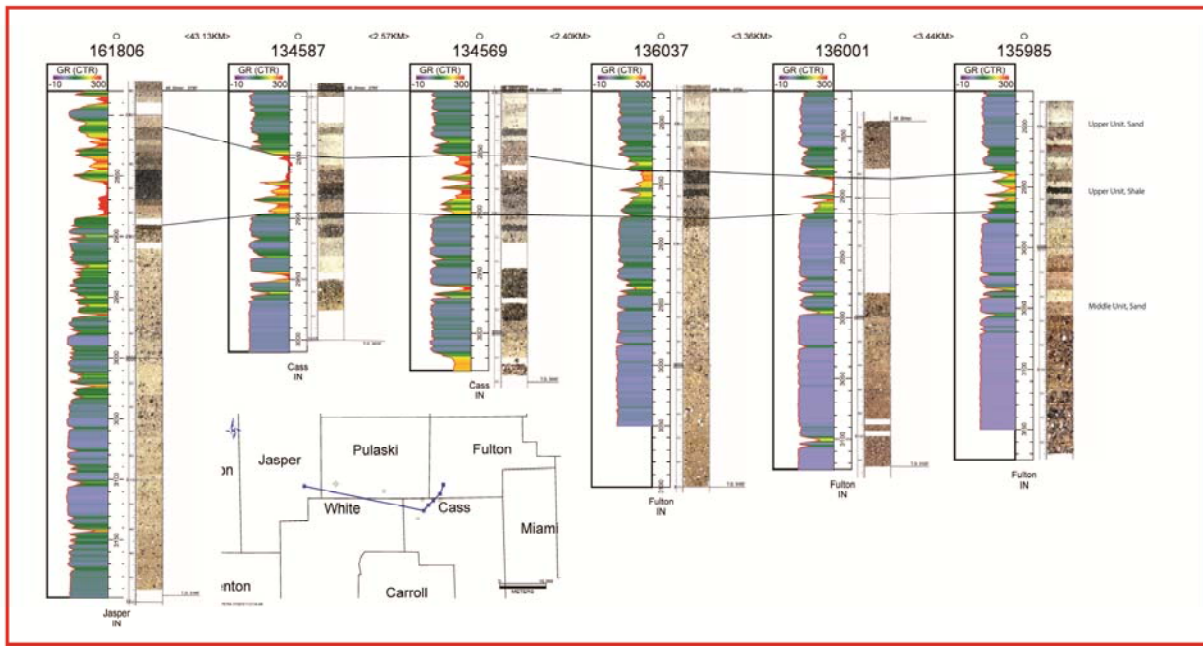
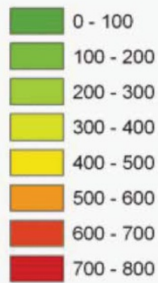
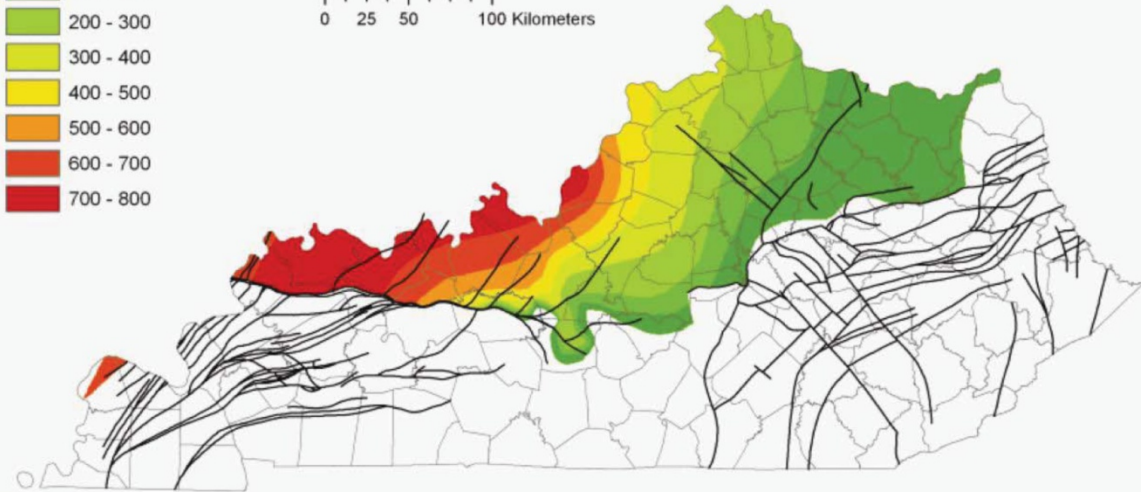


Figure 2-10. Example Geologic Cross Section in Northern Indiana

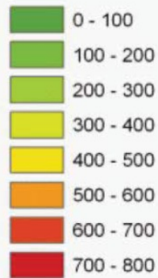
A major result of this portion of this research was revision to the southern margin of the Mt. Simon sandstone into Kentucky. This area is important for the Arches Province because many large CO₂ sources are located along the Ohio River. New seismic interpretations and well data collected from recent CO₂ injection tests were used to re-interpret the southern boundary of the Mt. Simon sandstone and examine the manner in which the sandstone thins south- and eastward. Structures associated with Cambrian rifting in the Rough Creek Graben (western Kentucky, Illinois basin) and Rome Trough (eastern Kentucky, Appalachian basin) influence the southern limit of the sandstone, causing thinning or absence on structural highs. The sandstone deepens to more than 8,000 ft west of the Owensboro Graben in Hancock County, Kentucky, where reservoir quality appears to decrease based on depth-porosity relationships in the basin. Figure 2-11 illustrates the new interpretation of the southern limit of the Mt. Simon. Based on these results, the structure maps for the Precambrian and Mt. Simon were revised in the southern portion of the model. In addition, some data from the area south of the Mt. Simon limit was removed from some data analysis because these points suggested inaccurate reservoir quality/capacity. Details on the analysis of the southern margin of the Mt. Simon are provided in Appendix A.



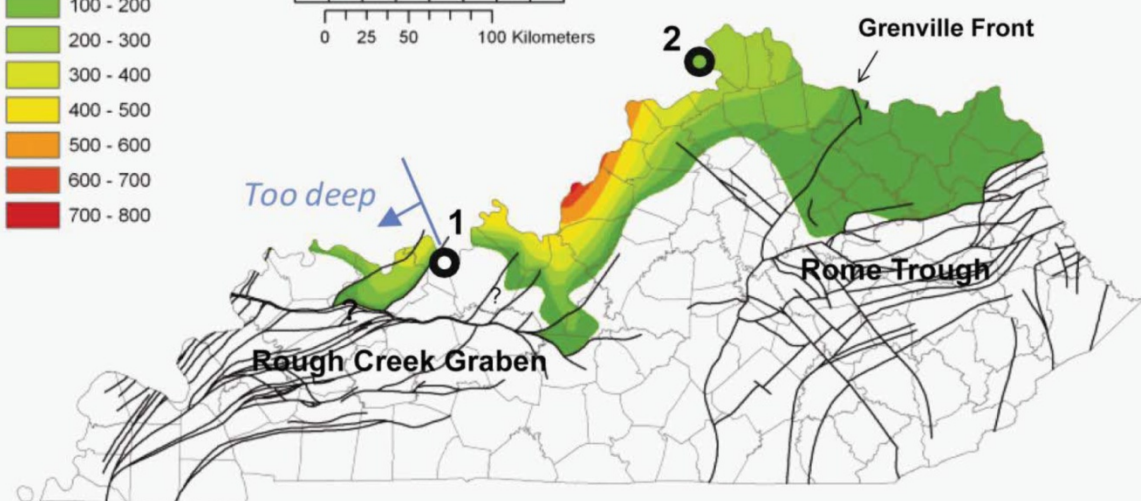
0 25 50 100 Miles
0 25 50 100 Kilometers



A. 2005



0 25 50 100 Miles
0 25 50 100 Kilometers



B. 2011

Figure 2-11. Comparison of Isopach Maps for the Mt. Simon Sandstone in Kentucky (from (A) 2005 with the (B) new map updated for this study. Label 1 is the Kentucky Geological Survey No. 1 Blan well. Label 2 is the Battelle No. 1 Duke Energy well)

2.6 Structure Maps

Based on cross sections and well log analysis results, structure maps for the Knox, Eau Claire, Mt. Simon, and Precambrian formations were completed. These maps reflect data from 496 deep wells in the general study area (Medina and Rupp, 2010). The maps build on MRCSP maps for similar intervals, but include updates in some areas where the relationship between the Mt. Simon and the Eau Claire formations were re-evaluated. The maps also match regional cross sections generated as part of the project. To ensure the geological model accuracy, a quality assurance/quality control (QA/QC) check was completed. Formation tops for all wells in the Arches Province were independently collected for each state and verified against the PETRA model.

Information concerning the stratigraphic tops for the Cambro-Ordovician units in the Arches Region was collected for existing subsurface well records. Using stratigraphic information for the Knox Supergroup, Eau Claire formation, Mt. Simon sandstone, and Precambrian basement, structure and isopach maps for each of these units were generated for the region. These maps were generated in geographic information system (GIS) software with interpolation methods that interpolate a raster surface from point, line, and polygon data. Figure 2-12 illustrates the resulting rasterized surfaces for the top (structure) and thickness (isopach) of each unit. These data were then exported as ASCII files, representing a finite-difference grid that can be used as input in numerical simulations. Maps were exported into GIS format at 4,000 m grid spacing.

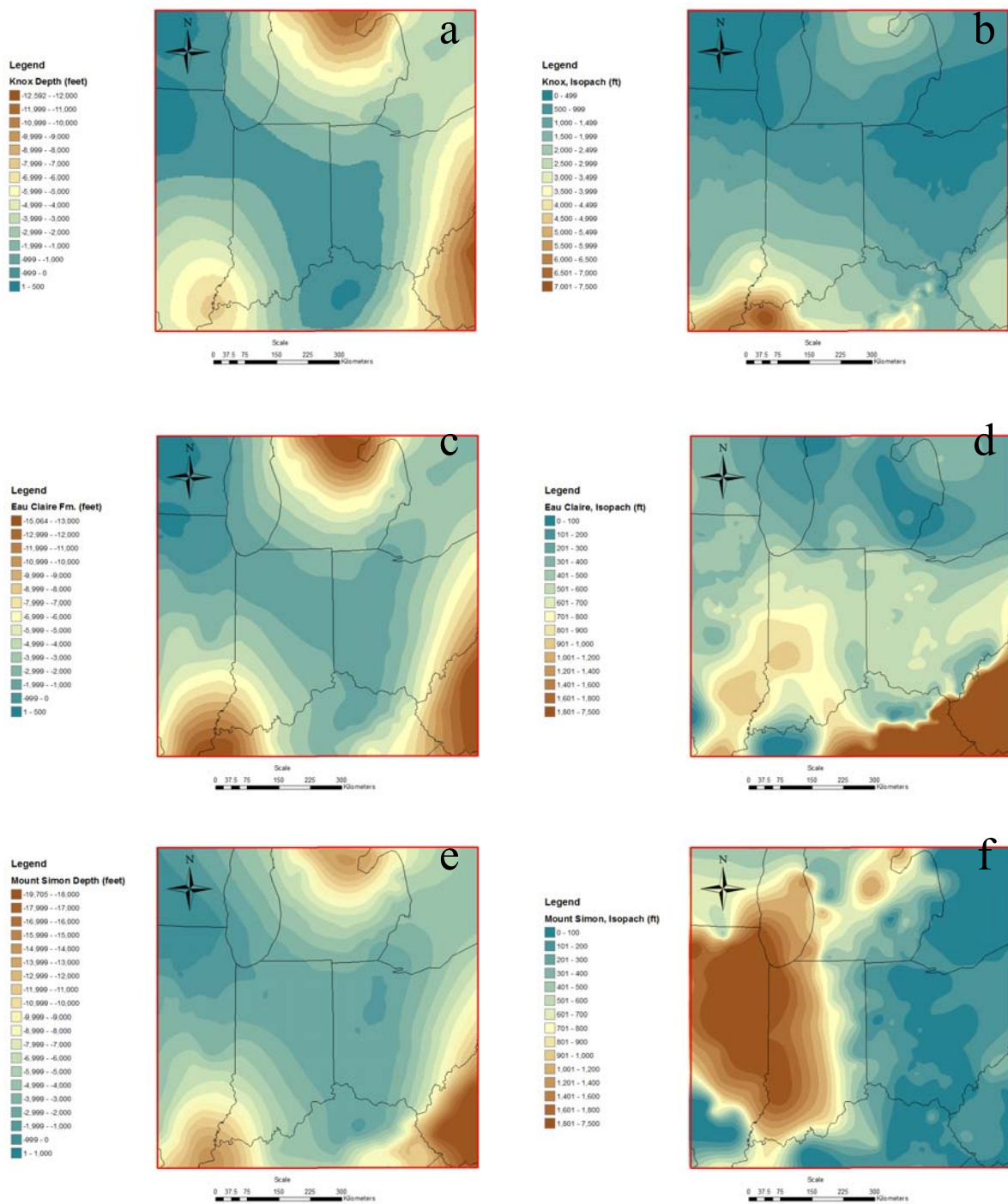


Figure 2-12. Study Area Showing Structure and Isopach Maps Respectively for the Knox (a, b), Eau Claire Formation (c, d), and Mt. Simon Sandstone (e, f)

Section 3.0: HYDRAULIC PARAMETERS

Input parameters were assembled for the numerical simulation based on geophysical well logs, rock core test results, reservoir tests, and other geotechnical methods. These parameters include the various geotechnical, hydraulic, and physical information necessary to run the simulations. The STOMP-WCS (water, CO₂, salt) code has a built-in database on thermodynamic properties of supercritical CO₂ and brine fluid. Therefore, the main input necessary for the model are related to rock properties and initial physical conditions in the Mt. Simon formation and adjacent formations. Since the model covers a 600 x 600 km area, smaller scale variability may not be fully portrayed in the numerical model. Other parameters follow relatively consistent trends across the model area, so a uniform value or gradient may be applied.

3.1 Rock Core Testing Program

This section is intended to provide the core test methods and results from the analyzed conventional cores in the Arches Province as well as provide a summary of the existing historical core data within the study area. The analyses conducted through the Arches Simulation project were performed by Weatherford Laboratories in Houston, Texas (Note: all described sample testing and data gathering methodologies in this document may be specific to the techniques used at that laboratory). The core samples were provided by various state geological surveys including Indiana, Ohio, Kentucky, and Michigan. All new analysis was performed on cores that had not already been examined and have been previously drilled and stored at the respective state geological surveys.

The Arches Simulation study has been focused, primarily, on the storage capacity and injectivity potential for the Mt. Simon formation in the Midwestern U.S. Core sample analysis and data collection, therefore, were limited to wells that had preserved cores from the Mt. Simon and Eau Claire intervals. Existing, or historical, rock core data from 76 wells were gathered from Indiana, Ohio, Kentucky, and Michigan. In addition, core samples were taken from existing sections of previously unanalyzed conventional core in the region and were subjected to routine and special core analyses. In total, core samples from eight additional wells were analyzed for comparison and integration into the historical dataset for, primarily, porosity and permeability attributes within the Mt. Simon. However, for six of the eight wells, additional special core analysis was conducted in order to provide accurate estimates of various rock properties including pore throat radius, capillary entry pressure, relative permeability, and rock strength (including compressive and tensile measurements).

Data collected from historical sources as well as those gathered through testing efforts in this project are scheduled to be used for model calibrations and direct model input parameters for flow simulations in the Mt. Simon. The data gathered from cores will serve as a “ground truth” throughout the model-building phase of the project.

3.2 Core Testing Methods/Types

Core analysis is the acquisition of data measured on core material for determining parameters used for developing and managing a reservoir from initial discovery to mature field development. There are two main reasons for core analysis. First, core analysis data are used by petrophysicists to calibrate wireline logs in the determination of reservoir properties. Such data include routine core analyses as well as special core analyses. Second, reservoir engineers use core analysis measurements such as relative permeability and pore volume compressibility to provide input parameters for reservoir simulations. Core analysis data can also be used to determine injectivity and to quantify acoustic rock properties.

Core analysis encompasses techniques used to derive formation properties from core material taken from the wellbore. The techniques generally involved measurement of plug samples of the core material. In

most cases, the sample should be maintained in or restored to a state that would be representative of the state of the material in the formation and may, for example, necessitate the application of appropriate stresses and/or temperature. In other cases, measurements are made on the matrix material itself without regard to representative state.

Routine core analysis refers to the set of measurements normally carried out on core plugs or conventional whole core. These include porosity, grain density, horizontal permeability, and a lithologic description. Routine core analyses also include a core gamma log and occasionally vertical permeability. Measurements are made at room temperature and at either atmospheric confining pressure, formation confining pressure, or both. Basic measurements are generally collected at 1-foot intervals for porosity, permeability, and mineralogy.

Special core analysis refers to any measurements that are not part of routine core analysis. Reservoir properties that can be measured include relative permeability and capillary pressure. While not performed in this study, measurements of electrical properties include formation factor, resistivity index and cation-exchange capacity. Petrographic and mineralogical studies, also not performed here, may include thin sections and X-ray diffraction.

Thin sections were created from cuttings and core samples in the Mt. Simon from the Kentucky Dupont Montague #1 well. Standard petrographic analysis of the characteristics of the samples was then conducted at 25, 50, 100, and 200X magnification.

3.2.1 Routine Analysis

Routine analysis begins with core plugs undergoing Dean Stark Extraction to clean and prepare the samples. The samples are flushed with gas phase toluene, which results in produced water. The water volume is monitored multiple times daily until the volume has not changed over a 24-hour period. Then the sample is further extracted using chloroform-methanol azeotrope to remove any residual salts. Finally, plugs are dried to a constant weight.

Grain volume is calculated using a Frank Jones helium porosimeter, which relies on Boyle's principle of gas expansion. The porosimeter is calibrated by measuring grain volume on three standards: Berea Sandstone, Lead, and Titanium. Then, the core plugs are tested wherein grain density is calculated from grain volume and dry weight data.

$$\text{Grain Density (g/cm}^3\text{)} = \text{weight of sample in air (g)}/\text{Grain Volume (cm}^3\text{)}$$

Porosity is the ratio of the void space volume to the bulk volume of a porous media. It is necessary to determine the volume of potentially available space for injection in a given reservoir. Pore volume measurements are also calculated on a Frank Jones helium porosimeter and also derived from Boyle's Law. The pore volumes of the sample plug are tested against stainless steel check plugs and Berea sandstone of known porosity at reservoir net confining stress.

Steady-state permeability is measured at net confining stress using a Frank Jones permeameter. Equivalent Klinkenberg permeability is calculated from the observed data, correcting for "air bounce" error related to laboratory methods.

The thin section analyses conducted on whole core and drill cuttings samples were conducted to determine petrologic properties of the Mt. Simon sandstone including quartz overgrowth and grain cementation. The samples were mounted on a glass slide before being cut to an approximate thickness of 0.03 mm (30 microns). The samples were then stained for specific mineral identification.

3.2.2 Special Core Analysis (SCAL)

Special core analysis, or SCAL, is a less defined set of tests wherein samples are tested for specific parameters that often go beyond the standard, or routine, capabilities of test equipment in the lab. With respect to the Arches project, SCAL tests included mercury injection capillary pressure (MICP), geomechanical analyses, and threshold pressure on samples from several select wells within the study area.

MICP tests are conducted in order to obtain measurements of the pore throat radius and capillary pressure, or entry pressure (Daniel and Kaldi 2008). Once the sample is cleaned and the total pore volume has been calculated (from routine testing), a known volume of mercury is introduced at an increasing pressure (maximum 5000 psia for the Arches tests) to the sample chamber. Material balance is then used to determine the volume of the accessed pores and, through calculation, the pore throat size distribution. Dimensionless capillary pressure (Leverett J function) for porous media that have the same pore structure but different permeability and porosity will have the same J-function. Therefore, if the different capillary pressure curves of the porous media are re-scaled as a J-function, they should plot as one curve. This curve then provides the means to average the capillary pressure data. Contrarily, if the porous media have different pore structures, then the Leverett J-functions for the different rocks will be different and will not plot as one curve.

$$\text{Pore Throat Radius (1m} \times 10^{-9}) = [2T \text{ (dynes/cm)} * \cos \Theta * C]/P_c \text{ (psia)}$$

where,

T = air-mercury interfacial tension

Θ = air-mercury contact angle

C = constant

P_c = mercury injection pressure

$$\text{Dimensionless Capillary Pressure } J(S_w, T) = P_c \text{ (psi)} * (k \text{ (md)} / \Phi \text{ (fraction)})^{1/2} * (\sigma \text{ (dynes/cm)} * \cos(\Theta))^{-1/2}$$

where,

$J(S_w, T)$ = Dimensionless Capillary Pressure

P_c = capillary pressure

Φ = porosity

k = permeability

σ = interfacial tension

Θ = contact angle

Relative permeability refers to the ratio of the effective permeability to the absolute permeability for a specific fluid in a porous system. Generally, relative permeability refers to multiphase flow conditions and is related to the viscosity of the phases. The relative permeability tests conducted for this project measured the specific permeability to both CO₂ as well as brine.

The rock mechanic tests for this project consisted of a triaxial compressive strength test and a Brazilian indirect tensile strength test. The triaxial test determines the compressive strength of the rock as well as Young's modulus and Poisson's ratio. In this test, the sample was loaded into a chamber, put under the desired hydrostatic pressure conditions, and axially stressed until the sample was fractured. The Brazilian tensile test is similar in that the sample was stressed until failure occurred; however, the tensile strength of the rock was measured (generally $\sim 1/10^{\text{th}}$ of the compressive strength).

3.3 Results from Core

The results presented here are organized into three categories: existing/historical routine analyses, new/arches project routine analyses, and new/arches SCAL analyses. Figure 3-1 shows the locations of the wells where core data were obtained. Table 3-1 gives the combined number of wells, the number of samples, average porosity, and average permeability for all analyzed data (i.e., historical/existing and new/arches). Figures 3-2 and 3-3 show maps of porosity and permeability, respectively, derived from both the historical/existing and new/Arches project datasets. Full results of the Arches core test are presented in Appendix B.

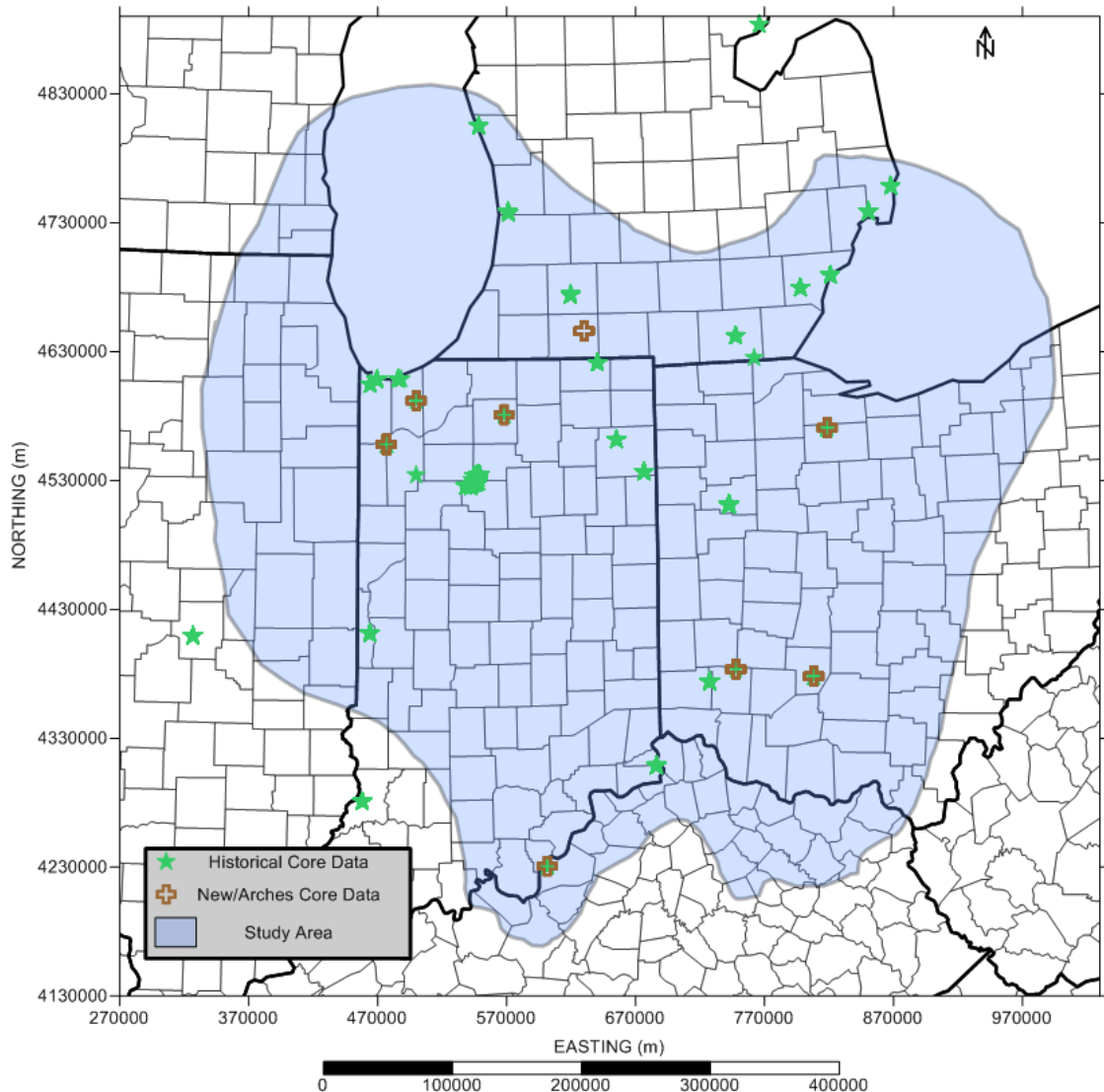


Figure 3-1. Map Showing Historical and New/Arches Core Data Well Locations

Table 3-1. Summary of Average Permeability and Porosity Measured in Core Samples from Existing and New/Arches Project Samples (by well)

Formation	Number of Wells	Number of Samples	Average Permeability to Air (mD)	Average Porosity (%)
Eau Claire	15	439	55.5	10.0
Mt. Simon	66	3,714	115.0	10.7

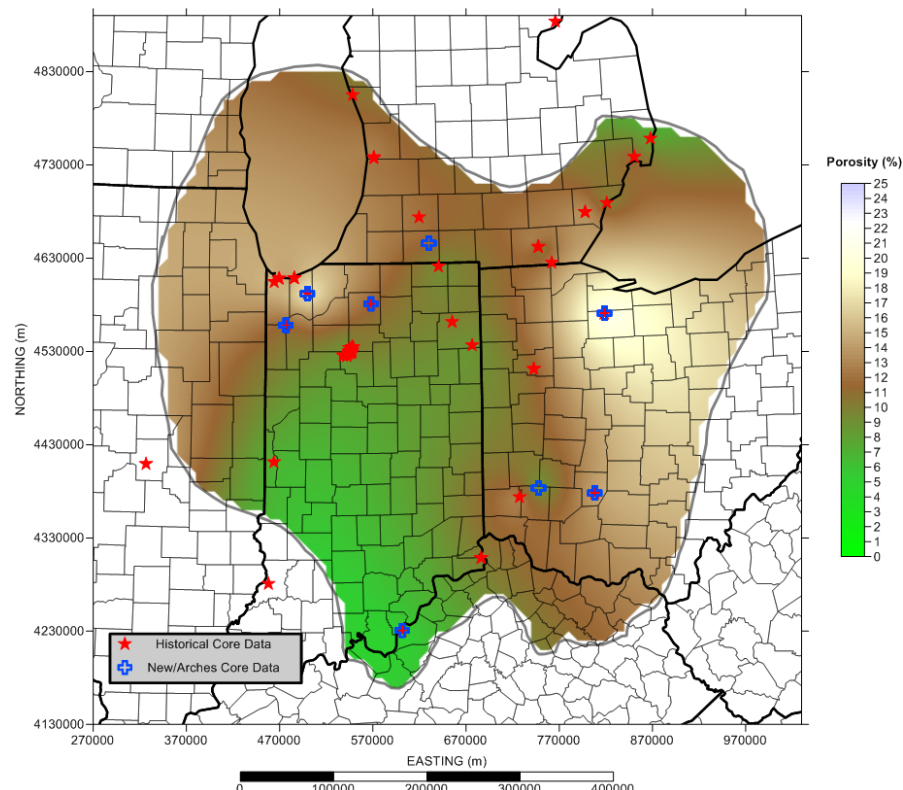


Figure 3-2. Map Showing Mt. Simon Historical and New/Arches Average Core Porosity Data

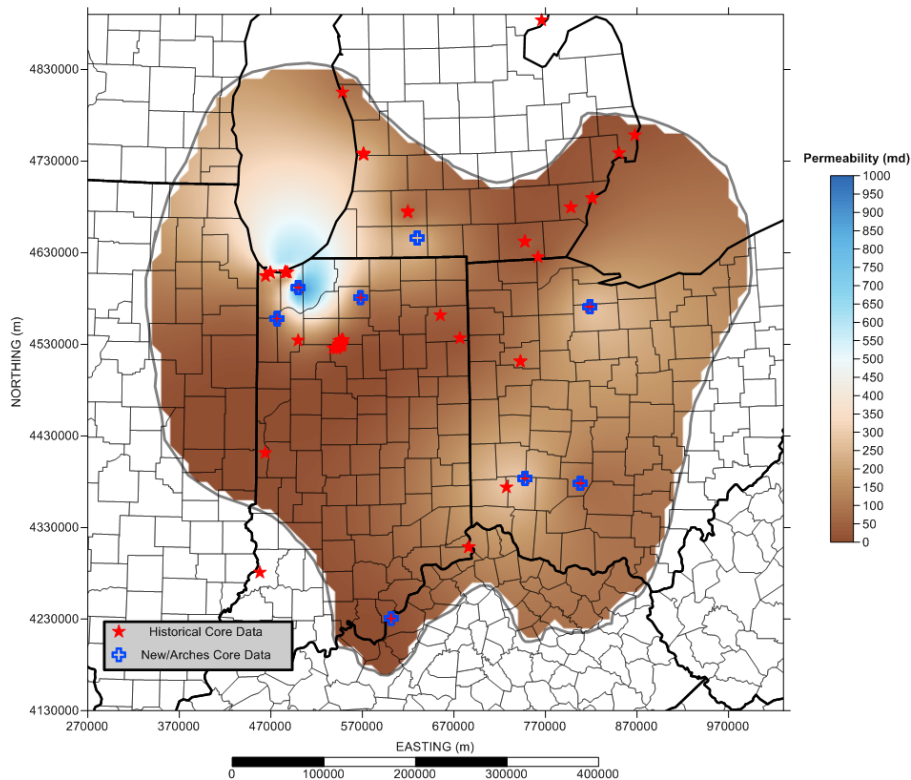


Figure 3-3. Map Showing Mt. Simon Historical and New/Arches Core Permeability Data

3.3.1 *Historical/Existing Core Data Results*

The existing core data were submitted by the various state geological surveys and represents the bulk of the routine analysis dataset for the Arches project. In all, over 4,000 rock core porosity/permeability test data were compiled from 71 wells in the Mt. Simon or the overlying Eau Claire. Table 3-2 provides the average permeability and porosity values from the existing core dataset. Figures 3-4 and 3-5 show the distribution of porosity and permeability, respectively, in the Mt. Simon, based on the historical core data, throughout the study area.

Overall, the regional trends observed in the historical core analyses agree with other lines of evidence such as wireline logs and reservoir testing data. That is, porosity increases generally follow a depth trend (structural/arch) while permeability increases toward the north and west of the study area, with minor pockets of increased permeability along the arch.

Table 3-2. Summary Average Permeability and Porosity Measured in Core Samples from Existing Samples (by well)

Formation	Number of Wells	Number of Samples	Average Permeability to Air (mD)	Average Porosity (%)
Eau Claire	12	412	31.8	8.5
Mt. Simon	59	3,636	114.7	10.6

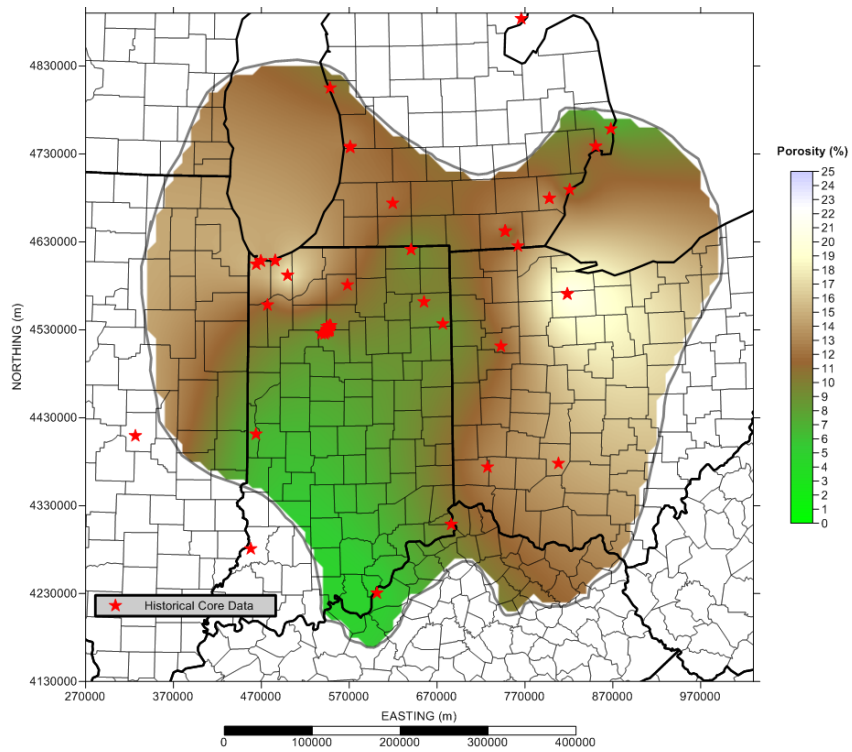


Figure 3-4. Map Showing Mt. Simon Historical Core Porosity Data

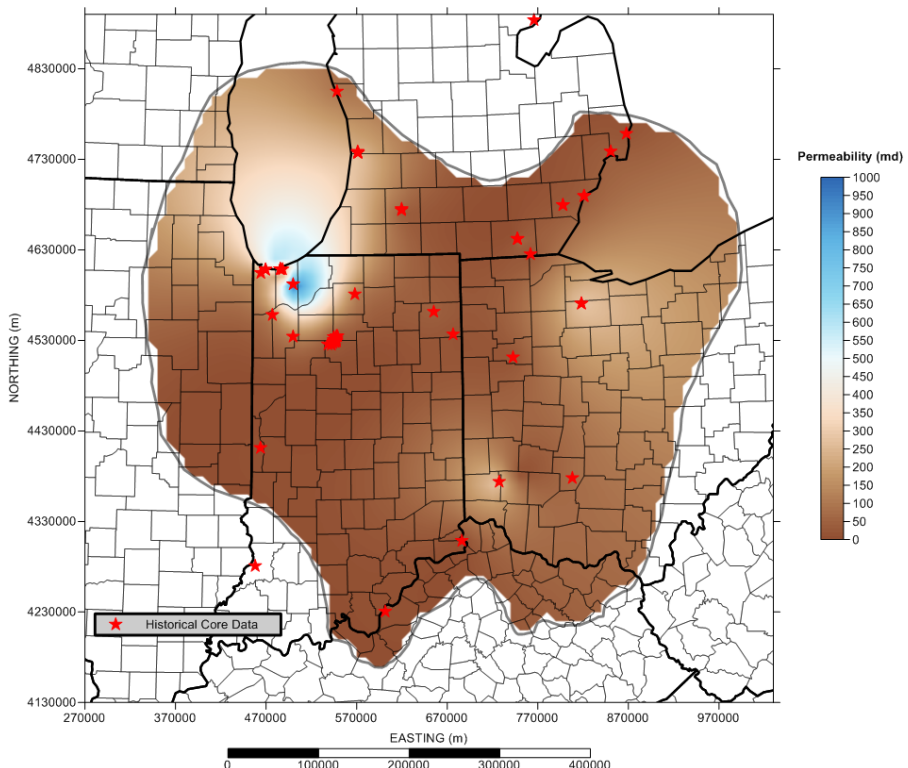


Figure 3-5. Map Showing Mt. Simon Historical Core Permeability Data

3.3.2 Routine Porosity/Permeability Core Analysis Results from Arches Study

Routine porosity/permeability core analysis was conducted as part of the Arches Simulation Project on 105 samples from eight wells in the study area. Table 3-3 gives the average permeability and porosity values from the new/Arches Project core dataset. Figures 3-6 and 3-7 show the distribution of porosity and permeability, respectively, in the Mt. Simon, based on new core data, throughout the study area.

Because of the sparseness of data in the new/Arches Project dataset, the regional trends are not as obvious as compared to more complete datasets, such as historical core. That is, during gridding, the porosity and permeability distributions tend to include a higher degree of coarseness in the interpolation and, therefore, smooth out many of the subtle trends in the data. Overall, however, the new/Arches Project core data agree well with the existing core data as well as other datasets, such as wireline logs and reservoir testing. Figure 3-8 shows the permeability-porosity crossplot for the core data gathered in the Arches Project analysis. As expected, the permeability scales exponentially with porosity, as shown by the best-fit line.

Table 3-3. Summary of Average Permeability, Average Porosity, and Average Grain Density Measured in Core Samples from New/Arches Project Samples (by well)

Formation	Number of Wells	Number of Samples	Average Permeability to Air (mD)	Average Porosity - NCS (%)	Average Grain Density (g/cc)
Eau Claire	3	27	127	14.9	2.67
Mt. Simon	7	78	280	11.9	2.63

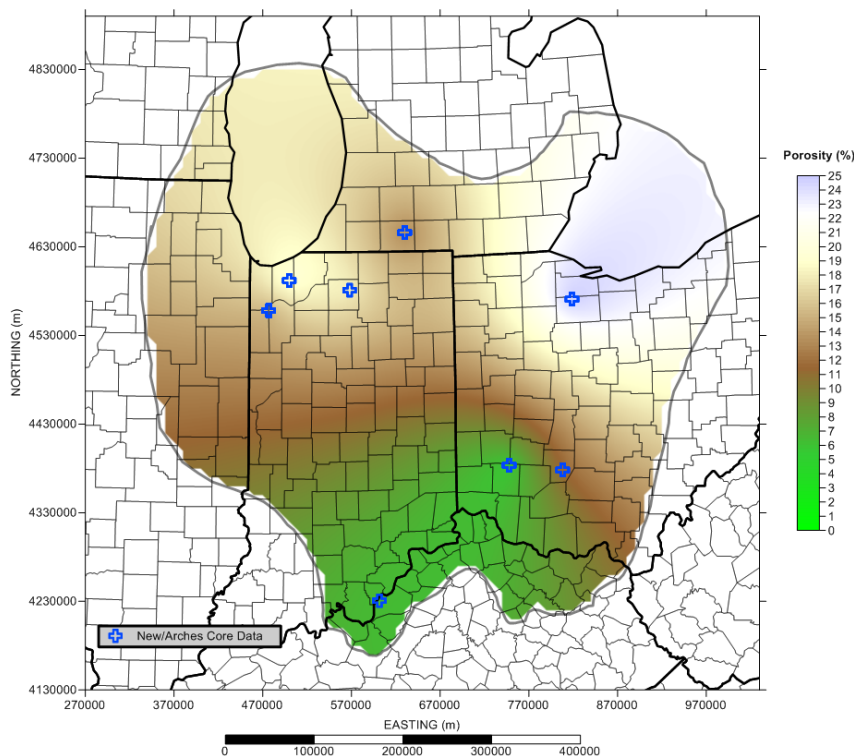


Figure 3-6. Map Showing Mt. Simon New/Arches Project Core Porosity Data

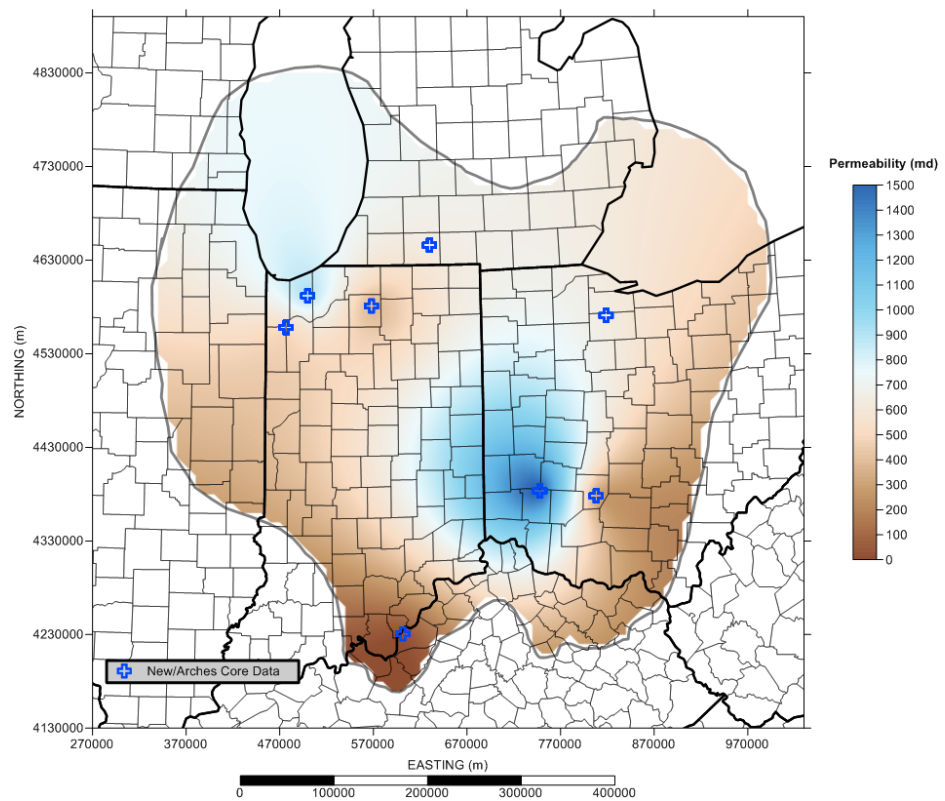


Figure 3-7. Map Showing Mt. Simon New/Arches Project Core Permeability Data

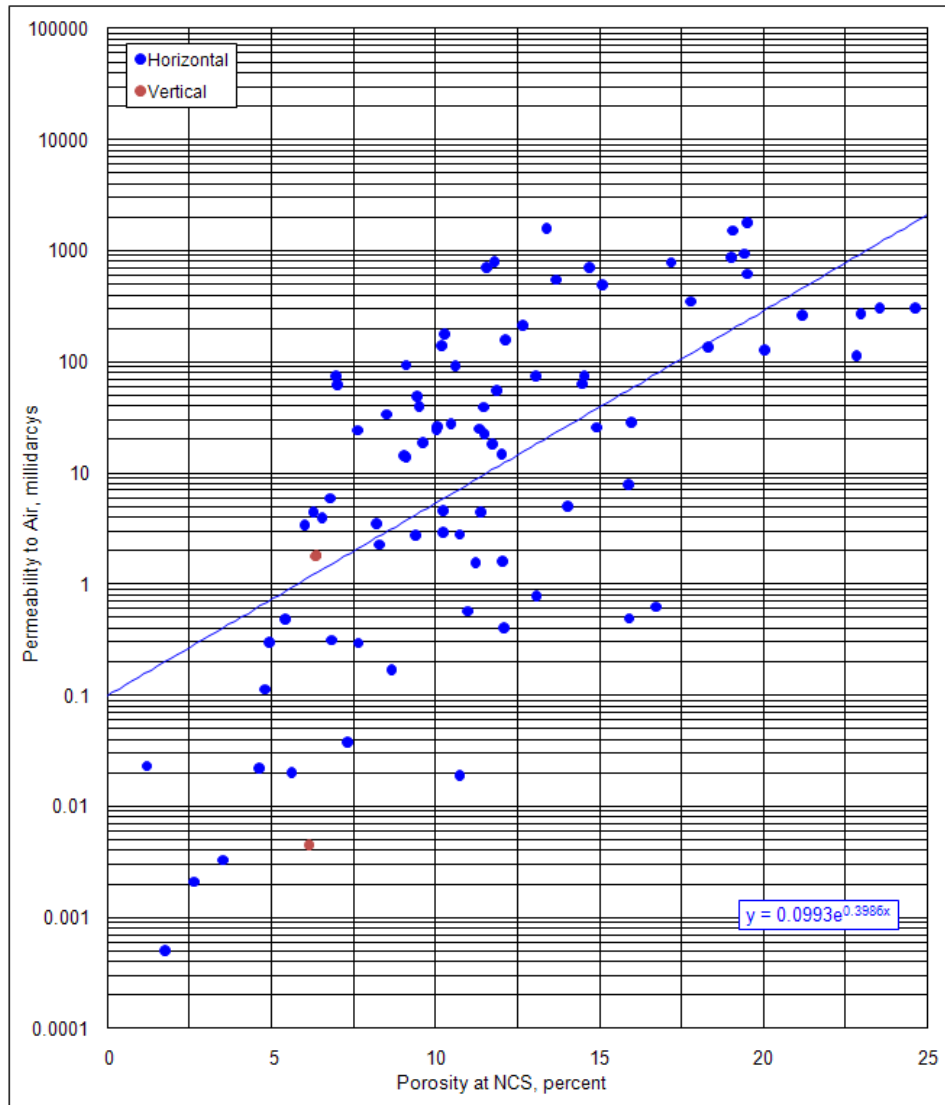


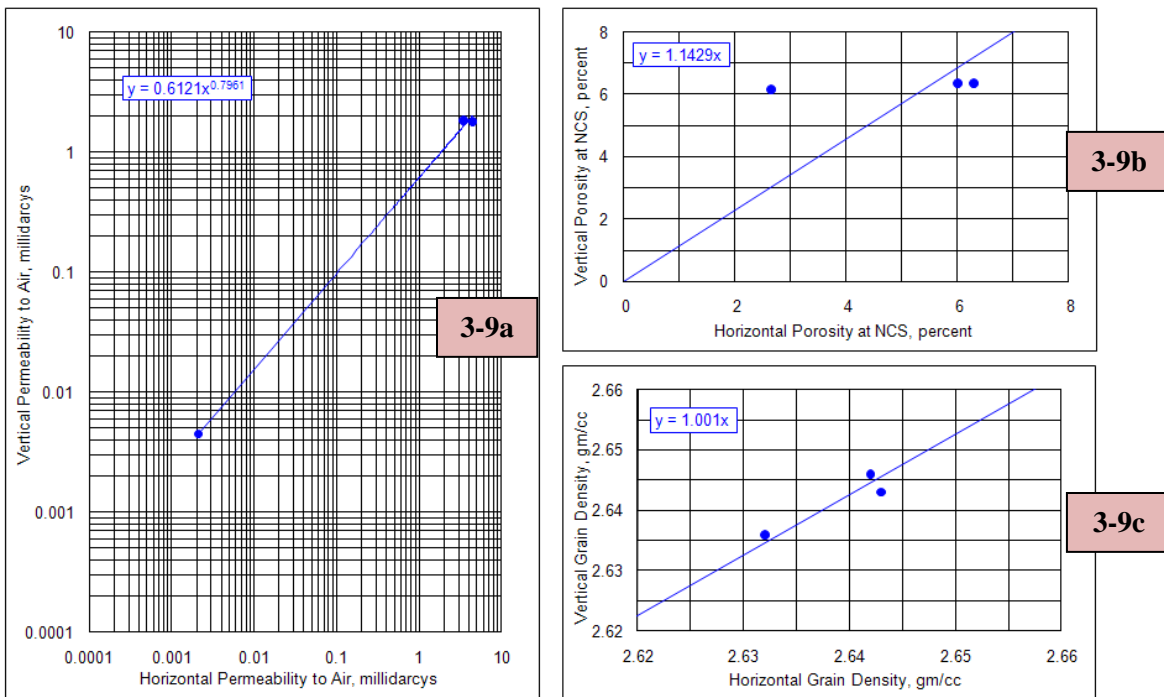
Figure 3-8. Permeability-Porosity Crossplot Showing Data from Routine New/Arches Core Analysis

Permeability and porosity measurements were also taken in the vertical direction for three samples from DuPont well KY11169, located in Louisville, Kentucky, in order to approximate the horizontal-to-vertical attribute ratio in the Mt. Simon. Table 3-4 compares the results of the measured horizontal and vertical features for the three samples. Figures 3-9 a-c show graphical representations of the horizontal-to-vertical attributes via crossplot. The data, while limited, indicate that the relationship between vertical and horizontal lithologic attributes remains near 1:1 in the x-y or z (vertical) direction for the three parameters measured in this test.

Table 3-4. Summary Comparison of Vertical and Horizontal Permeability, Porosity, and Grain Density Measured from New/Arches Core Samples in Mt. Simon

Sample Depth (ft)	Orientation	Klinkenberg Permeability (mD)	Porosity - NCS (%)	Grain Density (g/cc)
5731	Horizontal	2.7	6.0	2.64
5731	Vertical	1.5	6.4	2.65
5736	Horizontal	3.6	6.3	2.64
5736	Vertical	1.4	6.4	2.64
5740	Horizontal	0.0005	2.6	2.63
5741	Vertical	0.0012	6.2	2.64

NCS: net confining stress.



Figures 3-9 a-c. (a) Crossplot of Horizontal and Vertical Permeability to Air, (b) Crossplot of Horizontal and Vertical Porosity, (c) Crossplot of Horizontal and Vertical Grain Density

3.3.3 SCAL Results from Arches Study

The SCAL tests conducted as part of the Arches Simulation Project include MICP, geomechanical, and relative permeability. For MICP testing, core samples from 10 wells were analyzed while data from six wells were analyzed in both the geomechanical and relative permeability tests. The results from each of these analyses are discussed in detail below.

3.3.3.1 MICP Results. MICP tests conducted as part of the Arches Simulation study were conducted on 16 samples from 10 wells. The results of the analysis are listed in Table 3-5. Fourteen of the 16 samples were taken from the Mt. Simon, while the remaining two were taken from the overlying Eau Claire unit.

Figure 3-10 presents the results of the mercury injection in terms of the injection pressure and mercury saturation of the sample. The volume of mercury introduced into each sample is equivalent to the volume of porosity accessed during the test (Olson and Grigg 2008). Using the equation presented earlier in this section, pore throat radii were plotted against various mercury injection pressures (Figure 3-11) and a median value was calculated (Table 3-5). The median pore throat radius is generally best-calculated at roughly 50% saturation, using an approximate straight line observed on the semi-log plot. Figure 3-12 shows the dimensionless capillary pressure (Leverett J-function) curves created from the raw data for all 16 samples. Figures 3-13 and 3-14 show the Mt. Simon and Eau Claire J-function plots, respectively, with the accompanying best-fit curve.

The Leverett J-function plots for the two formations do not indicate similar pore structures within the respective dataset, as evidenced by the scatter in the overlying curves. It is possible that scatter in the data is from the inherent error in the laboratory measurements. Therefore, the best-fit curve approximation for J-function will be used in the modeling scenarios in the Eau Claire and Mt. Simon throughout the model domain. The approximation curves determined for the Eau Claire and Mt. Simon formations are:

$$\begin{array}{ll} \text{Eau Claire} & y = 6.2455e^{-6.638x} \\ \text{Mt. Simon} & y = 31.67e^{-8.15x} \end{array}$$

Table 3-5. Summary of Test Results from MICP

Sample Number	Well	Formation	Permeability to Air (mD)	Porosity (fraction)	Grain Density (g/cc)	Median Pore Throat Radius (μm)
1	Vistron #1	Mt. Simon	65.870	0.192	2.565	3.9269
2	Vistron #1	Mt. Simon	97.321	0.157	2.632	5.5207
3	Lloyd Cupp #1-11	Mt. Simon	0.138	0.117	2.660	0.0865
4	Kalamazoo	Mt. Simon	0.005	0.022	2.691	0.0306
5	Kalamazoo	Mt. Simon	182.695	0.108	2.640	12.4511
6	Ottawa	Mt. Simon	78.878	0.106	2.640	6.9670
7	Ottawa	Mt. Simon	145.415	0.114	2.628	10.5600
8	Montague #1	Eau claire	0.001	0.012	2.805	0.0702
9	Montague #1	Eau claire	0.254	0.087	2.631	0.3007
10	Midwest #2	Mt. Simon	55.355	0.125	2.648	1.4311
11	Midwest #2	Mt. Simon	146.711	0.116	2.626	10.3852
12	NIPSCO - Wakeland #1	Mt. Simon	4.194	0.100	2.646	1.4740
13	Duke East Bend	Mt. Simon	0.0001	0.017	2.84	0.0186
14	Duke East Bend	Mt. Simon	1.07	0.110	2.62	0.5131
15	Inland Steel	Mt. Simon	0.0005	0.025	2.68	0.0044
16	US Steel	Mt. Simon	0.00003	0.015	2.69	0.0046

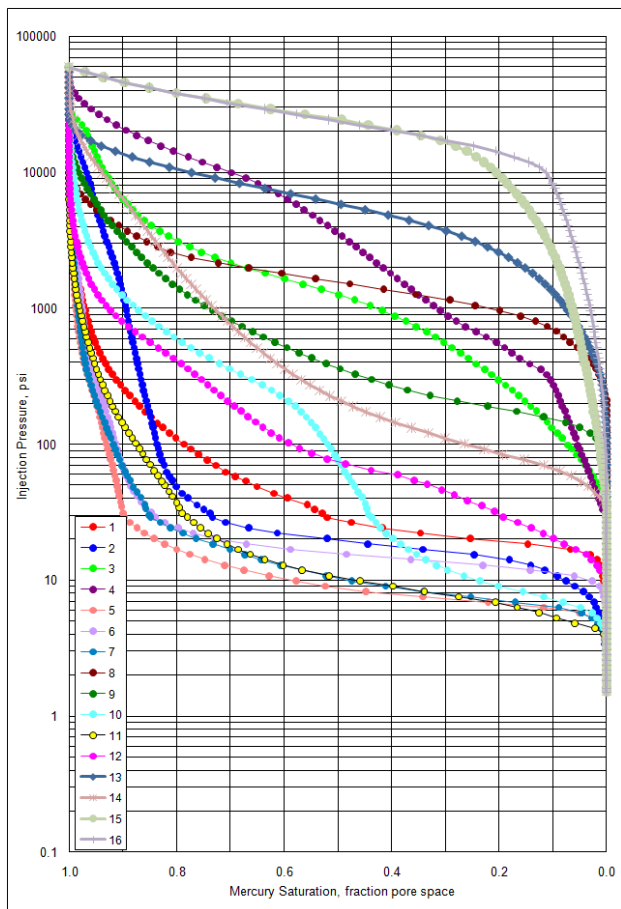


Figure 3-10. Mercury Saturation Plot for MICP Test Samples

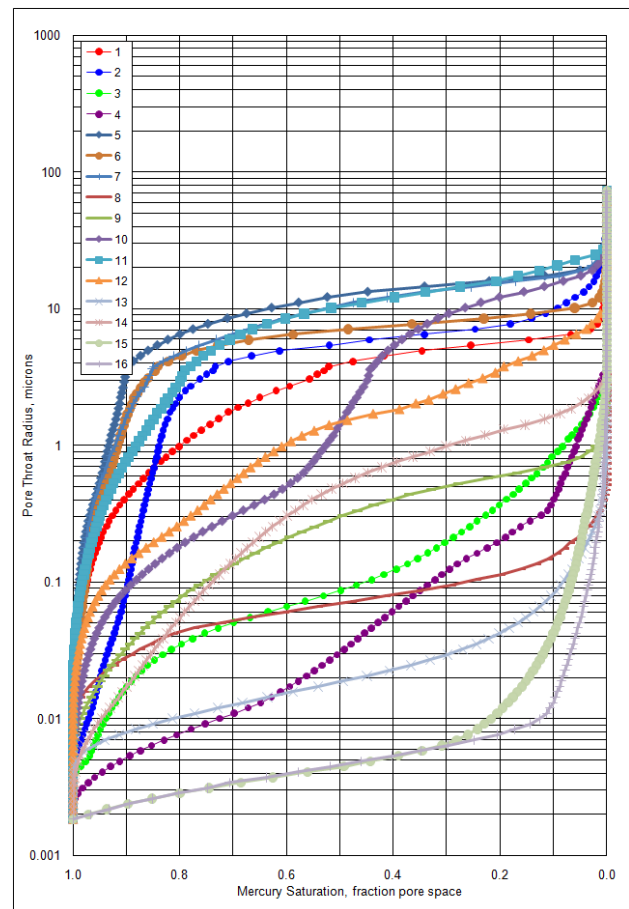


Figure 3-11. Pore Throat Radius Plot for MICP Test Samples

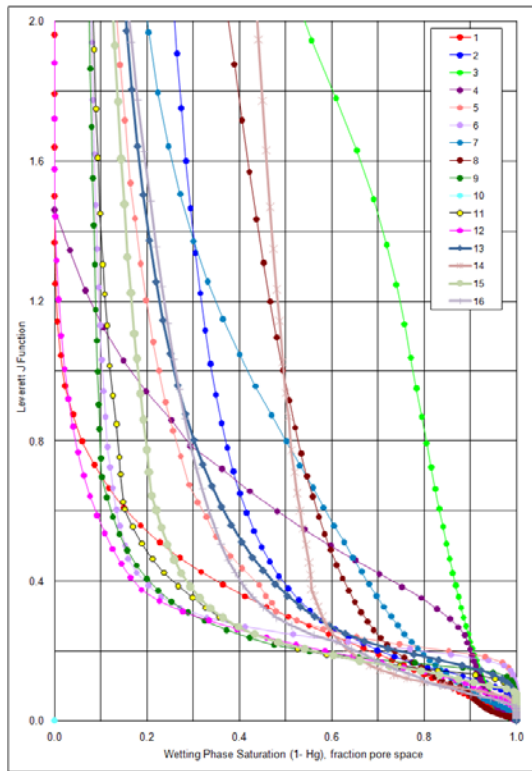


Figure 3-12. Leverett J Function Plot for MICP Test Samples

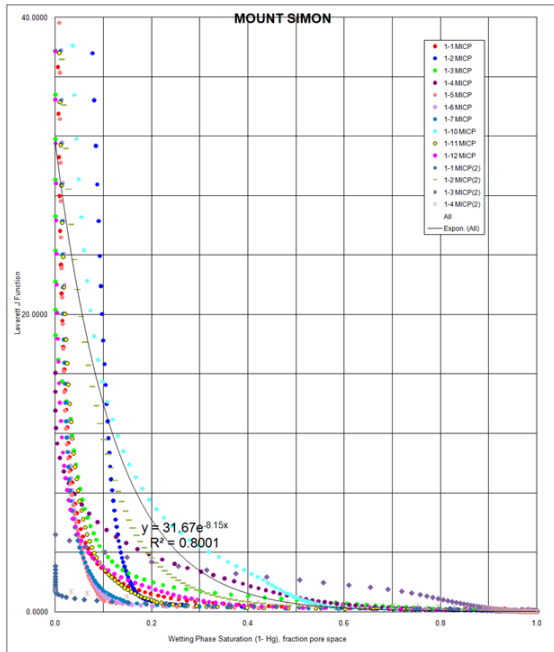


Figure 3-13. Leverett J-Function (Dimensionless Capillary Pressure) Plot of Mt. Simon MICP Data

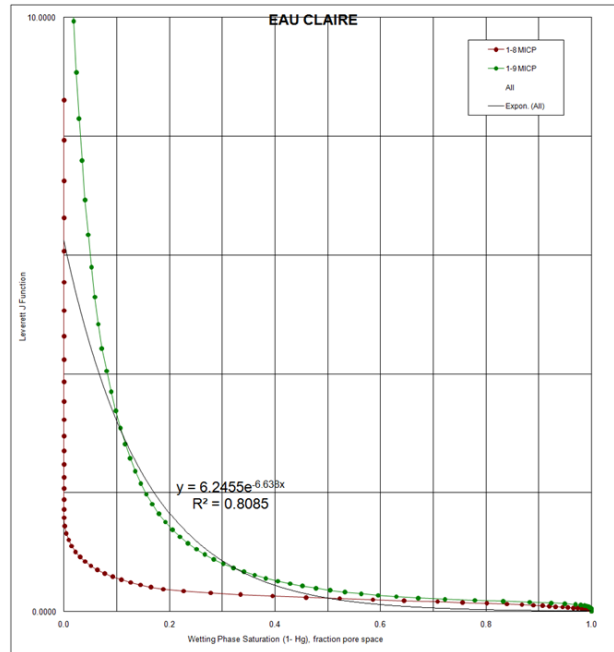


Figure 3-14. Leverett J-Function (Dimensionless Capillary Pressure) Plot of Eau Claire MICP Data

3.3.3.2 Geomechanical Results. Two geomechanical tests for the Arches Simulation project were performed on several core samples. A total of 11 samples were subjected to the triaxial compressive test, while nine samples were subjected to the Brazilian indirect tensile strength test. Figure 3-15 gives an example of the stress-strain curves generated by the triaxial compressive test for sample #1. The summary results of each test are presented in Tables 3-6 and 3-7.

The results from these tests provide key model inputs for the Arches Simulation project. The measured compressive strength of the samples is critical for understanding the upper pressure limits of the modeled formation in terms of failure mechanisms. Additionally, the rock properties measured in these tests will aid in defining the mode of deformation during the modeled injection scenarios.

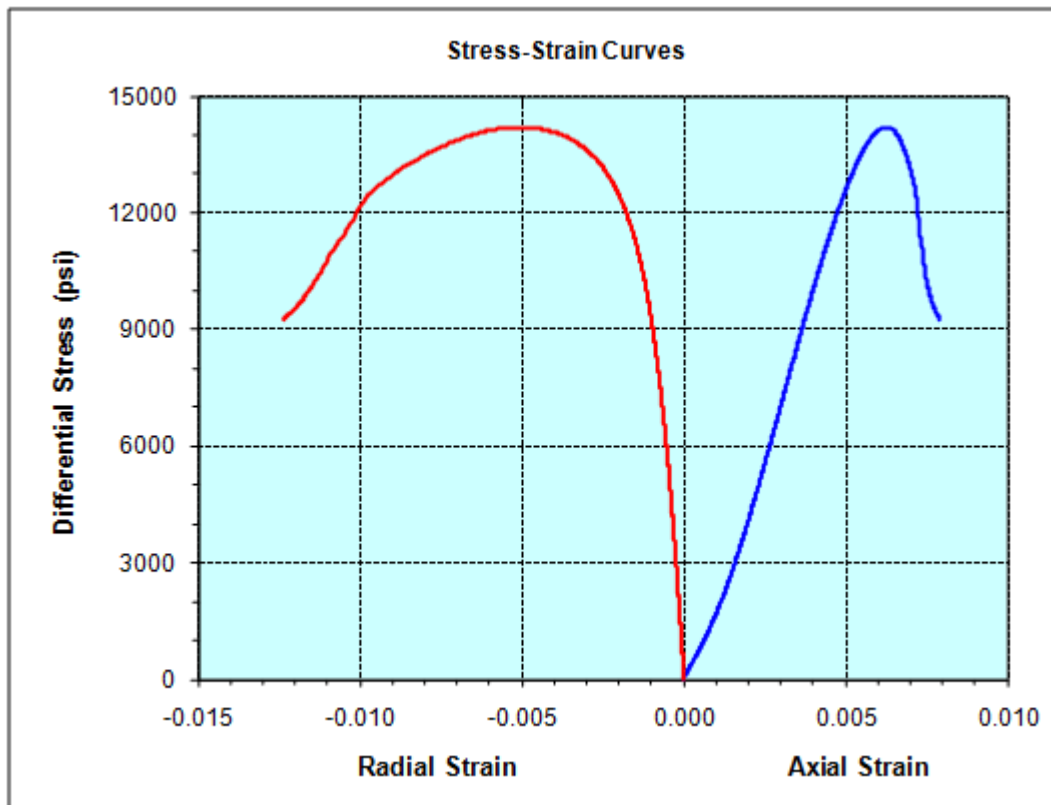


Figure 3-15. Plot of Stress-Strain Curve Results from Sample #1

Table 3-6. Summary of Triaxial Compressive Test

Sample Number	Well	Formation	Compressive Strength (psi)	Static Young's Modulus ($\times 10^6$ psi)	Static Poisson's Ration
1	Vistron #1	Mt. Simon	15202	3.027	0.362
2	Vistron #1	Mt. Simon	15729	3.338	0.32
3	Lloyd Cupp #1-11	Mt. Simon	17259	2.334	0.308
4	Kalamazoo	Mt. Simon	36729	6.451	0.288
5	Kalamazoo	Mt. Simon	31557	5.546	0.208
6	Ottawa	Mt. Simon	32376	4.957	0.347
7	Ottawa	Mt. Simon	28477	4.54	0.173
8	Montague #1	Mt. Simon	41184	7.862	0.253
9	Montague #1	Mt. Simon	30082	4.647	0.3
10	Midwest #2	Eau Claire	15161	3.634	0.282
11	Midwest #2	Eau Claire	24259	4.148	0.169

Table 3-7. Summary of Brazilian Indirect Tensile Test

Sample Number	Well	Formation	Density (g/cc)	Max. Load (lb)	Brazilian Tensile Strength (psi)
1	Vistron #1	Mt. Simon	2.05	2286	622.6
2	Lloyd Cupp #1-11	Mt. Simon	2.29	975	278.6
3	Kalamazoo	Mt. Simon	2.55	1220	391.1
4	Kalamazoo	Mt. Simon	2.38	2369	736.1
5	Ottawa	Mt. Simon	2.36	1761	507.1
6	Ottawa	Mt. Simon	2.40	2082	578.4
7	Montague #1	Mt. Simon	2.75	3087	900.3
8	Midwest #2	Eau Claire	2.31	2751	697.5
9	Midwest #2	Eau Claire	2.27	2843	743.9

3.3.3.3 Relative Permeability Results. Samples from eight wells in the Mt. Simon were selected for relative permeability testing as part of the Arches Simulation project. However, upon laboratory receipt, only six samples were suitable for liquid permeability testing. Of those remaining six samples, only two were mechanically suitable (i.e., sufficient physical condition) for CO₂ measurements. Table 3-8 gives a summary of the relative permeability tests conducted here while Figures 3-16 and 3-17 show plots of the fluid production during the relative permeability testing.

The results of the relative permeability testing performed here will require a few key assumptions prior to full model integration. For instance, true relative permeability measurements between synthetic brine and CO₂ were not made during these tests. That is, only the saturation end members, or 100% saturation with either brine or CO₂, were recorded (rather than multiple saturation points throughout the saturation curve). Further, because of significant degradation of several samples, the limited results of these tests will require a thorough review of the implications for the regional Arches Province model. A review of relative permeability in the literature may be invoked for the full model integration in order to provide more representative values.

Table 3-8. Summary of Relative Permeability Tests

Well	Formation	Permeability to Carbon Dioxide (mD)	Permeability to Brine (mD)
M & B Asphalt Co.	Eau Claire	*	231.00000
American Aggregates	Eau Claire	0.00879	0.00152
American Aggregates	Mt. Simon	*	25.40000
Kewanee Oil Co.	Eau Claire	*	26.70000
Marshall County	Mt. Simon	2.66000	2.46000
Porter County	Mt. Simon	*	261.00000
M & B Asphalt Co.	Eau Claire	*	231.00000

* Unable to create sufficient differential pressure for permeability measurement.

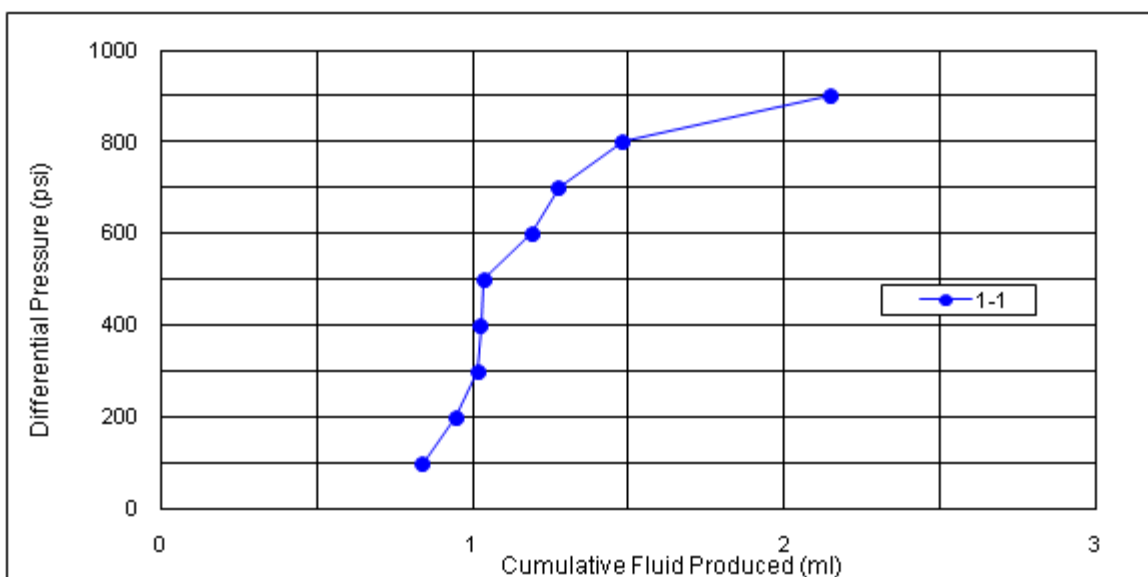


Figure 3-16. Liquid Production from Eau Claire Sample from CO₂ Relative Permeability Test in Well 3416560005, Warren County, Ohio (sample depth 3153 ft)

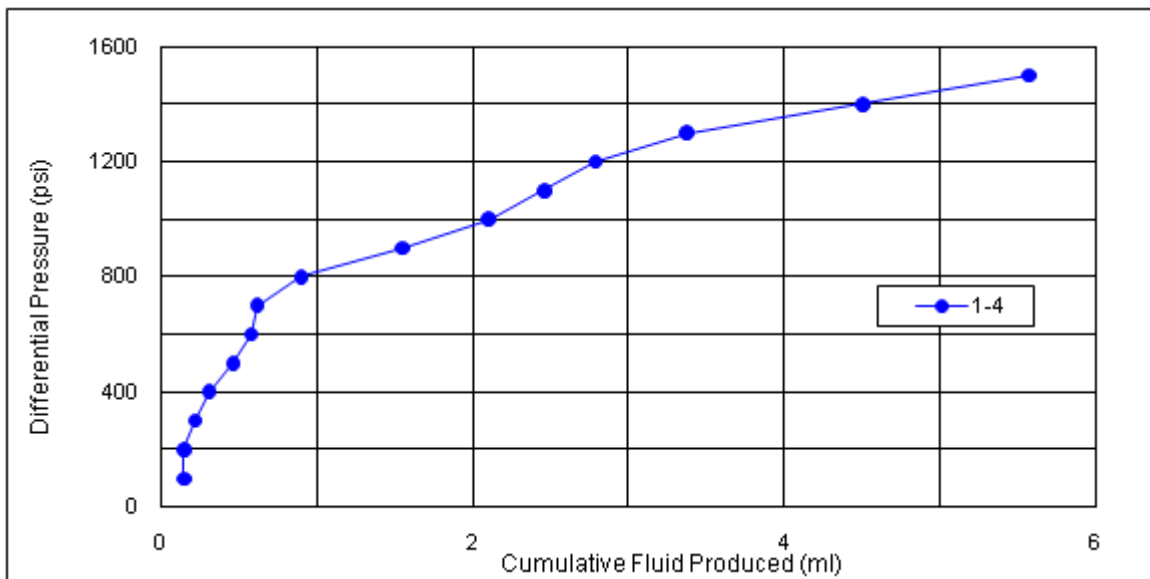


Figure 3-17. Liquid Production from Mt. Simon Sample from CO₂ Relative Permeability Test in Well IN16209, Jasper County, Indiana (sample depth 3087 ft)

3.4 Knox and Precambrian Layer Porosity and Permeability

Rock core test permeability and porosity data for the Knox and Precambrian layers were compiled from available rock core tests. In general, these formations are not tested as much as the Mt. Simon because they have not been used for deep well injection in the Arches Province. A total of 14 permeability values were compiled from the crystalline basement rock. One test suggested fairly high permeability of 14 millidarcies (mD), which may be a weathered sample at the contact with Mt. Simon. The other 13 tests had average permeability of 0.0008 mD and porosity of 1.8%, which appears suitable for dense crystalline rock. Review of 17 core test data from the Knox Supergroup indicates that the Knox is a much more variable unit. Permeability showed a large range from 0.00005 mD to 24 mD permeability and porosity of 0.10% to 24%. Because the Knox is not the focus of this study, average permeability of 4.4 mD and porosity of 2.6% will be assigned to the layer for the simulation. As described in the subsequent section, the Eau Claire and Mt. Simon formations will be represented with variable permeability and porosity distributions. As a follow on to previous rock core testing, several cores were also scheduled for more advanced mineralogy and CO₂ related hydraulic parameters (capillary entry pressure, CO₂ specific permeability, brine permeability). These test results are designed to better understand the multi-phase flow conditions in the Mt. Simon due to CO₂/brine mixtures. These advanced tests are currently being completed in the laboratory.

3.5 Reservoir Pressure

Available Mt. Simon reservoir pressure data were compiled for the study area. These data reflect drill stem tests, pressure fall-off tests, and shut-in tests performed in the Mt. Simon over the past 50+ years (Table 3-9). Tests were completed in different intervals in the Mt. Simon. Many different methods were also used to measure reservoir pressure. Therefore, there is variation in quality of these measurements. To help resolve these variations, pressure fall-off test data were reviewed from Mt. Simon injection wells. These tests are run under controlled conditions where the test interval is isolated with a packer assembly. The tests are also run until reservoir pressure stabilizes to a background level. In general, the pressure-fall-off data provided better definition to the nature of reservoir pressure.

Review of the Mt. Simon pressure data shows a clear trend with depth, as may be expected (Figure 3-18). Consequently, pressure gradients (pressure/depth) were also examined. The pressure gradients are generally 0.43 to 0.48 psi/ft in the Arches Province area and increase into the deeper geologic basins where formation fluid is denser. Given this trend, a uniform pressure gradient of 0.45 psi/ft may be suitable for the model.

Table 3-9. Mt. Simon Reservoir Pressure Data

Site	State	Well ID	Gage Depth (ft)	Pressure (psi)	Gradient (psi/ft)	Density	Source
LimaChem	OH	3400320067	2950	1303	0.44	1.10	Falloff
LimaChem	OH	3400320071	2950	1412	0.48	n/a	Falloff
LimaChem	OH	3400320084	2950	1403	0.48	n/a	Falloff
LimaChem	OH	3400363691	2950	1279	0.43	1.08	Falloff
ARMCO	OH	3401720004	2950	1275	0.43	1.12	Falloff
Mountaineer	WV	4705300423	8068	3954	0.49	1.24	Battelle (2008)
Mahomet	IL	120190015300	3942	1700	0.431	1.059	Bond (1972)
Tuscola	IL	120410105100	3995	1757	0.440	1.081	Bond (1972)
Louden	IL	120510362200	7978	3666	0.460	N/A	Bond (1972)
Crescent City	IL	120750091700	3971	1768	0.445	1.061	Bond (1972)
Herscher	IL	120910009300	3109	1045	0.336	1.013	Bond (1972)
HerscherNW	IL	120910046801	2204	976	0.443	1.004	Bond (1972)
Troy Grove	IL	120990103700	1421	600	0.422	1.00	Bond (1972)
Ancona	IL	121050026600	2178	945	0.434	1.011	Bond (1972)
Pontiac	IL	121050073900	3008	1335	0.444	1.034	Bond (1972)
Lake Blmtn	IL	121130052800	3608	1565	0.434	1.045	Bond (1972)
St. Jacob	IL	121190087601	4940	2153	0.436	1.07	Bond (1972)
Salem	IL	121210519800	8892	4050	0.455	1.17	Warner (1988)
Humble Oil	IL	121810010600	7978	3666	0.460	n/a	Warner (1988)
Cent. Ill E&G	IL	122010070500	820	279	0.433	1.00	Warner (1988)
Boyd	MI	211470015180	4496	2088	0.464	1.191	Bond (1972)
RES	OH	3400760010	5950	2733	0.459	1.21	Gupta (1991)
Calhio	OH	3408520142	5886	2760	0.469	1.22	Gupta (1991)
Empire Rvs.	OH	3413920448	4961	2050	0.413	1.21	Warner (1988)
Ohio Liq Disp	OH	3414320210	2745	1132	0.412	1.09	Warner (1988)
Ohio Liq Disp	OH	3414320226	2530	1053	0.416	1.10	Gupta (1991)
USS Chem	OH	3414520212	5514	2625	0.476	1.23	Gupta (1991)
Pensinger	IN	IN117407	6681	3033	0.454	1.13	Warner (1988)
FMC	IN	IN125110	5805	2427	0.418	1.15	Keller (1980)
Hoskins MFG	IN	IN135895	3417	1454	0.426	1.09	Warner (1988)
Royal Center	IN	IN135991	2880	1179	0.409	1.075	Bond (1972)
US Steel	IN	IN142097	3300	1420	0.430	1.07	Warner (1988)
Inland	IN	IN142098	3523	1525	0.433	1.01	Warner (1988)

Table 3-9. Mt. Simon Reservoir Pressure Data (continued)

Lake	IN	IN143816	2982	1217	0.408	1.100	Bond (1972)
Burns Har	IN	IN144456	3500	1589	0.45	1.05	Falloff
Midwest	IN	IN144461	3449	1433	0.415	1.08	Warner (1988)
Lakeside	IN	IN144500	2639	1100	0.417	1.05	Bond (1972)
Criterion Cat	IN	IN159265	2920	1283	0.44	n/a	Falloff
IN-DOT	IN	IN163282	3500	1480	0.42	1.02	Falloff
Dupont	KY	KY25578	3360	1469	0.437	1.14	Gupta (1991)
EastBend	KY	KYV0048	3351	1545	0.46	1.13	Falloff
Dupont	MI	M0002	5887	2748	0.47	1.16	Falloff
Heinz	MI	M0051	5032	2398	0.48	n/a	Falloff
Heinz	MI	M0052	4624	2381	0.51	n/a	Falloff
Heinz	MI	M0053	5013	2360	0.47	n/a	Falloff
Detroit Coke	MI	M0069	4112	2000	0.49	n/a	Falloff
Chemetron	MI	M0070	5000	2290	0.46	n/a	Falloff
BASF Chem	MI	M0071	5000	2325	0.47	n/a	Falloff
Pfizer	MI	M0129	5200	2460	0.47	n/a	Falloff
Pfizer	MI	M0130	5121	2460	0.48	n/a	Falloff
Upjohn	MI	M0137	4915	2144	0.44	1.16	Falloff
Honeywell	MI	M0155	4109	1755	0.43	n/a	Falloff
Ford	MI	M0184	4307	1838	0.43	n/a	Falloff
BASF Chem	MI	M0217	5900	2683	0.45	n/a	Falloff
Honeywell	MI	M0226	3700	1735	0.47	n/a	Falloff
Gelman	MI	M0328	5460	2550	0.47	n/a	Falloff
Bio-Lab	MI	M0357	4241	2004	0.47	1.13	Falloff
Pfizer	MI	M0373	5287	2430	0.46	n/a	Falloff
EDS	MI	M0376	4020	1866	0.46	n/a	Falloff
EDS	MI	M0462	4600	1972	0.43	n/a	Falloff
EDS	MI	M0463	4550	2012	0.44	n/a	Falloff
Mirant Z.	MI	M0509	5276	2508	0.48	n/a	Falloff
Mirant Z.	MI	M0510	5150	2490	0.48	n/a	Falloff

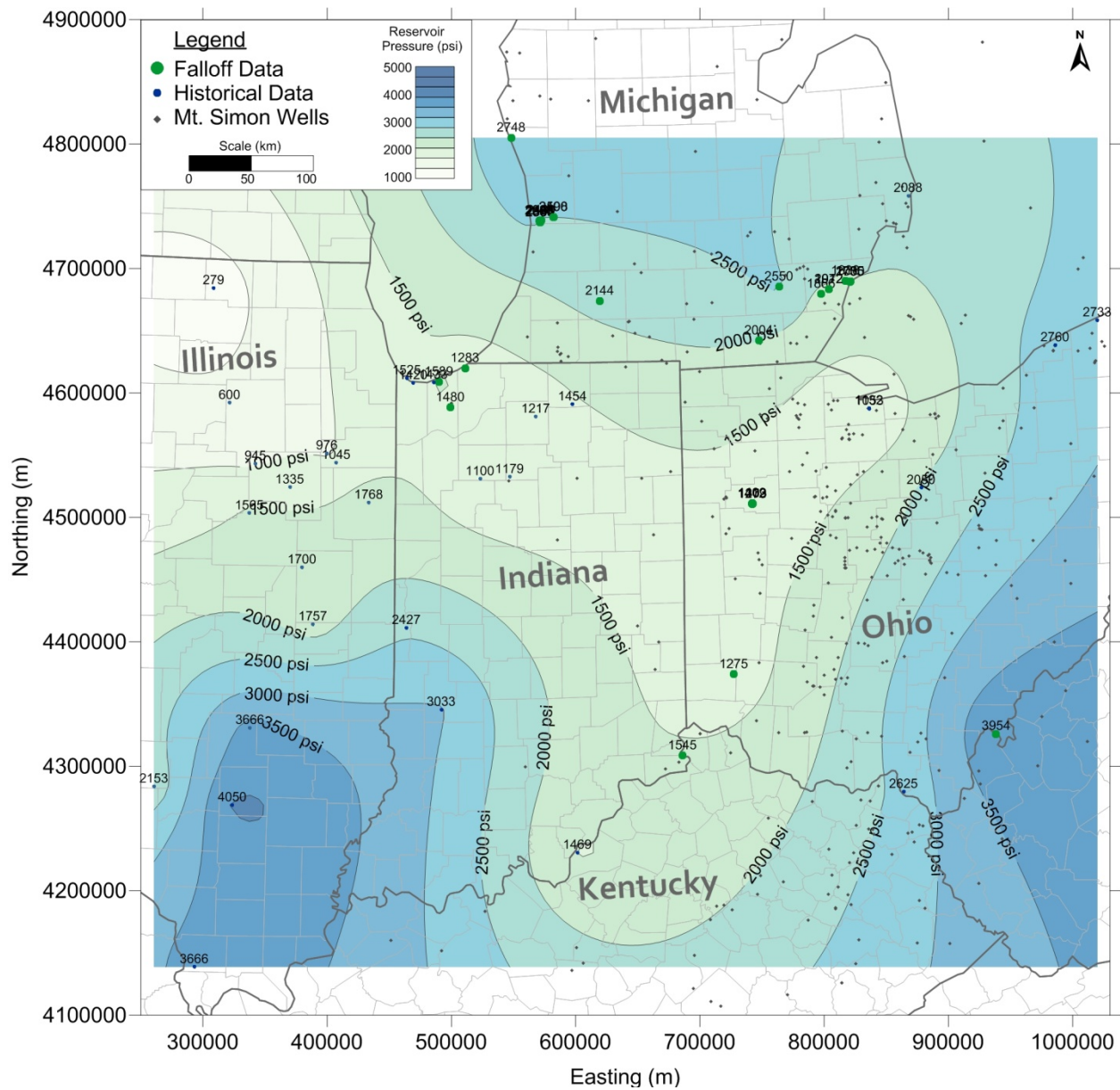


Figure 3-18. Mt. Simon Reservoir Pressure (psi)

3.6 Density/Salinity

Fluid density information was also compiled for the Mt. Simon. Fluid density shows a similar trend to pressure, with density increasing into the basins (Figure 3-19). However, there is a more substantial change in density, so variable distribution can be input into the model. Very little information is available on fluid density of the Eau Claire formation because it is typically a low permeability containment zone that does not produce fluid. Therefore, it may be necessary to estimate fluid density in the unit based on gradient observed in the underlying Mt. Simon. Density was not evaluated in the Knox or Precambrian intervals. Several other studies have examined vertical fluid movement across formations (Lampe, 2009;

Eberts and George, 2000; Gupta, 1993; Brower et al., 1989). Limited salinity data is available for the Mt. Simon and a simple relationship was used to estimate salinity based on density.

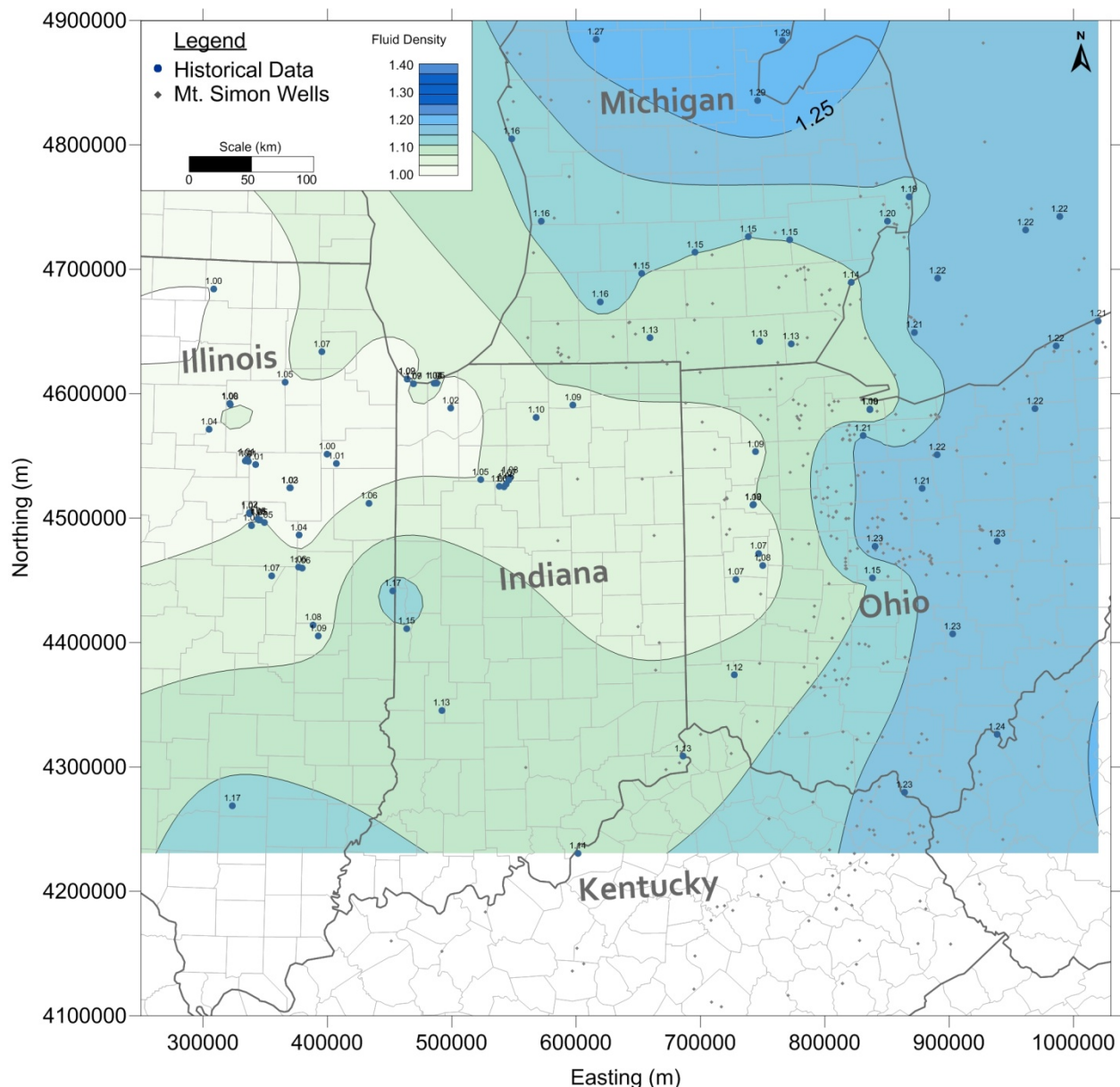


Figure 3-19. Mt. Simon Fluid Density

3.7 Reservoir Temperature

Downhole temperature data were also compiled for the study area to evaluate reservoir temperature variations in the Mt. Simon sandstone. Published historical temperature data for wells existing in the study area were collected. Within the study area, data from Indiana, Illinois, Ohio, and Kentucky were analyzed and screened for temperature gradient calculations. Data were evaluated to determine an average temperature gradient for the Arches Province for subsequent application to the regional model.

The source data included the well location, depth, ambient surface temperature, and bottomhole temperature (Table 3-10).

A uniform average surface temperature (55 deg F) was used throughout the study area as it is shown to insignificantly vary, from north to south, in Indiana (Foust et al., 2003). Wells shallower than 2,000 ft were screened out of the final dataset as they can be strongly influenced by near-surface phenomena (Vaught 1980). The remaining wells were then screened using a depth to the top of Mt. Simon cutoff equal to 6,000 ft SS (subsea).

Table 3-10. Example of Source Data

Well Lat.	Well Long.	Depth (ft)	Bottomhole Temp (deg F)	Ambient Surface Temp (deg F)	Gradient (deg/100 ft)
38.8412	-86.3092	6790	120	55	0.96

The dataset was comprised of 123 wells which included wells deeper than 2,000 feet located in the established study area. However, a high degree of data scatter existed within the dataset and therefore the 20 most extreme outliers were removed. Wells that showed the 10 lowest and highest temperature gradients were removed from the final dataset to account for possible errant data collection. Temperature gradients are displayed for each well on an isopach map of the study area (Figure 3-20). The average temperature gradient of the final dataset was calculated to be 1.02 deg F/100 ft.

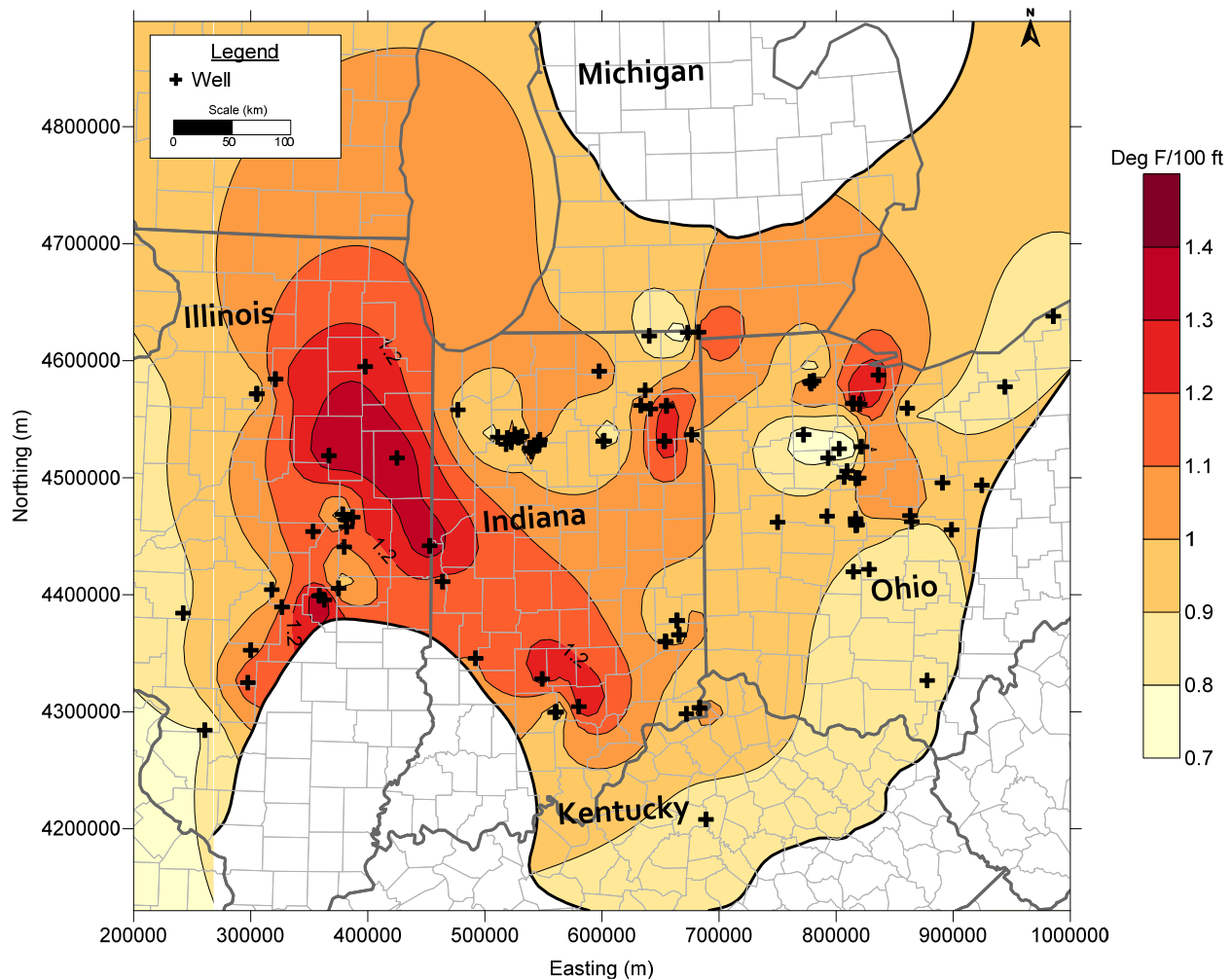


Figure 3-20. Isopach of Final Temperature Gradient Dataset

3.8 Compressibility/Geomechanical

Geomechanical parameters were also compiled from rock core test data and reservoir testing for Mt. Simon wells in the study area. In general, geomechanical tests are specialized methods, not routinely performed on rock cores. Therefore, few test data were available. Table 3-11 summarizes geomechanical data for the Eau Claire and Mt. Simon formations. A total of 37 bulk compressibility test data were compiled. These tests had bulk compressibility of 3.0E-7 to 7.0E-6 1/psi. Data were also obtained for bulk compressibility of the Knox, Eau Claire, and Precambrian layers. To supplement this information, 11 rock samples from the Mt. Simon and two Eau Claire rock samples were identified from the state core repositories and sent to a geotechnical laboratory for geomechanical testing. The samples will be tested for Poisson's ratio, Young's modulus, sonic velocity, and rock density. This testing will better define geomechanical characteristics for the Mt. Simon in the Arches Province. Overall, data suggest average compressibility of 2E-06 1/psi for the Mt. Simon sandstone, which is in the normal range for fine-medium grained sandstones. Compressibility for the Eau Claire had an average value of 6E-07 1/psi.

Table 3-11. Summary of Geomechanical Data for Eau Claire and Mt. Simon Formations

Well ID	Well Name	Depth (ft)	Porosity (%)	Bulk Compressibility (1/psi)	Formation	Source
3400363691	BP Strat	2125	0.4	3.02E-07	Knox	BP Chem., 1991
3400363691	BP Strat	2150	0.3	3.66E-07	Knox	BP Chem., 1991
3400363691	BP Strat	2169	0.6	1.28E-07	Knox	BP Chem., 1991
3400363691	BP Strat	2211	8.4	2.71E-07	Knox	BP Chem., 1991
3400363691	BP Strat	2326	5.6	2.94E-07	Knox	BP Chem., 1991
3400363691	BP Strat	2375	5.4	4.85E-07	Knox	BP Chem., 1991
3400363691	BP Strat	2490	4.8	1.42E-07	Eau Claire	BP Chem., 1991
3400363691	BP Strat	2516	0.2	1.11E-06	Eau Claire	BP Chem., 1991
3400363691	BP Strat	2552	0.2	1.41E-07	Eau Claire	BP Chem., 1991
3400363691	BP Strat	2625	4.0	5.00E-07	Eau Claire	BP Chem., 1991
3400363691	BP Strat	2634	9.8	4.48E-07	Eau Claire	BP Chem., 1991
3400363691	BP Strat	2645	10.1	6.72E-07	Eau Claire	BP Chem., 1991
3400363691	BP Strat	2676	9.8	6.15E-07	Eau Claire	BP Chem., 1991
3400363691	BP Strat	2685	8.6	4.18E-07	Eau Claire	BP Chem., 1991
3400363691	BP Strat	2789	16.6	1.18E-06	Eau Claire	BP Chem., 1991
3400363691	BP Strat	2809	7.1	6.08E-07	Eau Claire	BP Chem., 1991
3400363691	BP Strat	2838	15.8	1.14E-06	Mt. Simon	BP Chem., 1991
3400363691	BP Strat	2847	13.9	5.86E-07	Mt. Simon	BP Chem., 1991
3400363691	BP Strat	2882	8.2	7.34E-07	Mt. Simon	BP Chem., 1991
3400363691	BP Strat	2889	16.5	9.53E-07	Mt. Simon	BP Chem., 1991
3400363691	BP Strat	2901	13.7	6.15E-07	Mt. Simon	BP Chem., 1991
3400363691	BP Strat	2950	16.1	3.92E-07	Mt. Simon	BP Chem., 1991
3400363691	BP Strat	2971	15.0	5.65E-07	Mt. Simon	BP Chem., 1991
3400363691	BP Strat	2997	8.7	1.13E-06	Mt. Simon	BP Chem., 1991
3400363691	BP Strat	3048	5.5	4.99E-07	Mt. Simon	BP Chem.
3400363691	BP Strat	3071	10.2	1.75E-06	Mt. Simon	BP Chem., 1991

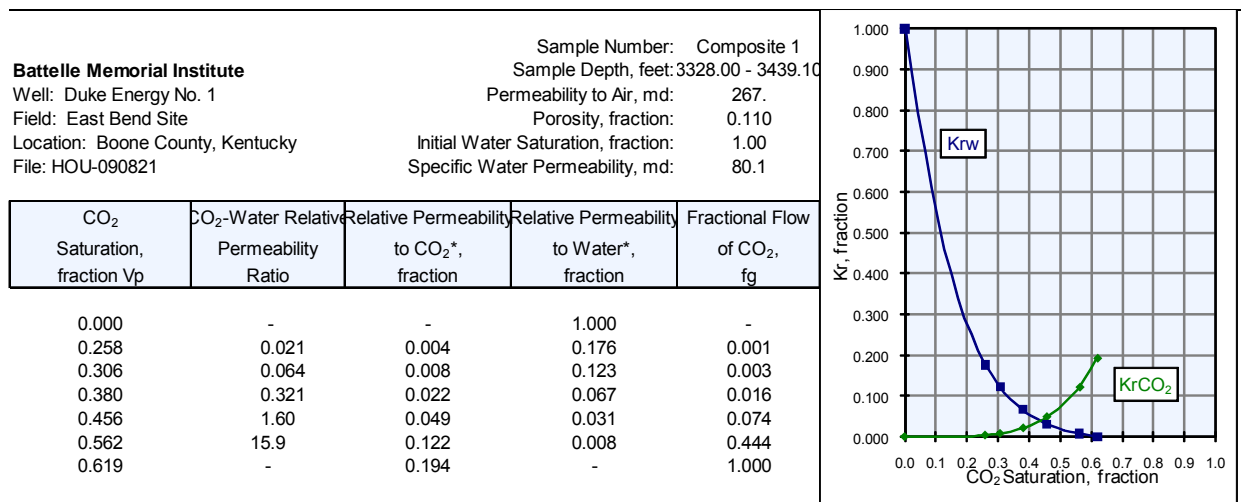
Table 3-11. Summary of Geomechanical Data for Eau Claire and Mt. Simon Formations (continued)

Well ID	Well Name	Depth (ft)	Porosity (%)	Bulk Compressibility (1/psi)	Formation	Source
3400363691	BP Strat	3105.9	14.1	1.24E-06	Mt. Simon	BP Chem., 1991
3400363691	BP Strat	3130.2	13.5	2.91E-06	Mt. Simon	BP Chem., 1991
3400363691	BP Strat	3144.8	5.5	2.22E-06	Mt. Simon	BP Chem., 1991
3400363691	BP Strat	3146.0	0.12	7.96E-07	Mt. Simon	BP Chem., 1991
3400363691	BP Strat	3158.3	na	7.79E-07	Middle Run?	BP Chem., 1991
3400363691	BP Strat	3211.2	0.03	7.91E-07	Middle Run?	BP Chem., 1991
144458	Beth.Steel	2730.0	na	7.00E-06	Mt. Simon	Beth.St.BrnsHrb, 1990
21139000517	Heinz#2	5020.0	12	4.50E-06	Mt. Simon	UIC reports
21077001377	UpJohn#3	4915.0	na	4.36E-06	Mt. Simon	UIC reports
21091003577	BioLabIW#1	4241.0	13	4.23E-06	Mt. Simon	UIC reports
21091004207	EDS#2	4475.0	13	4.23E-06	Mt. Simon	UIC reports
34003200670000	Vistron#1	2967.6	na	2.77E-07	Mt. Simon	Arches Sims, 2011
34003200670000	Vistron#1	3066.4	na	3.23E-07	Mt. Simon	Arches Sims, 2011
21149313350000	Lloyd Cupp	5022.4	na	4.89E-07	Mt. Simon	Arches Sims, 2011
21077003277000	Kalamazoo	4970.6	na	1.95E-07	Mt. Simon	Arches Sims, 2011
21077003277000	Kalamazoo	4978.9	na	3.14E-07	Mt. Simon	Arches Sims, 2011
21139000707000	Ottawa	5528.6	na	1.81E-07	Mt. Simon	Arches Sims, 2011
21139000707000	Ottawa	5334.1	na	4.36E-07	Mt. Simon	Arches Sims, 2011
21121000000000	Montague#1	5730.2	na	1.91E-07	Mt. Simon	Arches Sims, 2011
21121000000000	Montague#1	5731.5	na	2.58E-07	Mt. Simon	Arches Sims, 2011
IN159092	Midwest#2	2817.0	na	3.64E-07	Eau Claire	Arches Sims, 2011
IN159092	Midwest#2	3911.9	na	4.77E-07	Eau Claire	Arches Sims, 2011

3.9 Other Model Input

Other model input addressed in the conceptual model included parameters related to pore geometry and residual saturation necessary for the numerical simulations. Pore geometry was better defined with mercury injection capillary pressure tests, threshold pressure tests, and CO₂/brine specific permeability tests completed under the Arches Simulation project. Brine/CO₂ residual saturation curves were obtained from tests performed on Mt. Simon rock core samples from the MRCSP East Bend test well (Battelle, 2010). Table 3-12 summarizes results of this test. Experience with this dataset in numerical simulations performed as part of MRCSP research suggests that these curves may not represent actual field conditions. Therefore, results from MICP tests completed under the Arches Simulation project were analyzed to estimate saturation behavior in the Mt. Simon.

Table 3-12. Mt. Simon Rock Core CO₂-Water Relative Permeability Data from East Bend



Section 4.0: GEOCELLULAR MODEL DEVELOPMENT

As part of the conceptual model, a geocellular model was developed for the study area. The geocellular model includes structure, permeability, and porosity distribution for the key hydrostratigraphic units in the model. The geocellular model was based on a combination of geophysical logs, rock core test data, pressure fall-off testing in Mt. Simon injection wells, and other geotechnical data (Figure 4-1). These data were analyzed with geostatistics and processed to a 3D grid. The 3D grid contains regularly spaced porosity and permeability values in the study area. These parameters are the primary control on fluid flow and are considered the main input for the numerical simulations. Data for the geocellular model is provided in Appendix C in digital format.

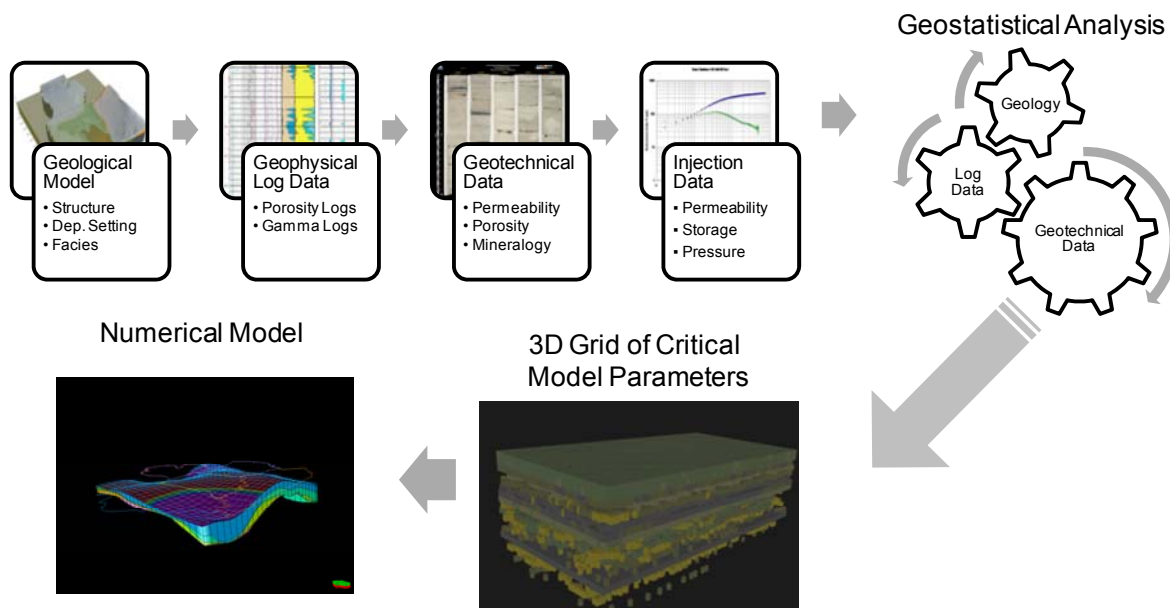


Figure 4-1. Schematic Diagram Showing Geocellular Model Development Process

4.1 Geophysical Log Database

Porosity logs for wells in the Arches Province were compiled to better define hydraulic conditions in the model domain. Best available geophysical porosity logs were compiled for 186 wells that penetrate the Eau Claire and Mt. Simon in the study area (Figure 4-2). Data were compiled into a “X, Y, Z, n” format based on well x-location, y-location, elevation, and logged porosity value.

Porosity was based on either sonic, neutron, or density geophysical log data based on the best available data for each well. Logs were analyzed with histograms for each porosity log in a preliminary quality assessment. When the histogram data were anomalous, the log was discarded if no other source of information was available. In those wells with core analyses, logs were calibrated versus porosity from core and corrected for the log value accordingly. If more than one porosity log was available in a well, the best available log was selected based on the hierachic order as follows: neutron porosity, then sonic, and then density logs. Neutron porosity was estimated as a function of neutron porosity equivalence relationships established for different rock types (Schlumberger, 1972). Porosity was estimated from sonic logs using methods relating transit time (Δt) values to sonic porosity, using charts developed by

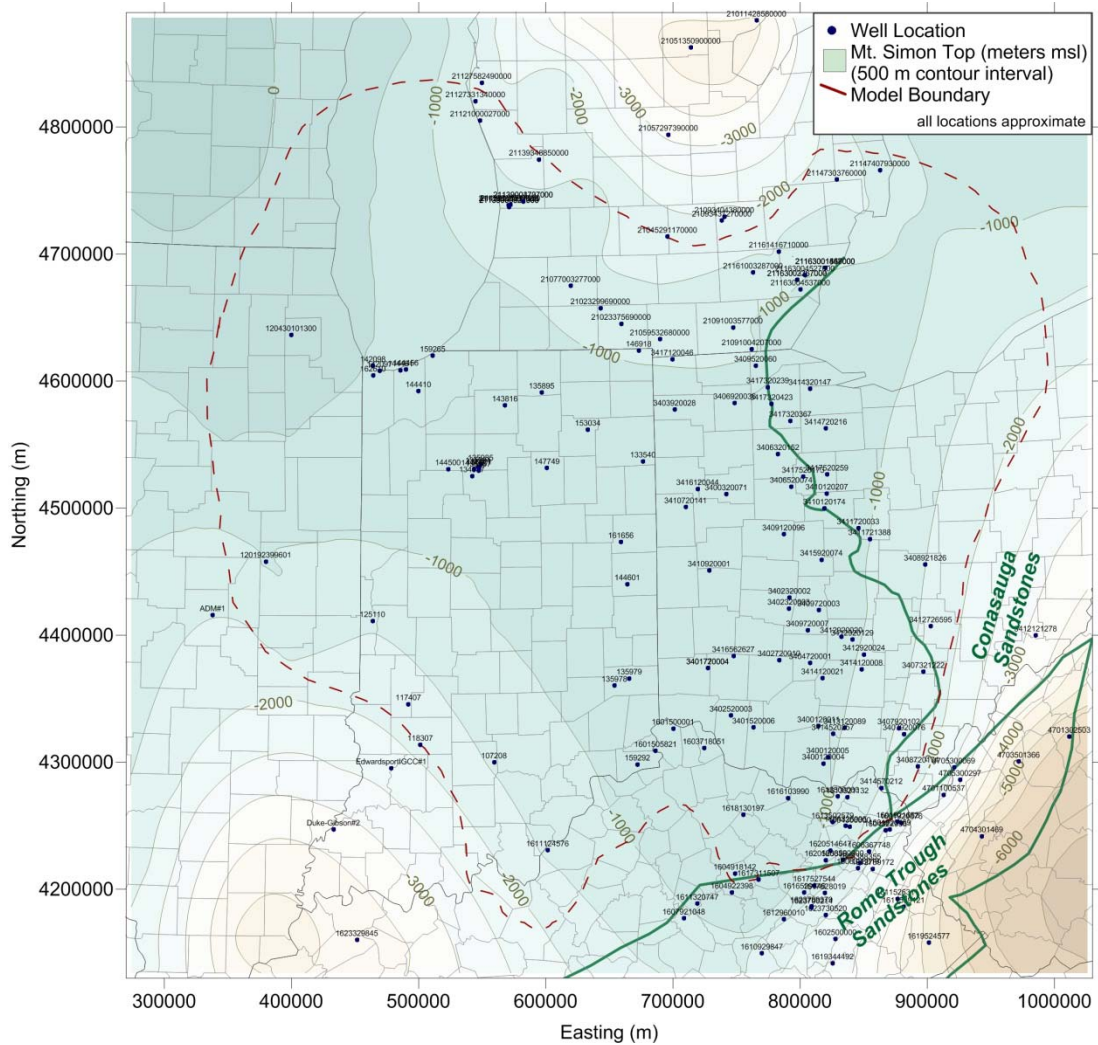


Figure 4-2. Location Map Showing Well Locations Where Geophysical Porosity Logs Were Evaluated

Asquith and Gibson (1982). Bulk density was transformed to porosity (ϕ) using a density-porosity formula (Asquith and Gibson, 1982) for matrix densities of common lithologies after Schlumberger (1972). Due to the large number of wells included in the assessment, these methods were not as detailed as more rigorous petrophysical analyses that may be completed on an individual well basis.

The logs provide a fairly continuous estimate on rock porosity with depth. Data were compiled in digital format from the Knox formation to total depth. A total of over 950,000 porosity data points were collected. The data were screened for outliers and classified with indicator parameters based on formation (Knox, Eau Claire, Upper Mt. Simon, Middle Mt. Simon, Lower Mt. Simon, or Precambrian). The porosity data supplements the ~3,700 core test data and 31 injection well pressure fall-off tests. As shown on the map, there are large areas where no data are available because no wells have been drilled into the Eau Claire or Mt. Simon.

Porosity data were evaluated with two-dimensional (2D) maps of average porosity in the Mt. Simon sandstone interval. Based on evaluation of these data, several wells outside the southern and eastern limit of the Mt. Simon sandstone were removed from the dataset because these wells resulted in false

indications of reservoir quality in these areas. In addition, some outliers were removed from the dataset because these wells had anomalous porosity values. Figure 4-3 shows estimated average porosity in the Mt. Simon sandstone based on the porosity log data. Large portions of the model domain have porosity in the range of 10 to 15%, which matches the central tendency of Mt. Simon rock core test results. Porosity generally decreases to less than 5% into the Michigan and Appalachian Basins.

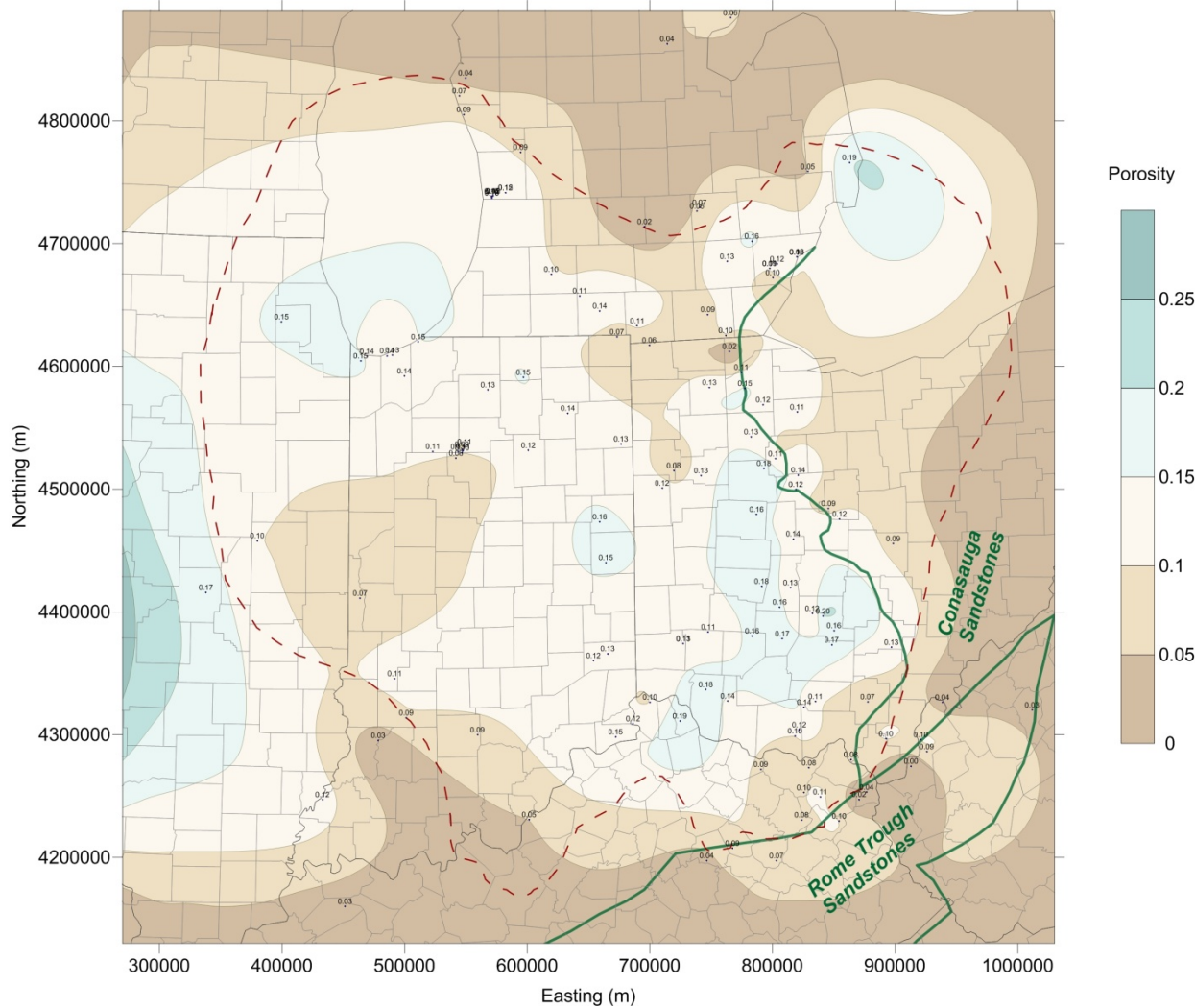


Figure 4-3. Average Porosity in Mt. Simon Sandstone Based on Log Data

4.2 Geostatistical Analysis

Geostatistical analysis was completed on the porosity data from the Mt. Simon and the Eau Claire rock formations. The goal of the geostatistical analysis was to determine any valid spatial trends in porosity that may reflect reservoir quality in the study area. Analysis was also completed on the Eau Claire formation to determine caprock quality in the Arches Province. Based on porosity log data, geostatistical parameters, and structural boundaries, a 3D grid of porosity is being developed throughout the model domain. The end product will be a 3D grid of permeability and porosity which depicts regional variations in the Mt. Simon.

The Mt. Simon porosity dataset consisted of a total of 129,893 unique porosity records (excluding records with missing or unacceptable values). The locations of the wells were concentrated in the states of Michigan, Ohio, Indiana and Kentucky. The lower Mt. Simon has larger spans with no well data. There is less coverage toward the north, particularly in the middle and lower layers. The northern-most wells in the middle layer are on the order of 150 km further north than the remaining wells of that layer. The western-most well in the upper and middle layers is on the order of 80 km further west than the remaining locations. Given that the range of covariance within the region spans a smaller extent than these distances, wells at the furthest extents were not as useful for producing empirical variograms, contributing only to the estimate of the sill. This also means that in the gridding process, predicted porosities in areas with less well coverage (much of the Arches Province) will be represented by the overall mean porosity.

Data preprocessing included adjusting for the structure in the formation layers by flattening each of the lower, middle and upper layers. The flattening was accomplished by referencing the vertical direction with respect to the top elevation of the wells of that layer. In the covariance modeling, this implies that the distance will use the vertical offset (in meters) in the computation of the Euclidean distance (i.e., if j represents the index of the well and d represents the index along the vertical in the well, the offset used as the z coordinate is $z_{jd}^* = \max_j(z) - z_{jd}$). The porosity profiles (trace of porosity vs. depth) of each well were examined for each layer. Many profiles have high-frequency variation in porosities. Some of the profiles exhibited spikes in porosity, which may suggest a spurious reading due to local discrepancies between the assumed lithography and the true form at some depths. Spikes in the profiles contribute to erratic fluctuations in the empirical measures of spatial covariance. A few wells in the middle Mt. Simon had one or two spikes that were reduced or eliminated.

Many of the well profiles have only short segments of readings, extending just tens of meters because the wells only penetrate a portion of formations. Other, newer well logs have thousands of observations at 0.1-m intervals. This results in differential influence on variogram estimation and can be particularly problematic in configurations where one well is a major contributor to a particular distance bin. To reduce the substantial differences in influence, the well profiles were subsampled by randomly sampling 30 observations from any well profiles with over 30 observations, and retaining all observations from any wells with fewer than 30 observations. The histograms of the porosities of the combined profiles for the complete profiles and the subsampled profiles were examined to verify that subsampling did not substantially change the observed distribution of porosities in each of the layers. In the final analysis using subsampled profiles, no wells were omitted from the analyses.

The standard deviations of the well porosities were examined for any spatial patterns. Plots of standard deviations along UTM-X and UTM-Y did not indicate any directional patterns in variance. The porosity spatial characteristics are consistent with a stationary process. The general patterns of locations of higher or lower median porosities are indicative of spatial covariance, with an effective range on the order of tens of kilometers. In the lateral direction, the empirical variograms produced from the complete profile data tended to have somewhat sporadic fluctuations, even with some spikes eliminated on certain wells. Variograms on the subsampled profiles revealed a more systematic pattern of overall increase in the observed semivariance as the distances increased from 10 km to upwards of 50 km or so. Directional variograms were examined to look for patterns in anisotropy. These variograms did not manifest a consistent orientation of ranges of covariance. The covariance structure in each of the three layers was modeled as isotropic in the horizontal direction. Models were developed by iteratively examining the ranges and sills of empirical variograms produced with increasing sizes of bin intervals – 1 km, 5 km, 10 km and 20 km. Typically the most useful bin interval settings were the 10 km and the short range, which each exhibited more stable increases in semivariance as range increased. Empirical variograms were produced using Stanford Geostatistical Modeling Software (SGeMS). Models were fit by eye using the SGeMS interactive tool for exploring variogram models. As a model was being refined, the model was

examined on each of the empirical variograms of the various bin interval sizes to verify that the model was not inconsistent with observed semivariance at any of the ranges.

Table 4-1 summarizes the parameters for each layer of the Mt. Simon formation determined using the SGeMS tool. Figure 4-4 shows the 10-km bin interval and short-range empirical variograms of each layer, with the line overlay indicating the variogram described by that layer's model. The vertical ranges of the middle and lower layers were set higher than the range suggested by the empirical variograms so that the semivariance observed in these ranges is honored with a single exponential structure with a lateral range that is two orders of magnitude larger.

Table 4-1. Covariance Parameters Determined Using SGeMS Variogram Tools

Parameter	Upper	Middle	Lower
Type	-----Exponential-----		
Nugget	20	8	10
Sill (combined nugget and partial sill)	55	40	54
Range Major axis (m)	63000	45000	50000
Range Orthogonal axis (m)	63000	45000	50000
Range Vertical axis (m)	500	1000	500

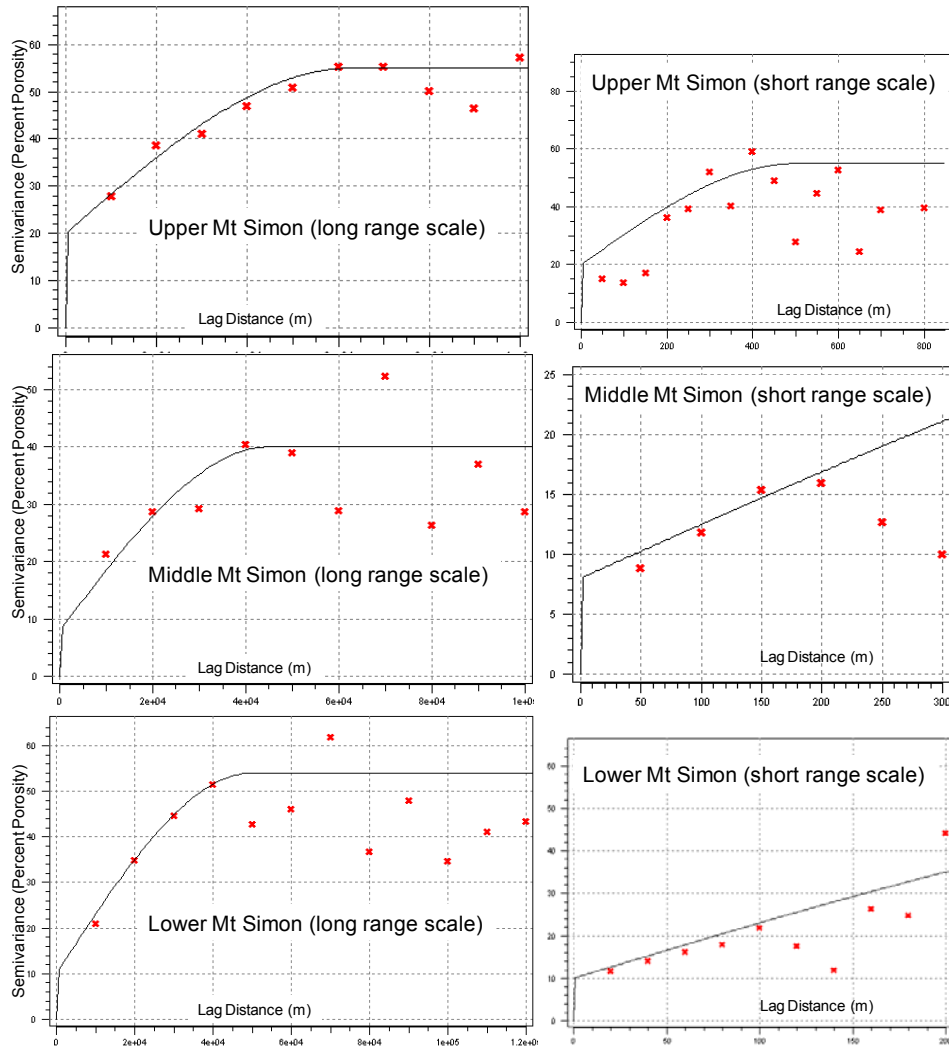


Figure 4-4. Empirical Variograms of the Mt. Simon Formation (Long range has 10 km bin intervals; short range has 20 to 50 m bin intervals. The superimposed curve represents the covariance structure of each layer [parameters as specified in Table 4-1])

Indicator geostatistical analysis was used to analyze the Eau Claire porosity data set, because porosity values in the formation are generally within a small range where trends are difficult to detect. The indicators were based on gamma ray geophysical log data. A '1' indicator was assigned if the gamma ray log value was less than 100, indicating mostly dolomite lithology. A '2' indicator was assigned to the Eau Claire if the gamma ray log value was greater than 100, indicating mostly shale lithology. The Eau Claire dataset consisted of categorical shale/dolomite indicators from 176 wells. The Eau Claire data contained a total of 229,017 records (excluding records with missing data). The geometry of the data was adjusted using the same method as the Mt. Simon data, with the z values expressed with respect to the top of the layer.

Indicator data showed a large area with north-south orientation in the center of the Arches Province which is mostly shale (Figure 4-5). The percent dolomite increases from there at roughly 5 units per 10 km out toward the outer extent of the region. There is one well in Indiana (#21149313350100) with unusually high numbers of dolomite readings compared to the surrounding wells. Because the observations at this well were unusually high for dolomite, this well was excluded from the variogram analysis. The indicator

analysis showed an area of low dolomite content extending for much of the north-south extent in the middle of the region, which might suggest a very long range of covariance along this orientation; outside of this area the range along this direction or any direction is obviously limited to a shorter distance. Empirical variograms (Figure 4-6) in the Eau Claire layer indicate some anisotropy, with a longer range in the north-south orientation (roughly 10 km) and about half that in the east-west orientation (Table 4-2). The vertical range is roughly 300 m.

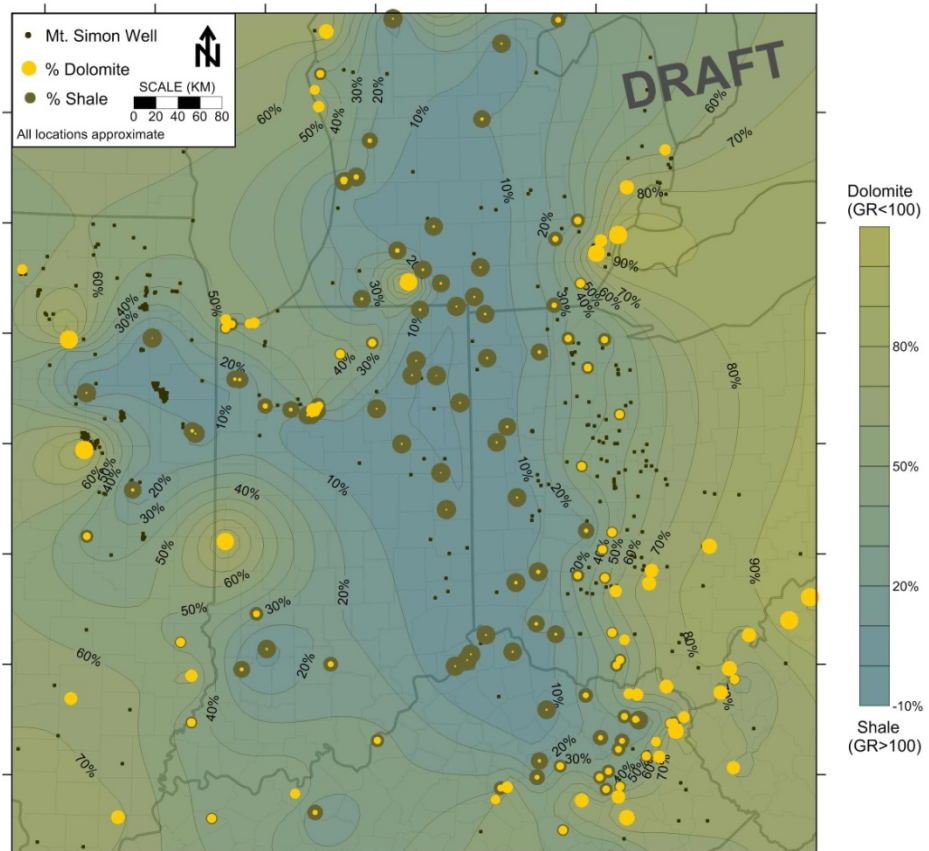


Figure 4-5. Map Showing Ratio of Dolomite to Shale Based on Gamma Ray Logs in the Eau Claire Formation

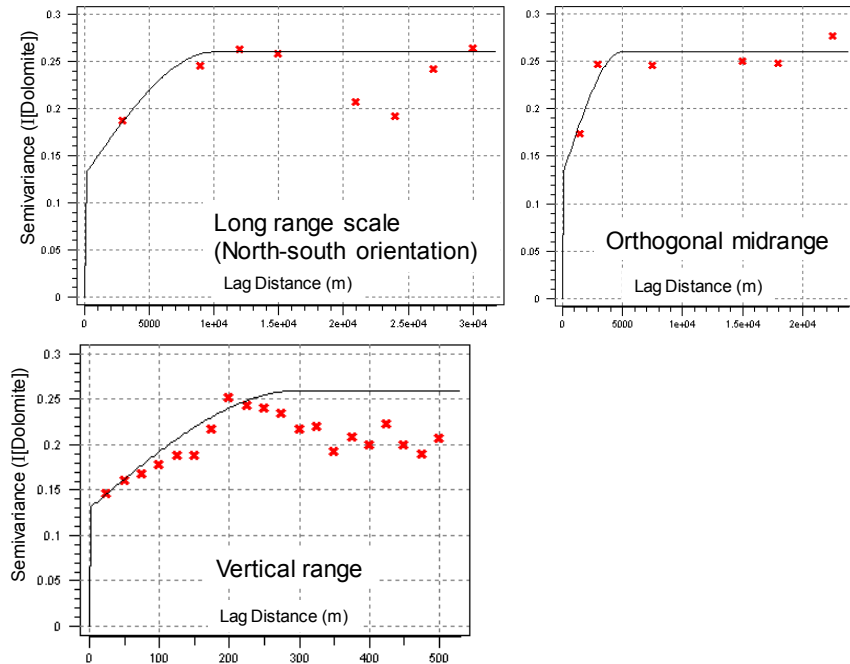


Figure 4-6. Empirical Variograms of Eau Claire Dolomite

Table 4-2. Parameters of Eau Claire Dolomite Covariance Structure

Parameter	Eau Claire
Type	Exponential
Nugget	0.13
Sill (<i>combined nugget and partial sill</i>)	0.26
Range Major axis (m)	10000
Range Orthogonal axis (m)	5000
Range Vertical axis (m)	300

4.3 3D Porosity Grid

The 3D porosity grid for the study area was finalized in EarthVision geologic interpretation and visualization software. The 3D block contains porosity data for the Eau Claire and Mt. Simon rock formations. The 3D block was based on 3D gridding of 360,000 porosity data from geophysical log data. The data were gridded in EarthVision geologic interpretation and visualization software with conformal gridding methods. Conformal gridding is a specialized variation of the minimum tension gridding technique available in EarthVision. Conformal gridding is designed for cases where a parameter's spatial distribution is related to variations in a surface. The conformal gridding was set to mimic the shape of the top surface grid for the Eau Claire and the bottom surface grid for the Mt. Simon.

The grid covers a total area of 700 by 700 km. X,Y spacing was 5,000 m by 5,000 m in a 140 by 140 grid arrangement. Z-spacing was set at 2 m from 0 to -2,500 elevation. Total grid size was 24,500,000 cells. Figure 4-7 shows the 3D porosity model visualization in EarthVision. The model reveals discrete layers with similar porosity. Figure 4-8 shows the Eau Claire porosity model. The Eau Claire is generally lower

in porosity, but there are zones where higher porosity is present. This demonstrates that the geocellular model has captured variations within the unit so the Eau Claire is not portrayed as a uniform confining layer. Average absolute error in the model was 1.8%, indicating suitable prediction of porosity. Figure 4-9 shows the Mt. Simon porosity model. The Mt. Simon includes zones of higher porosity. Some indication of grouping into upper, middle, and lower intervals is apparent. Average porosity of the scattered data for the Mt. Simon was 0.14 and the gridded data average was 0.12, suggesting the Mt. Simon grid model slightly underestimates porosity. Average absolute error in the model was 1.6%, indicating suitable prediction of porosity.

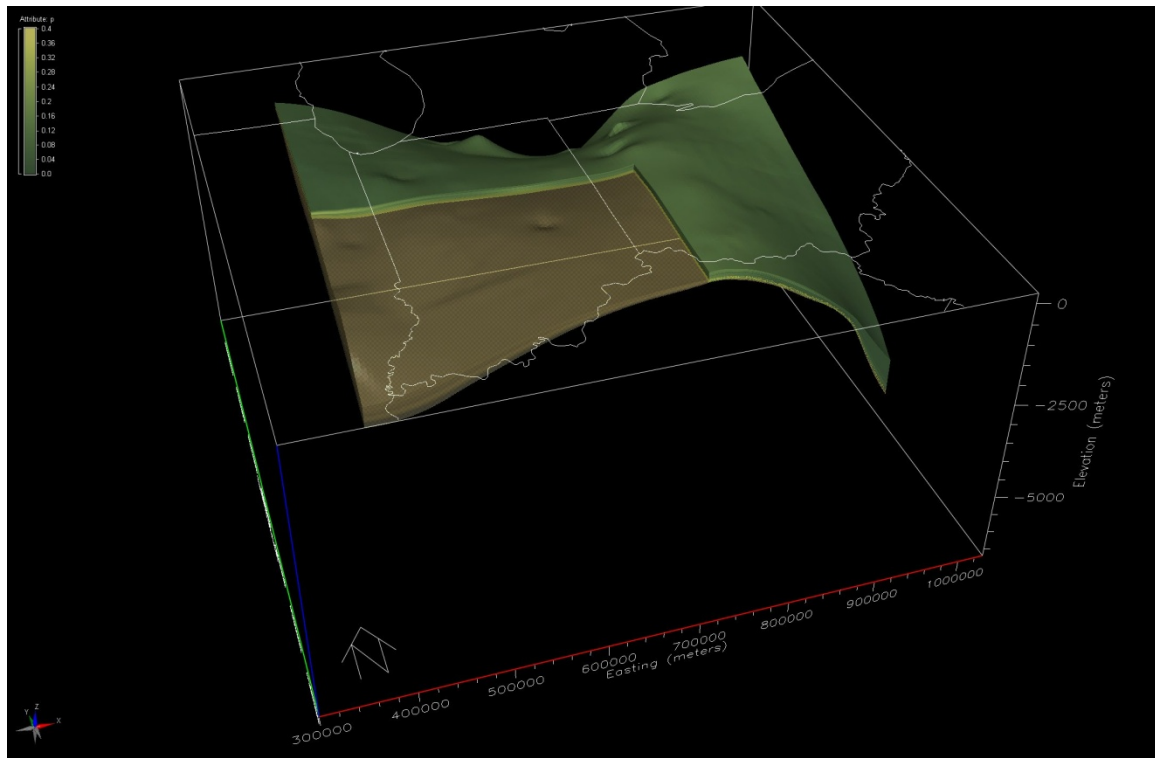


Figure 4-7. 3D Porosity Model

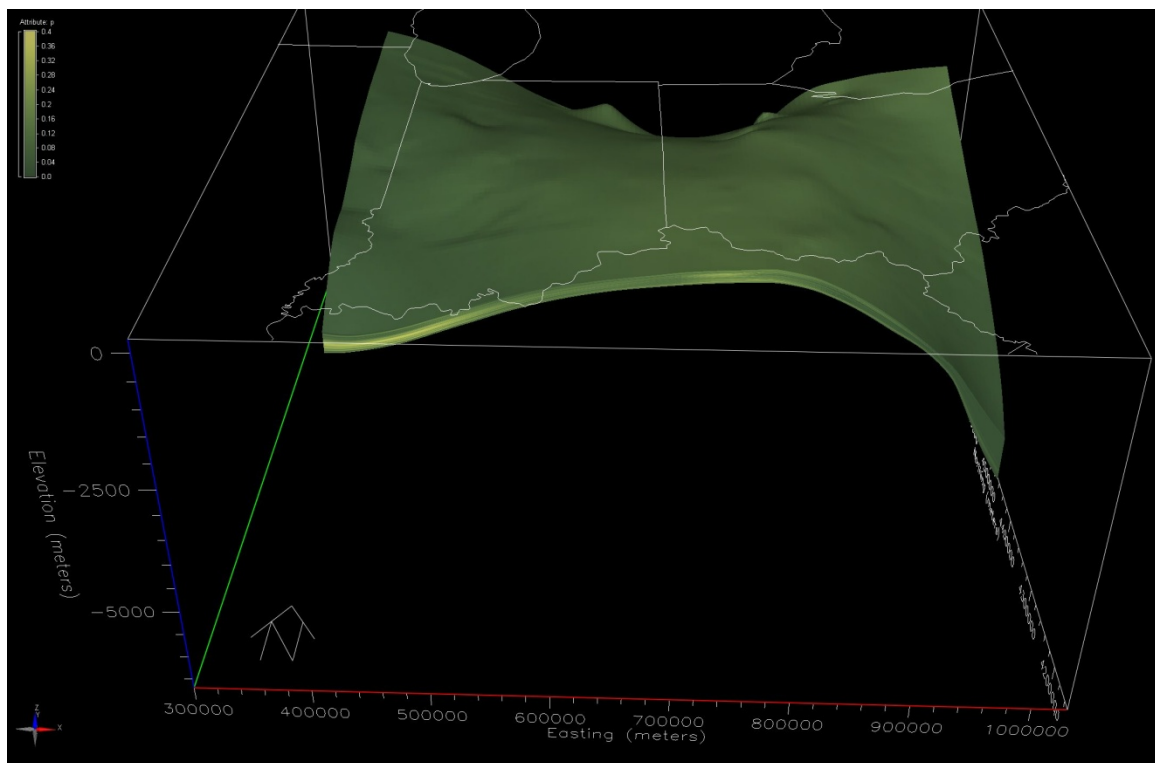


Figure 4-8. 3D Porosity Distribution for Eau Claire

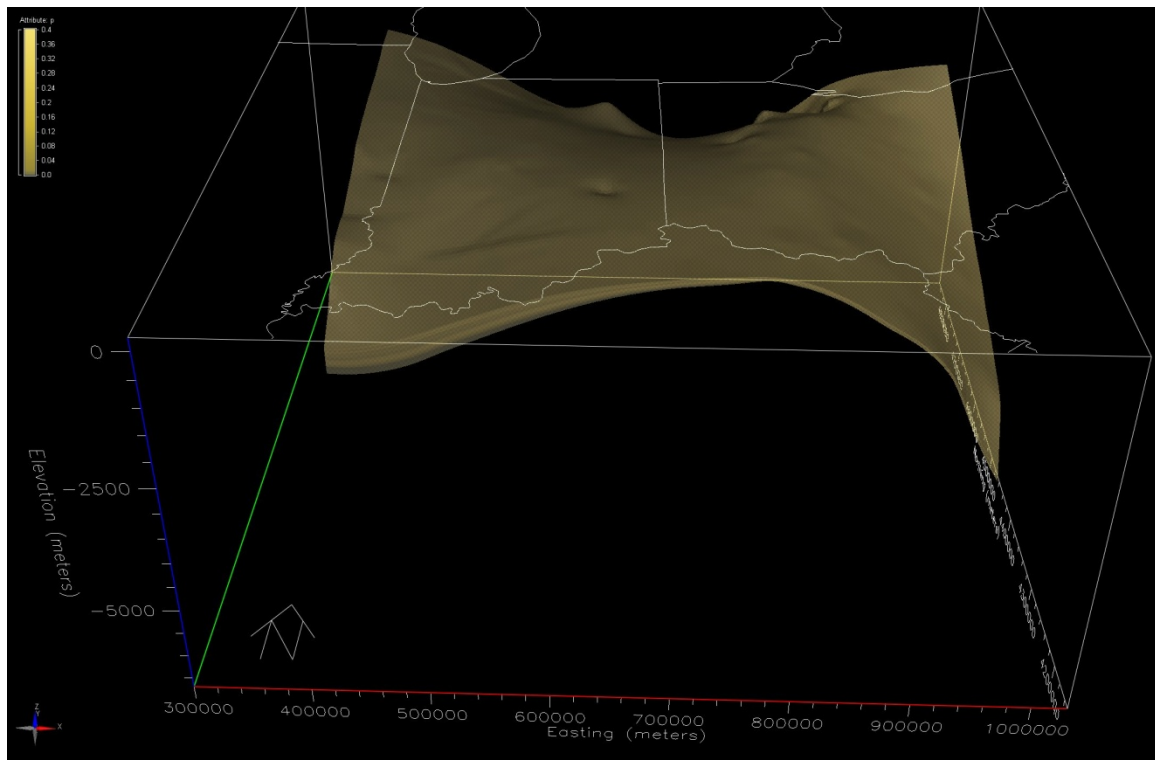


Figure 4-9. 3D Porosity Distribution for Mt. Simon

4.4 Porosity-Permeability Transform Estimate

Core data analyses combined with wireline logs for porosity were used to determine if there is a regional trend in porosity and permeability and how these values vary with depth within the reservoir (Medina et al., 2011). This published work along with other studies (i.e., Birkholzer et al., 2009) constitutes the basis for populating the 3D mesh with values according to published data. Vertical variations within the Mt. Simon were also evaluated by isolating different trends in porosity/permeability with depth interval.

Lateral variations and dividing of the study area into ‘subregions’ were also assessed to determine if there were regional trends in petrophysical properties of the Mt. Simon. This subdivision was based on a shaly unit within the upper unit of the Mt. Simon sandstone, which was originally defined in northwestern Indiana as the “B-Cap” (Becker et al., 1978). A subdivision of the Mt. Simon sandstone is being proposed and will certainly improve the quality of the conceptual model in a qualitative basis (Medina and Rupp, 2010).

The properties assigned to the conceptual geological model for use in the flow simulator were based on the relationship with the properties of the geologic material occurring at the location of each grid cell and porosity and permeability from rock core tests. Several different approaches have been used to represent permeability distribution of the Mt. Simon (Figure 4-10). The k - ϕ relationship used in this study was described by the exponential equation determined by Medina et al. (2008):

$$k(\phi) = 0.7583 * e^{0.283 * \phi}$$

where k is permeability in millidarcies (mD) and ϕ is porosity (percent). This equation was based on the curve fit of 3,800 rock core porosity and permeability results from the Mt. Simon. Since permeability can vary across many orders of magnitude, there is a fair amount of uncertainty in these types of equations. However, as described earlier, much of the 3D porosity model has a porosity of 15%. As such, most of the permeability transform model is near 70 mD.

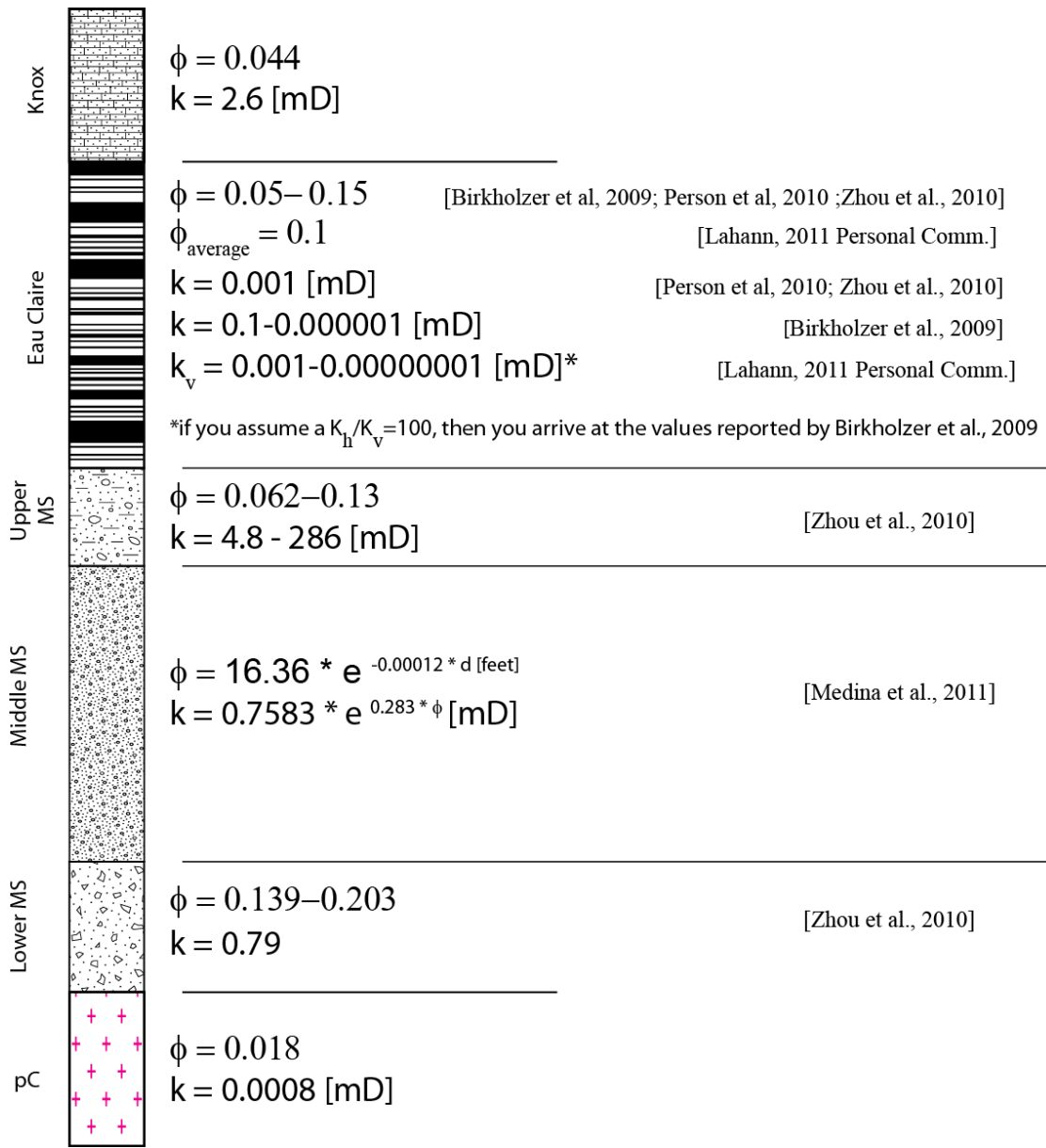


Figure 4-10. Ranges of Values for Porosity and Permeability within the Eau Claire and Mt. Simon Formations (pC=Precambrian; MS=Mount Simon sandstone)

Eau Claire permeability distribution is even more problematic because shale lithology may have relatively high porosity but very low permeability. Approximately 300 core test porosity and permeability data were evaluated from the Eau Claire formation for this study. Rock core tests show very poor correlation of porosity to permeability for the unit. Many of the tests were below detection limits for permeability, which makes interpretation difficult. Overall, these data suggest average porosity of 4.3% and permeability of 1.2 mD. However, the median permeability is 7.6E-5, suggesting there are several high outliers in the Eau Claire dataset. Based on the $k-\phi$ relationship of this Eau Claire data, the following exponential equation was used for porosity-permeability transform for the Eau Claire interval:

$$k(\phi) = 0.000226 * e^{37.27 * \phi}$$

where k is permeability in millidarcies (mD) and ϕ is porosity (percent). This equation is a very general relationship. A more detailed evaluation of Eau Claire confining layer properties should be completed for site specific CO₂ storage applications.

4.5 Injection Well Reservoir Test Permeability Correction Factors

A method was developed to normalize 3D permeability grid to pressure fall-off and rock core test data. The method involves transforming the 3D porosity grid to a permeability 3D grid, based on the best available method for estimating permeability from porosity. The preliminary 3D permeability grid was then normalized by multiplying the initial permeability data by a correction factor. The correction factor basically normalizes data to the pressure fall-off and core test data, thereby providing the most accurate permeability distribution.

The availability of wireline log data (i.e. porosity data) for the Mt. Simon in the Arches Province far surpasses that of available pressure fall-off data, which determine the bulk reservoir permeability. However, the log-derived (i.e., transformed) permeability data often under represented permeability values throughout the study area, with respect to fall-off data. For this reason, a correction factor was used to calibrate the log-derived permeability dataset to create a 3D permeability block. Reservoir permeability is a key input in the geocellular model for controlling darcy flow in a porous system. The permeability transform equation used to transform log porosity data into permeability is discussed in the previous section.

Unfortunately, the accuracy of a simple transformation of porosity to permeability decreases over large geographic distances and larger datasets with more scatter. For this reason, the 3D permeability block derived from wireline logs (i.e., transformed) was corrected using the correction factor f_{corr} , which is the ratio of permeability data derived from pressure fall-off data to those derived from the porosity-permeability transform. The result is a corrected 3D permeability volume throughout the study area that reflects the completeness of the wireline log data as well as the operational accuracy of the fall-off data.

$$f_{corr} = k_{PFO}/k_{LOG}$$

where k_{PFO} = pressure falloff permeability value

k_{LOG} = permeability transform (from porosity) value

$$k_{corr} = k_{LOG} * f_{corr}$$

Table 4-3 provides the number of wells used in determining the correction factor for both the pressure fall-off and log porosity data. Figures 4-11 and 4-12 show contoured images of the gridded data for both log-derived and pressure fall-off permeability, respectively. Figure 4-13 shows a map of the resulting f_{corr} values throughout the study area.

Core data analyzed in the Arches Simulation Project were used to determine the maximum permeability cutoff for the corrected porosity-permeability transform data. That is, the maximum measured permeability from core was 1710 md; therefore, the upper permeability limit for the corrected data was designed not to exceed this threshold. A total of 137 wells existed in the study area, the Mt. Simon, and the average corrected permeability, by well, for these data was 69.1 md.

Table 4-3. Type of Data and Number of Wells Used to Determine the Permeability Correction Factor (f_{corr})

Date Type	Number of Wells	Average Permeability Value (mD)
Pressure Falloff	21	61.9
Log Porosity	172	49.5
Corrected Permeability	137	69.1

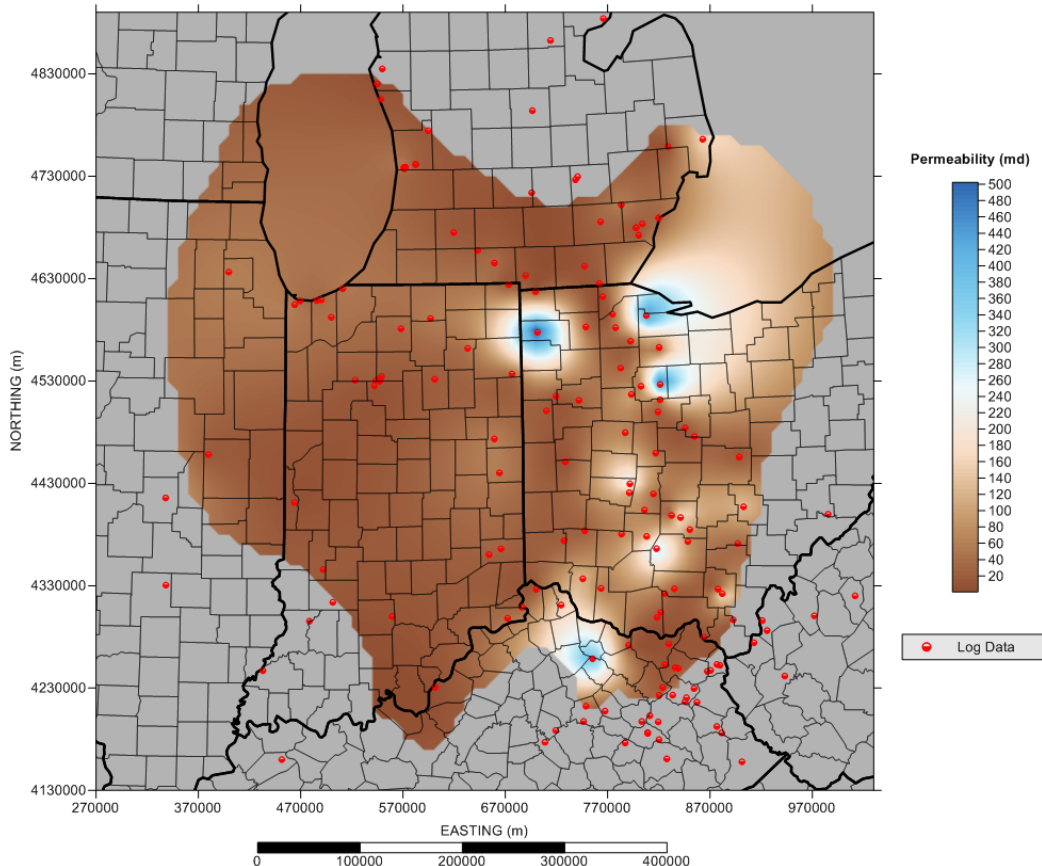


Figure 4-11. Map of Log-Derived Permeability Transform Data

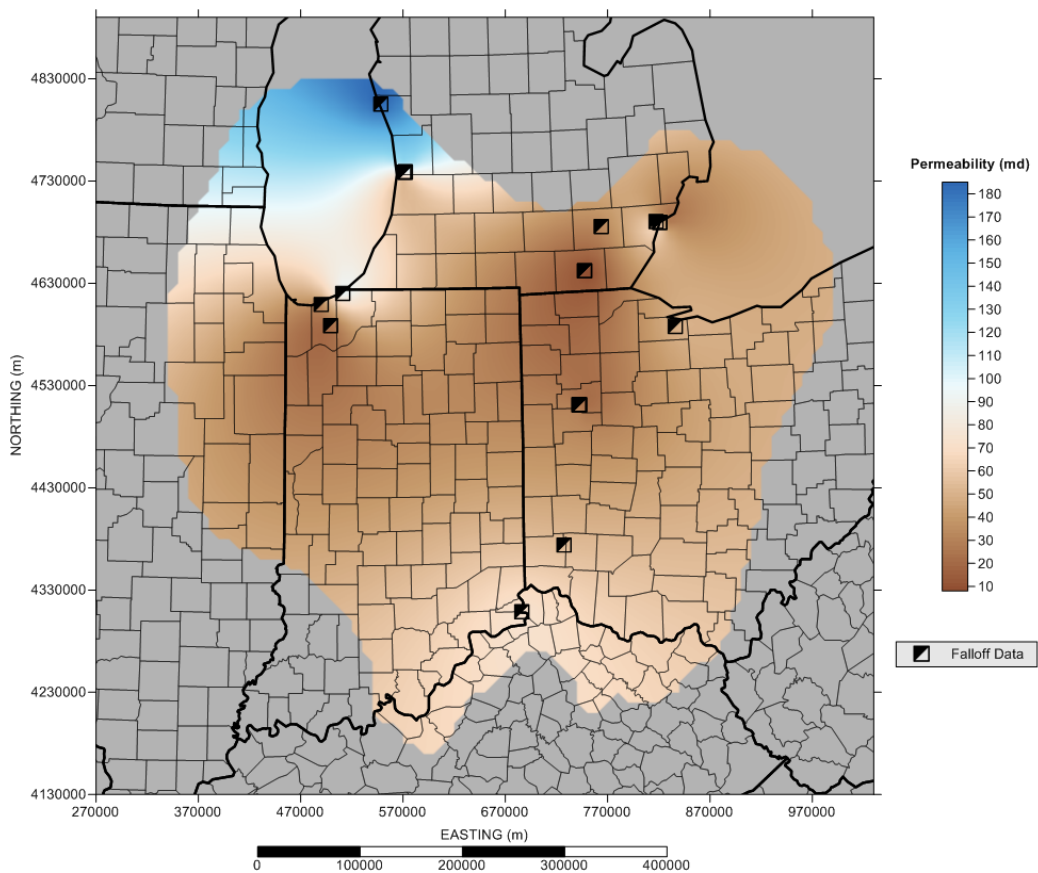


Figure 4-12. Map of Pressure Fall-off Permeability Data

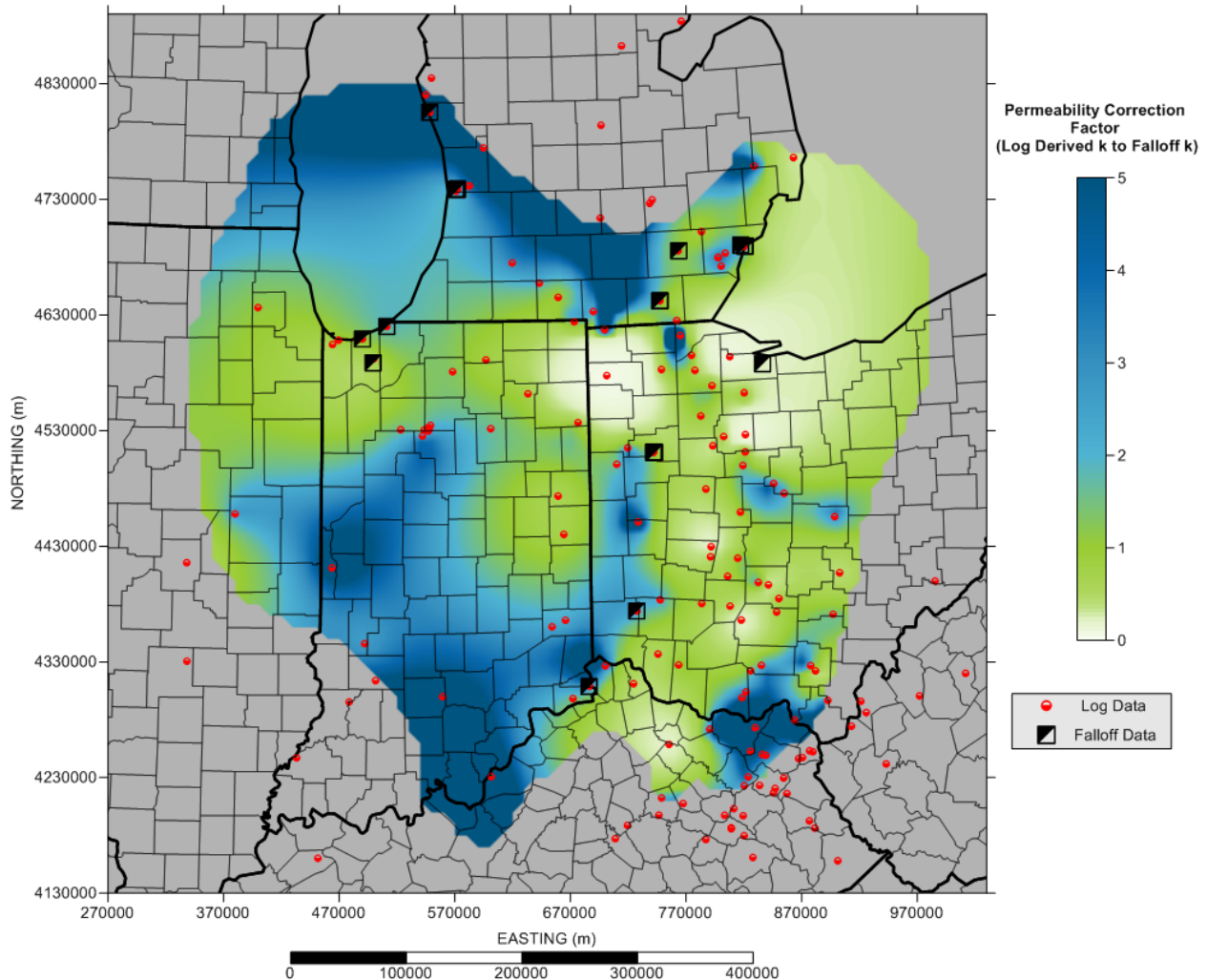


Figure 4-13. Map of Permeability Correction Factor

4.6 3D Permeability Grid

To develop the final 3D permeability grid, the geophysical log porosity dataset was transformed to initial permeability values. These data were then corrected with correction factors extracted from the injection well reservoir test permeability correction factor grid. This final set of permeability data represents permeability corrected with injection well information. The permeability data were capped at 1710 mD because this represents the maximum observed permeability from rock core tests and reservoir tests in the Mt. Simon. Consequently, it is unrealistic to include permeability zones greater than this value in the permeability model. The corrected permeability data were transformed into log values and gridded in EarthVision with conformal gridding methods. The conformal gridding was set to mimic the shape of the top surface grid for the Eau Claire and the bottom surface grid for the Mt. Simon.

Figure 4-14 shows the 3D permeability model visualization in EarthVision. Similar to the porosity grid, the model exhibits vertical layering and broad lateral trends in permeability. However, permeability varies across several orders of magnitude. Figure 4-15 shows the Eau Claire permeability model. The Eau Claire is much lower in permeability, but there are zones where permeability up to tens of mD is present. The Eau Claire is not portrayed as a uniform confining layer in the geocellular model. Average

absolute error in the model was 1.6%, indicating suitable prediction of permeability. The average of the scattered input data was -1.3 and the gridded mean was -1.6, indicating the grid slightly underestimates Eau Claire permeability. Figure 4-16 shows the Mt. Simon permeability model. This permeability distribution will be the main control on fluid flow in the numerical simulations. Average absolute error in the model was 1.6%. The average of the scattered input data was 1.6 and the gridded mean was 1.2, indicating the grid also underestimates Mt. Simon permeability. However, this variation is the result of some large areas in the corners of the model where permeability is low but few data points are present.

It should be noted that the visualizations include vertical exaggeration of 40X, which amplifies the structural features. Figure 4-17 shows a visualization of the porosity model with 5X vertical exaggeration. As shown, the rock layers in the area are mostly flat with very broad, gentle structural features most notable on a regional scale.

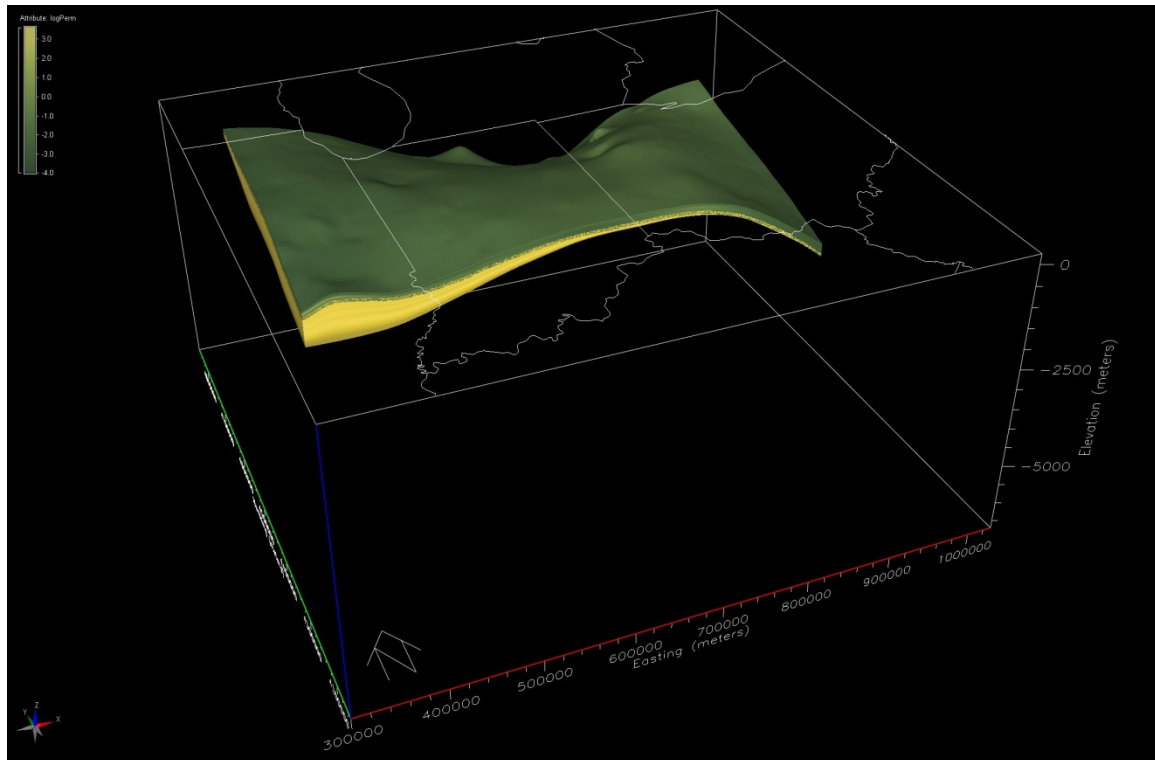


Figure 4-14. 3D Permeability Model

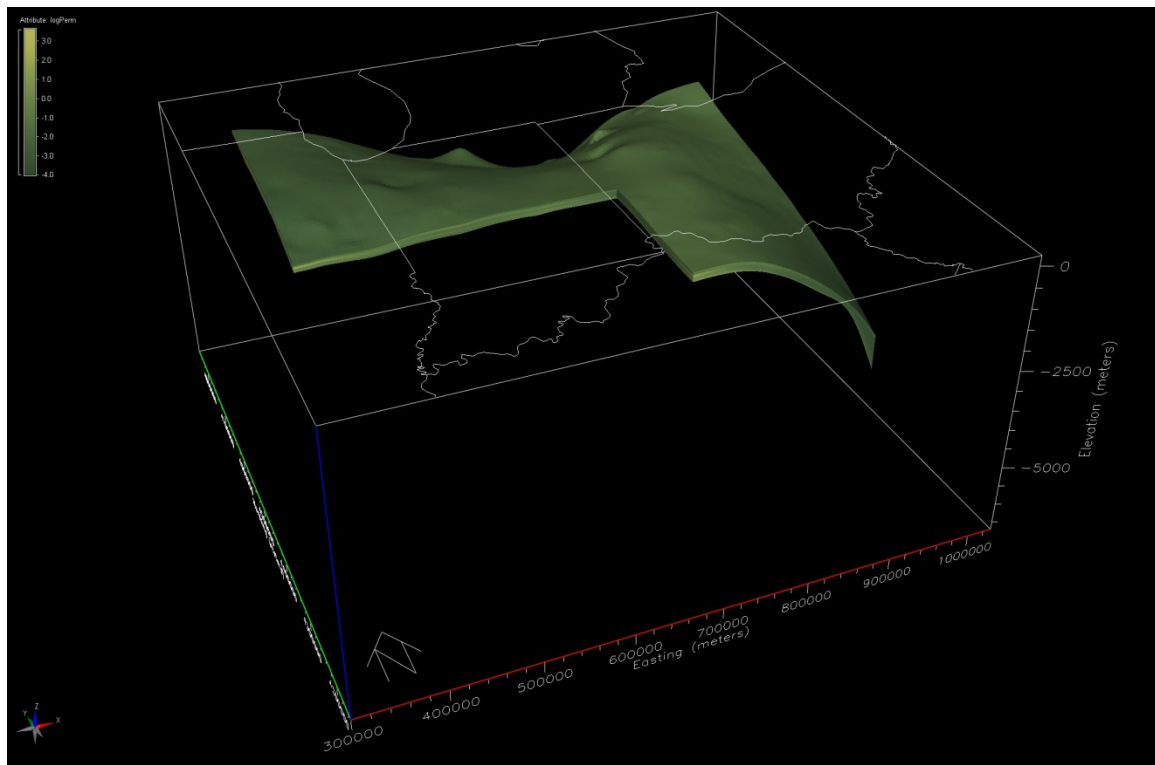


Figure 4-15. 3D Permeability Distribution for Eau Claire

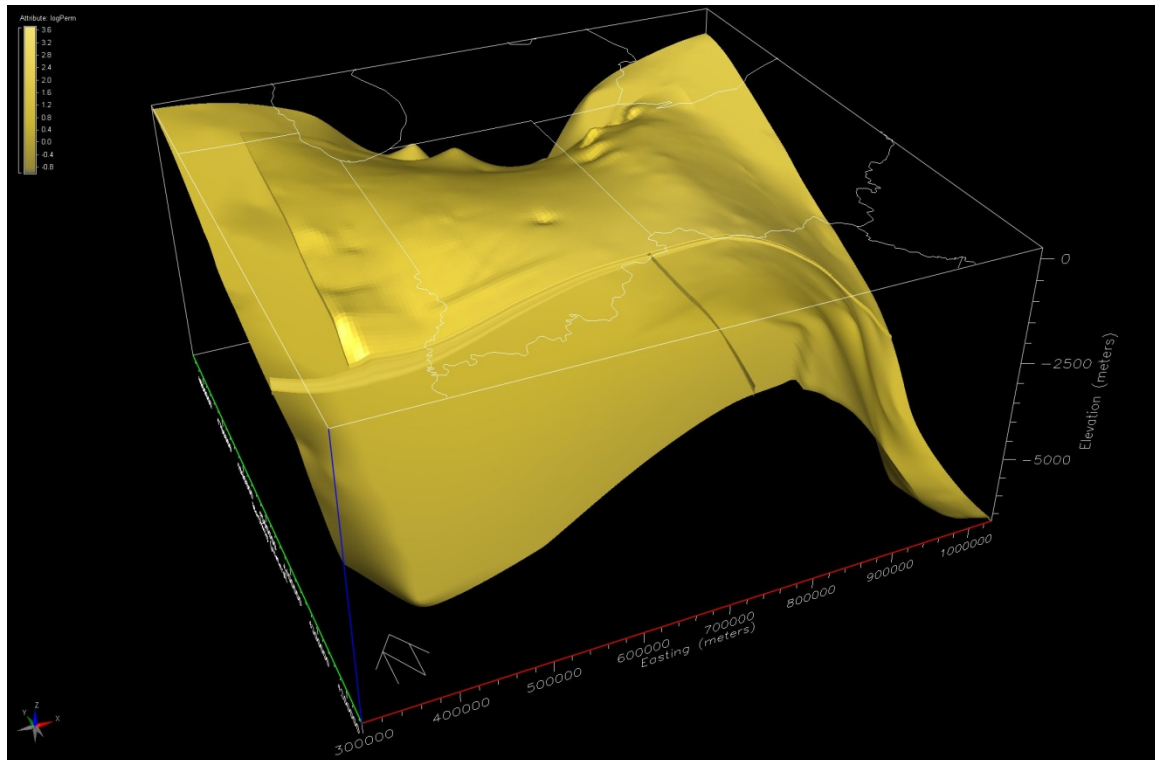


Figure 4-16. 3D Log Permeability Distribution for Mt. Simon

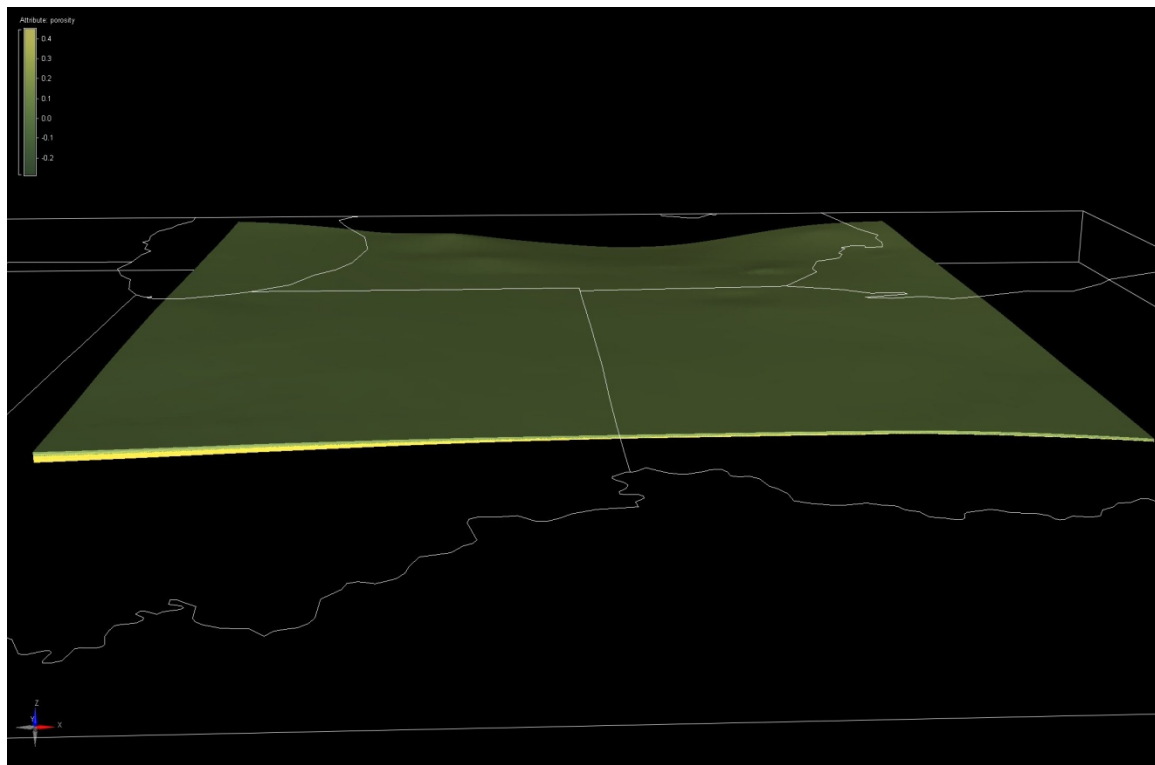


Figure 4-17. 3D Porosity Distribution at 5X Vertical Exaggeration

Section 5.0: SIMULATION SCENARIOS

CO₂ injection scenarios were developed for the numerical simulations. These scenarios include injection locations, rates, and schedules. The scenarios were based on review of CO₂ sources in the Arches Province region and pipeline routing analysis.

5.1 CO₂ Sources in the Arches Province

The distribution of large CO₂ point sources was analyzed for the Arches Province. Data on CO₂ point sources were obtained from the U.S. DOE Carbon Atlas database (2008). Review of these sources suggests that there are approximately 131 point sources in the area with emissions greater than 100,000 metric tons CO₂ per year (Figure 5-1). These sources have combined emissions of 286 million metric tons CO₂ per year. There are 53 point sources with emissions over 1 million metric tons per year which have total emissions of 262 million metric tons CO₂ per year. Thus, there are 233 smaller sources that account for only 8.4% of overall emissions. Approximately 221 million metric tons per year emissions are from power plants, mostly concentrated along the Ohio River Valley and the Great Lakes coastline. In addition, there are many sources in adjacent areas, which may access the Arches area with a pipeline distribution system.

In general, the source study provides some guidance related to realistic source sizes for the model. To reduce greenhouse gas emissions in the Arches Province by 25 to 50%, CO₂ storage projects with total storage rates of 70 to 140 million metric tons CO₂ per year would be necessary. The study also suggests that a pipeline distribution system would be required, since few sources are located in the central portion of the Arches Province.

Based on this source distribution, it was determined that on-site injection and regional storage field injection would be most useful for evaluating CO₂ storage potential in the Arches Province. The on-site scenario addresses whether it is feasible to implement CO₂ storage at the source locations, which is generally considered the most cost effective option for facilities. The regional storage scenario assumes a pipeline distribution system to transport CO₂ to regional storage fields with more suitable geology. Both scenarios are designed to address 25% and 50% reduction in emissions, or injection rates of approximately 70 to 140 million metric tons CO₂ per year.

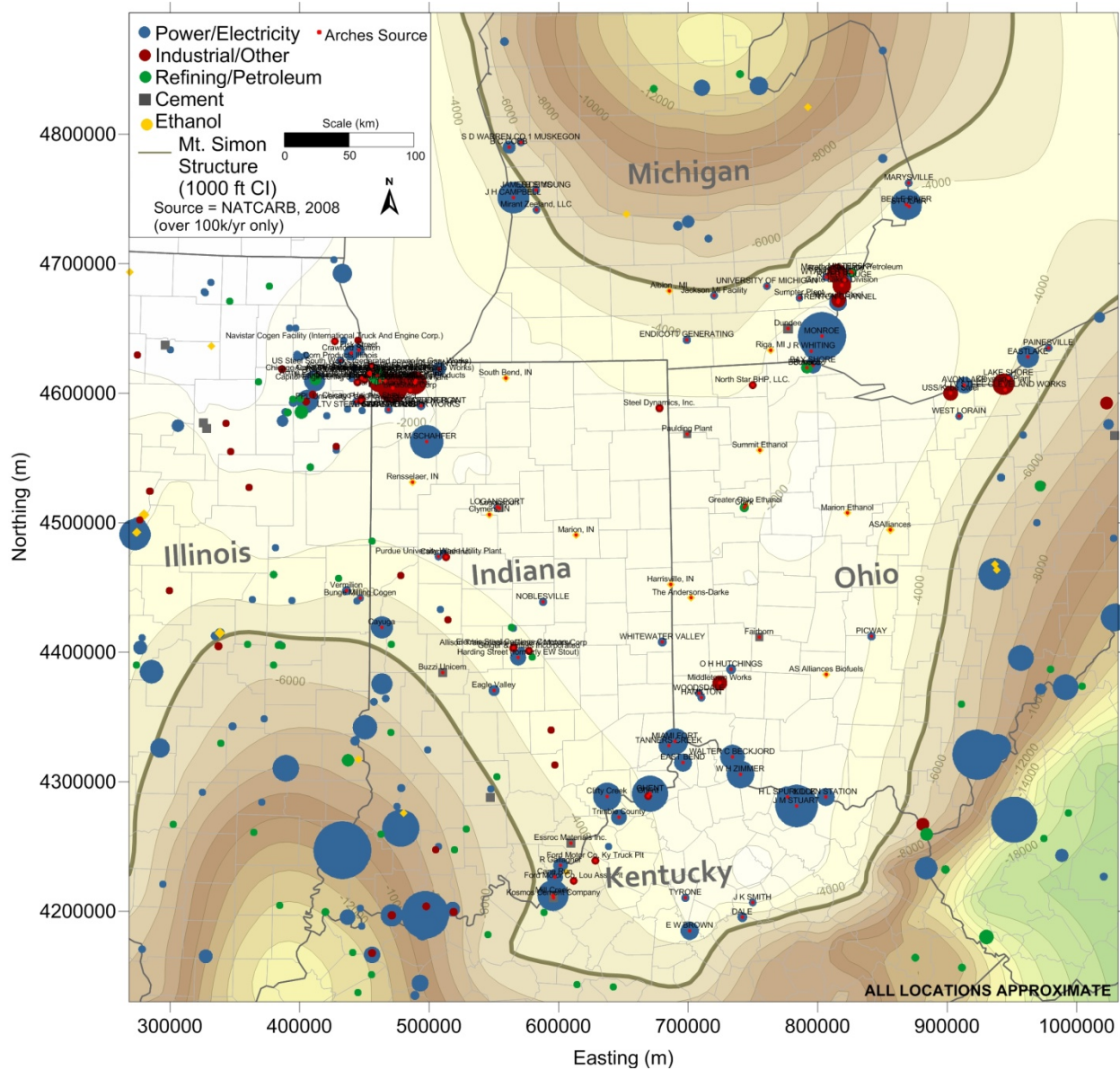


Figure 5-1. Distribution of Large CO₂ Point Sources in the Arches Province

5.2 On-Site Injection

The on-site injection scenario addresses point sources with emissions greater than 1 million metric tons CO₂ per year. These 53 sources account for 91.6% of point source emissions in the Arches Province. The sources are mostly clustered along the Great Lakes coastline and Ohio River Valley, which generally do not have the most appealing geologic setting for CO₂ storage.

5.3 Regional Injection Fields

The regional storage field scenario assumes that a pipeline distribution system will be constructed to transport CO₂ from sources to regional CO₂ storage fields. The regional scenario was prescribed for seven storage fields, each injecting at total rates of 10 to 20 million metric tons CO₂ per year. These fields will contain several wells to facilitate these injection rates. Separate scoping level simulations will

be completed to determine the most appropriate arrangement of injection wells in the storage fields. To determine geographical location of potential storage fields, a pipeline routing analysis was completed for the sources in the Arches Province.

5.4 Pipeline Routing Study

A least cost path study was conducted using the CO₂ pipeline transport cost estimation model developed by MIT's Carbon Capture and Sequestration Technologies Program. This program was used in conjunction with CO₂ source and carbon sink location data selected for the study. The objective of the analysis was to investigate least cost path trends for CO₂ transportation pipelines routed from significant point sources of CO₂ to pre-selected carbon sequestration sites in the Arches Province region. The MIT study focused on utilizing the Mt. Simon sandstone in the Arches Province as the target formation for carbon sequestration.

The MIT model was developed as a tool to be used within the ArcGIS software package to calculate a least cost path between two selected points and produce construction cost outputs associated with that path. The program package consists of three layers: A U.S. map layer, a states layer and the least cost path layer, or obstacles layer. The analytical power of the model is in the obstacle layer, which ArcGIS utilizes to perform the least cost path analysis. The obstacle layer is pre-built and cannot be modified by the user. A general description of how the obstacle layer was constructed by the MIT team for the program is described below:

Because pipeline construction cost varies considerably depending on the local terrain and the presences of infrastructure, an obstacle layer was created in ArcGIS to account for such variability. Locations and characteristics of these obstacles were uploaded into the GIS software as an obstacle layer. The obstacle layer reflected three types of general obstacles: land slope, protected areas, and crossings and three line type obstacles: waterways, railroads, and highways. This vector obstacle layer was then converted to a raster obstacle layer consisting of 1 km by 1 km cells. Obstacles occurring in the cells were assigned relative weights based on their associated difficulty of traversing. The assigned obstacle numbers were totaled for each 1 km² cell. That number total was then assigned to each cell, giving it a specific pipeline construction cost factor. The spatial analysis function in ArcGIS was then used to determine the least cost pipeline path from each CO₂ source and sink. (MIT 2009)

For the purposes of this study 20 CO₂ sources and three CO₂ sinks were selected to run the CO₂ pipeline transport cost estimation simulation in the Arches Province. The top 20 significant CO₂ point sources in the Arches Province were screened base on their annual CO₂ output. Three carbon point sink locations were selected based on their proximity to the selected CO₂ point sources and geologic conditions of the Mt. Simon sandstone favorable to carbon sequestration and storage within the MRCSP region. Carbon sink #1 is identified as Sink Central North and is located in south central Michigan. Carbon sink #2 is identified as Sink Central West and is located in central Indiana. Carbon sink #3 is centrally located on the border of Indiana and Ohio and is identified as Sink Central. Latitude and longitude coordinates of the 20 CO₂ point sources and three carbon sink sources were uploaded to the ArcGIS module. The uploaded CO₂ point source and carbon sink locations were then selected from the least cost path interface for each least cost path simulation.

Three scenarios were created in the model based on the three arbitrary carbon sequestration locations in the central portion of the Arches Province. Each scenario represents least cost pipeline routing from the 20 CO₂ point sources to one of the three sites selected for carbon sequestration. For each scenario a map

was created in ArcGIS displaying the least cost path for the 20 CO₂ transportation pipeline routes. Consequently, a total of 60 pipeline routes were determined (Figure 5-2).

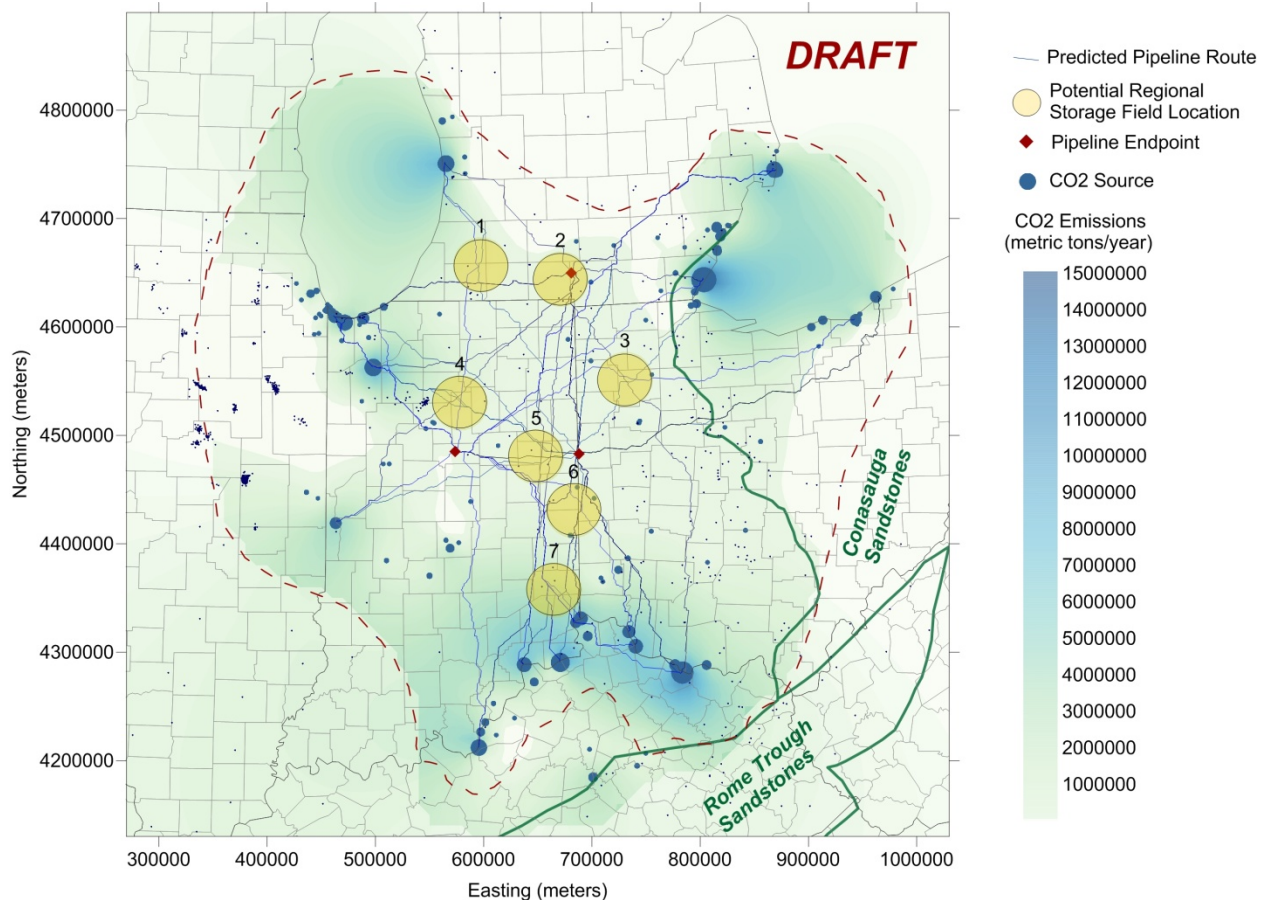


Figure 5-2. Pipeline Routing Analysis Results

These pipeline routes suggest there are some central areas where pipeline routes intersect or blend together. These locations may be practical potential regional storage fields. Seven locations were selected as potential regional storage field locations. These locations are fairly arbitrary. Several other locations may be feasible for regional storage fields. However, the seven locations do represent coverage across the Arches Province. The locations are separated by at least 50 km, which should minimize interference between storage fields. Total injection of 10 to 20 million metric tons CO₂ at each location would represent total injection rate of 70 to 140 million metric tons CO₂ per year (represents approximately 25 to 50% reduction of CO₂ emissions from large point sources across the Arches Province).

5.5 Other Simulation Scenarios

The project is designed to include several other simulation scenarios related to CO₂ storage processes. These scenarios are focused on issues related to geomechanical, geochemical, leakage, and monitoring aspects of CO₂ storage. Since these scenarios are focused on small-scale processes, the simulations will be completed with smaller 2D radial models. Geomechanical simulations will take advantage of the new dataset on geomechanical parameters completed as part of this project. The objective of the geochemical simulations is to evaluate the potential for mineral precipitation and/or dissolution in the Mt. Simon and Eau Claire formations. Leakage simulations are focused on assessing the potential for CO₂ migration through the confining layers and into freshwater zones. Finally, several simulations will be completed to evaluate what monitoring methods are most appropriate for the Arches Province.

Section 6.0: CONCLUSIONS

A conceptual model was developed for the Arches Province that integrates geologic and hydrologic information on the Eau Claire and Mt. Simon formations into a geocellular model. The conceptual model describes the geologic setting, stratigraphy, geologic structures, hydrologic features, and distribution of key hydraulic parameters. The geocellular model depicts the parameters and conditions in a numerical array that may be imported into the numerical simulations of CO₂ storage. Geophysical well logs, rock samples, drilling logs, geotechnical test results, and reservoir tests were evaluated for a 500,000 km² study area centered on the Arches Province:

- Information from over 500 wells that penetrate the Eau Claire formation or deeper zones in the Midwestern U.S.,
- Geophysical well logs from 496 wells,
- Approximately 4,000 rock core test results in Eau Claire or Mt. Simon intervals,
- 105 additional standard permeability and porosity tests on Mt. Simon/Eau Claire rock samples,
- Completion of geomechanical tests on 11 rock samples,
- 16 mercury injection capillary pressure tests on rock samples,
- 10 other advanced saturation tests on rock core samples,
- Deep well injection operational data from 48 wells in the study area,
- Pressure fall-off reservoir test data from 31 wells,
- Compilation and analysis of a total of 960,000 porosity data from geophysical logs,
- Many other geological maps, research, and publications.

The Precambrian interval, which includes crystalline and meta-sedimentary basement rock, was identified as the lower bound of the model. The Mt. Simon sandstone is considered the main injection interval for CO₂ storage. In the conceptual model, the unit includes other Cambrian basal sandstone formations, mainly identified in eastern Ohio and Kentucky. The nature of flow between these units is not entirely clear. Since the model covers some areas into eastern Ohio and Kentucky, the Conasauga sandstone units were binned with the Mt. Simon unit. The transition in rock character is captured by reduction of porosity and permeability into these areas. The Eau Claire includes variable shale, sandstone, and dolomite units that also grade into the Conasauga Group in the eastern portion of the study area. The Knox unit includes a group of several carbonate rock formations. Both the Knox and Precambrian were represented as simple, homogenous units in the conceptual model.

The geologic and hydraulic data were integrated into a geocellular model. The data were integrated into a 3D grid of porosity and permeability, which are key parameters regarding fluid flow and pressure buildup due to CO₂ injection. Permeability data were corrected in locations where reservoir tests have been performed in Mt. Simon injection wells. The final geocellular model covers an area of 600 km by 600 km centered on the Arches Province. The geocellular model includes a total of 24,500,000 cells representing estimated porosity and permeability distribution.

Development of the conceptual model revealed several key conclusions regarding the geologic framework for CO₂ storage in the Arches Province:

- The Arches Province covers a large area where the character of rock formations changes substantially. The Mt. Simon sandstone and equivalent basal sandstone interval are present from Iowa to West Virginia. The Arches Province is located along the east-central extent of the overall. Thus, the formation exhibits several facies changes across the study area and related to its original depositional setting and subsequent diagenetic alteration. Many of these trends were exhibited in maps of hydraulic and geotechnical parameters.

- Interpretation of the Mt. Simon was refined in the Arches Province to define the distribution of the formation in more detail. The mapping was based on detailed geologic cross sections which built upon previous work performed by the MRCSP and other research. In the Arches Province, the interval generally thickens from 100 ft on the edge of the Appalachian basin to over 2,000 ft in the northern portion of the Illinois basin.
- Hydrostratigraphic units were identified to aid in delineation of formation structure, which defines the overall framework of the model. However, a sharp contact between reservoir and confining unit was not explicitly defined in the conceptual model. In developing the conceptual model, it was determined that there is often no clear break between hydrostratigraphic units. Thus, the Cambrian basal sandstone and Eau Claire formation were represented with a variable distribution of input parameters.
- A major result of this portion of this research was revision to the southern margin of the Mount Simon sandstone into Kentucky. This area is important for the Arches Province because many large CO₂ sources are located along the Ohio River. New seismic interpretations and well data collected from recent CO₂ injection tests were used to re-interpret the southern boundary of the Mt. Simon sandstone and examine the manner in which the sandstone thins south- and eastward. Structures associated with Cambrian rifting in the Rough Creek Graben (western Kentucky, Illinois basin) and Rome Trough (eastern Kentucky, Appalachian basin) influence the southern limit of the sandstone, causing thinning or absence on structural highs.
- Geostatistical analysis of geophysical porosity data was completed for the Mt. Simon and Eau Claire intervals. Geostatistical analysis for the Mt. Simon suggests a fairly erratic dataset. Subsampling methods were necessary to interpret the data and indicated a lateral correlation range of 50 to 60 km. Indicator analysis for the Eau Claire showed an area of low dolomite content extending for much of the north-south extent in the middle of the region, which might suggest a very long range of covariance along this orientation; outside of this area the range along this direction or any direction is obviously limited to a shorter distance. Empirical variograms in the Eau Claire layer indicate some anisotropy, with a longer range in the north-south orientation (roughly 10 km) and about half that in the east-west orientation.
- There are 131 large CO₂ point sources in the Arches Province with combined emissions of approximately 286 million metric tons CO₂ per year. However, the 53 sources greater than 1 million metric tons CO₂ per year account for over 90% of total emissions. Based on review of these sources, on-site injection and regional storage field scenarios were identified for simulation. A pipeline routing study was used to identify seven potential locations for regional storage fields.

The model has several inherent assumptions and limitations related to depicting the nature of deep rock formations. This is a basin-scale simulation study, and many trends in geology and input parameters were generalized. In general, any CO₂ storage project would require more detailed investigation of rock formations in the project area. Research was focused on the Arches Province, and areas outside this region were not reviewed in detail. Data coverage is limited in some areas and should be considered when examining maps and figures. Geological information on the Mt. Simon has been collected over a period of many decades and the quality of the information varies. Implementation of a CO₂ storage project is a multi-year effort involving site screening, site assessment, characterization, testing, and system design. The conceptual model was intended to provide general guidance for a large region of the Midwestern U.S. A CO₂ storage project would require field work such as seismic surveys, drilling, geophysical logging, reservoir tests, detailed reservoir modeling, and system design. The results of this report shall not be viewed or interpreted as a definitive assessment of suitability of candidate geologic CO₂ storage formations, the presence of suitable caprocks, or sufficient injectivity to allow CO₂ sequestration to be carried out in an economic manner.

Section 7.0: REFERENCES

Asquith, G.B. and C.R. Gibson. 1982. *Basic Well Log Analysis for Geologists*. Methods in Exploration Series. American Association of Petroleum Geologists, Tulsa, OK.

Barnes, D., Bacon, D., and Kelley, S. 2009. Geological sequestration of carbon dioxide in the Cambrian Mount Simon Sandstone: Regional storage capacity, site characterization, and large-scale injection feasibility, Michigan Basin. *Environmental Geosciences*, v. 16, no. 3, p. 163-183.

Battelle. 2010. Appalachian Basin- CO2 Injection Test in the Cambrian-Age Mt. Simon Formation Duke Energy East Bend Generating Station, Boone County, Kentucky, Midwest Regional Carbon Sequestration Partnership. Prepared for U.S. DOE NETL by Battelle. 158 p.

Becker, L. E., Hreha, A. J., and Dawson, T. A., 1978, Pre-Knox (Cambrian) stratigraphy in Indiana. Department of Natural Resources: Geological Survey Bulletin 57, 72 p.

Birkhozer, J.T., Zhou, Q., Tsang, C.-F. 2008. Large-scale impact of CO2 storage in deep saline aquifers: a sensitivity study on the pressure response in stratified systems, *International Journal of Greenhouse Gas Control*, doi:10.1016/j.ijggc.2008.08.002.

Blakey, R. 2008. "Paleogeography and Geologic Evolution of North America," *Global Plate Tectonics and Paleogeography*. Northern Arizona University.

Bond, D.C. 1972. *Hydrodynamics in Deep Aquifers in the Illinois Basin*: Illinois State Geological Survey Circular 470.

Bowen, B.B., Ochoa, R. I., Wilkens, N. D., Brophy, J., Lovell, T. R., Fischietto, N., Medina, C. R., and Rupp, J. A. 2011. Depositional and diagenetic variability within the Cambrian Mount Simon Sandstone: Implications for carbon dioxide sequestration *Environmental Geosciences*, June 1, 2011; 18(2): 69 - 89.

Brower, R.D., A.P. Visocky, E.G. Krapac, B.R. Hensel, G.R. Peyton, J.S. Nealon, and M. Guthrie. 1989. *Evaluation of Underground Injection of Industrial Waste in Illinois Final Report*, ENR Contracts AD-94 and UI-8501, Illinois State Geological Survey.

Christopher, Charles and James Iliffe. "Reservoir Seals; How they Work and How to Choose a Good One," Available at: http://esd.lbl.gov/CO2SC/co2sc_presentations/Site_Select_Charact_Gen_Framework/Christopher.pdf.

Clifford, M.J. 1973. Hydrodynamics of Mount Simon Sandstone, Ohio and Adjoining Areas. *Underground Waste Management and Artificial Recharge*, Vol 1, p 349-356.

Daniel, R.F. and J.G. Kaldi. 2008. "Evaluating Seal Capacity of Caprocks and Intraformational Barriers for the Geosequestration of CO₂." PESA Eastern Australian Basins Symposium III. Sydney, 14-17 September.

Drahovzal, J.A., D.C. Harris, L.H. Wickstrom, D. Walker, M.T. Baranowski, B.D. Keith, and L.C. Furter. 1992. *The East Continent Rift Basin: A New Discovery*: Kentucky Geological Survey, ser. 11, Special Publication 18, 25 p.

Eberts, S.M. and L.L. George. 2000. "Regional Ground-Water Flow and Geochemistry in the Midwestern Basins and Arches Aquifer System in Parts of Indiana, Ohio, Michigan, and Illinois," U.S. Geological Survey Professional Paper 1423-C. 103 p.

Foust, M.L., J.B. Comer, and J.A. Rupp. 2003. "Geothermal Gradient Distribution in Indiana," Open File Study 03-02, Indiana Geological Survey, October 13.

Greb, S., Harris, D. C., Solis, M. P., Anderson, W. H., Drahovzal, J. A., Nuttall, B. C., Riley, R. A., Solano-Acosta, W., Rupp, J. A., and Gupta, N. 2009. Cambrian-Ordovician Knox carbonate section as integrated reservoirs and seals for carbon sequestration in the eastern mid-continent United States, in Grobe, M., Pashin, J., and Dodge, R. L., eds., Carbon dioxide sequestration in geologic media - state of the science: Tulsa, Okla., American Association of Petroleum Geologists, p. 241-259.

Gupta, N. 1993. "Geologic and Fluid-Density Controls on the Hydrodynamics of the Mt. Simon Sandstone and Overlying Geologic Units in Ohio and Surrounding States," PhD dissertation, The Ohio State University, Columbus, Ohio.

Lampe, D.C. 2009. "Hydrogeologic Framework of Bedrock Units and Initial Salinity Distribution for a Simulation of Groundwater Flow for the Lake Michigan Basin," U.S. Geological Survey Scientific Investigations Report 2009-5060. 49 p.

Leetaru, H., and McBride, J. 2009. Reservoir uncertainty, Precambrian topography, and carbon sequestration in the Mt. Simon Sandstone, Illinois Basin. *Environmental Geosciences*; December 2009; v. 16; no. 4; p. 235-243.

Medina, C., Barnes, D., and Rupp, J. 2008. Depth relationships in porosity and permeability in the Mount Simon Sandstone of the Midwest region: Applications for carbon sequestration. Eastern Section Meeting of the AAPG, Pittsburgh, PA, October 14, 2008.

Medina, C. R., Rupp, J. A., 2010 (poster), Reservoir Characterization and Lithostratigraphic Division of the Mount Simon Sandstone: Implications for Estimations of Geologic Sequestration Storage Capacity. AAPG Eastern Section, Annual Meeting, 9/26/10-9/28/10, Kalamazoo, Michigan.

Medina, C. R., Rupp, J. A., and Barnes, D. A., 2011, Effects of reduction in porosity and permeability with depth on storage capacity and injectivity in deep saline aquifers - a case study from the Mount Simon Sandstone aquifer: *International Journal of Greenhouse Gas Control*, v. 5, p. 146-156.

Midwest Geological Sequestration Consortium (MGSC). 2005. "An Assessment of Geological Carbon Sequestration Options in the Illinois Basin," U.S. DOE Contract: DE-FC26-03NT41994, The Board of Trustees of the Univ. of Illinois, Illinois State Geological Survey, Final Report December 31.

MIT Carbon Capture and Sequestration Technologies Program. 2009. Carbon Management GIS: CO₂ Pipeline Transport Cost Estimation. Report for NETL, DOE Contract: Contract DE-FC26-02NT41622.

Mossier, J.H. 1992. Sedimentary Rocks of the Dresbachian Age (Late Cambrian), Hollendale Embayment, Southeastern Minnesota. University of Minnesota Report of Investigations 40.

Nuefelder, R.J. 2011. Petrographic, Mineralogical, and Geochemical Evidence of Diagenesis in the Eau Claire Formation, Illinois Basin: Implications for Sealing Capability in a Carbon Dioxide Sequestration System. Master of Science Thesis, Purdue University, West Lafayette, Indiana. 153 p.

Ochoa, R.I. 2011. Porosity Characterization and Facies Analysis of the Cambrian Mount Simon Sandstone: Implications for Regional CO₂ Sequestration Reservoir. Master of Science Thesis, Purdue University, West Lafayette, Indiana. 151 p.

Olson, R.K. and M.W. Grigg. 2008. "Mercury Injection Capillary Pressure (MICP) A Useful Tool for Improved Understanding of Porosity and Matrix Permeability Distributions in Shale Reservoirs." Kerogen Resources, Inc., Houston, TX. Adapted from oral presentation at AAPG Annual Convention, San Antonio, TX, April 20-23.

Person, M., Banerjee, A., Rupp, J., Medina, C., Lichtner, P., Gable, C., Pawar, R., Celia, M., McIntosh, J., and Bense, V., 2010, Assessment of basin-scale hydrologic impacts of CO₂ sequestration, Illinois basin: International Journal of Greenhouse Gas Control, v. 4, p. 840-854.

Saeed, Aram. 2002. "Petroleum Analysis of the Cambrian Mt. Simon Sandstone Using Subsurface Facies Analysis and Digital Image Processing." M.S. Thesis, Bowling-Green State University.

Santos, J.O., Potter, P.E., Easton, R.M., Hartmann, L.A., McNaughton, N.J., and Rea, R., -Joao-Orestes, 2001, Proterozoic Middle Run Formation of eastern Midwest, USA; a Torridonian equivalent? (abs): Geological Society of America, v. 33, p. 93.

Schlumberger. 1972. Log Interpretation, Volume I - Principles.

Shrake, D.L., Wolfe, P.J., Richard, B.H., Swinford, E.M., Wickstrom, L.H., Potter, P.E., and Sitler, G.W. 1990. Lithologic and geophysical description of a continuously cored hole in Warren County, Ohio, including description of the Middle Run Formation (Precambrian?) and a seismic profile across the core site: Ohio Division of Geological Survey, Information Circular 56, 11 p.

Tóth, J. 1963. "A Theoretical Analysis of Groundwater Flow in Small Drainage Basins," *Journal of Geophysical Research*, Vol. 68, No. 16, pp. 4795-4812.

The University of Adelaide, "Mercury Injection Capillary Pressure Analysis," Available at: <http://www.asp.adelaide.edu.au/research/micp/background/>

U.S. DOE (U.S. Department of Energy). 2008. Carbon Sequestration Atlas of the United States and Canada. National Energy Technology Laboratory, Pittsburgh, PA, USA.

Vaught, Tracy L. 1980. "An Assessment of the Geothermal Resources of Illinois Base on Existing Geologic Data," Gruy Federal, Inc., Arlington, VA, December. Prepared for U.S. Dept. of Energy Division of Geothermal Energy Under Contract No. AC08-80NV10072.

Warner, D.L. 1988. *Hydrogeologic and Hydrochemical Assessment of the Basal Sandstone and Overlying Paleozoic Age Units for Wastewater Injection and Confinement in the North Central Region (Draft Final Report)*, Underground Injection Practices Council, Oklahoma City, OK.

Wickstrom, L. H., Gray, J. D., and Steiglitz, R. D. 1992. Stratigraphy, structure, and production history

of the Trenton Limestone (Ordovician) and adjacent strata in northwestern Ohio: Ohio Division of Geologic Survey Report of Investigations 143, 78 p.

Wickstrom, L.H., Venteris, E.R., Harper, J.A., McDonald, J., Slucher, E.R., Carter, K.M., Greb, S.F., Wells, J.G., Harrison III, W.B., Nuttall, B.C., Riley, R.A., Drahovzal, J.A., Rupp, J.A., Avary, K.L., Lanham, S., Barnes, D.A., Gupta, N., Baranoski, M.A., Radhakrishnan, P., Solis, M.P., Baum, G.R., Powers, D., Hohn, M.E., Parris, M.P., McCoy, K., Grammer, G.M., Pool, S., Luckhardt, C.M., Kish, P. 2005. Characterization of Geologic Sequestration Opportunities in the MRCSP Region: Phase I Task Report Period of Performance, October 2003–September 2005, p. 152.

Zhou, Q., Birkholzer, J.T., Mehnert, E., Lin, Y.-F., and Zhang, K. 2010. Modeling Basin- and Plume-Scale Processes of CO₂ Storage for Full-Scale Deployment: Ground Water, v. 48, p. 494-514.